UNIVERSITY of MISKOLC

FACULTY of EARTH and ENVIRONMENTAL SCIENCES & ENGINEERING

INSTITUTE of RAW MATERIAL PREPARATION and ENVIRONMENTAL TECHNOLOGIES

Mechanical Activation to Enhance the Reactivity of Coal Gangue for Tailoring Geopolymer Properties

A Dissertation Submitted Partial Fulfilment of the Requirement for the Degree of Doctor of Philosophy

Author

Siti Natrah Binti Abd Bakil

Scientific supervisor:

Prof Dr. Gábor Mucsi

Professor

Co-supervisor:

Dr. Ferenc Kristály

Senior research fellow

MIKOVINY SÁMUEL DOCTORAL SCHOOL of EARTH SCIENCES

Head of the doctoral school:

Prof. Dr. Péter Szűcs

Professor

Miskolc, Hungary

2025

Statement of Supervisors for the PhD Thesis

"MECHANICAL ACTIVATION TO ENHANCE THE REACTIVITY OF COAL GANGUE FOR TAILORING GEOPOLYMER PROPERTIES" by
Siti Natrah Binti Abd Bakil

Throughout her doctoral career, the candidate has consistently demonstrated exceptional intellectual rigour and highly innovative thinking, driving a research agenda with profound impact in geopolymer research and applications. Her work is fundamentally dedicated to advancing mechanical activation as a green technology to systematically overcome the low reactivity of coal gangue, a critical barrier that severely limits its widespread adoption as a viable secondary material. The candidate's thesis, which focuses on enhancing the reactivity of coal gangue for high-performance geopolymer applications, places her research decisively at the forefront of international efforts in sustainable construction materials and industrial waste valorisation. Crucially, she successfully developed and integrated mechanical activation into a comprehensive, robust framework for the rigorous evaluation of coal gangue waste reactivity from the Bükkábrány opencast lignite mine in Borsod-Abaúj-Zemplén County, Hungary.

The candidate's doctoral research presents findings with immediate and significant translational value for the sustainable construction sector. The work extends the use of coal gangue as a crucial secondary raw material, moving beyond established geopolymer development to offer a versatile methodological framework that can be readily adapted to optimise sustainable cement production. The first investigation empirically quantifies how different mechanical stress regimes, such as compression, shear (attrition), impact, and collision, fundamentally alter and systematically enhance the reactivity of coal gangue powder. This produced a predictive framework capable of accurately forecasting the resulting powder characterisation for different grinding devices, along with the associated specific energy consumption of mechanical activation. Finally, the candidate provided a crucial and comprehensive characterisation of the mechanically activated coal gangue powder, rigorously focusing on key parameters that directly determine the subsequent geopolymerization reaction kinetics and ultimate material performance. Collectively, these innovations establish a robust pathway for high-impact resource

valorisation. This work transforms a problematic waste into a high-performance resource, directly contributing to a competitive and resilient market.

The candidate has published high-impact research, resulting in several peer-reviewed publications in leading, high-impact (Q1) journals, underscoring the rigour, quality, and international relevance of her scientific contributions. In addition to these technical achievements, the candidate has consistently demonstrated outstanding academic and professional qualities, including an unwavering work ethic, deep intellectual curiosity, and the ability to address complex resource valorisation challenges with creativity, determination, and innovative solutions. We confidently recommend that she be awarded the PhD degree, as she has successfully fulfilled all the academic and research requirements for this qualification. We certify that this dissertation contains only valid data, and the presented results represent the candidate's own work. In our opinion, it meets the scope and quality requirements set by the Mikoviny Sámuel Doctoral School of Earth Sciences.

NOVEMBER 2025, MISKOLC

Scientific Supervisors:

Prof Dr. Gábor Mucsi

University Full Professor

Dr. Ferenc Kristály

Senior research fellow

ACKNOWLEDGEMENT

My success in this Ph.D. program could not have been achieved without the deep cooperation, invaluable assistance, and ongoing support I was fortunate to have from many people. Through these few sentences, I would like to express my thanks to them. First and foremost, I would like to express my immense appreciation to my supervisors ***Professor Dr. Gábor Mucsi*** *and* ***Dr. Ferenc Kristály****. Their overwhelming support, insightful advice, constant encouragement, supervision was instrumental from the very beginning of my PhD candidature at the University of Miskolc, guiding me through to its midway point. Their expert guidance, invaluable suggestions, and the exceptional opportunities they provided have truly allowed me to develop and cultivate my passion as a researcher.*

My deepest appreciation also goes to my beloved family, my husband, ***Saifullah Umar****, my children, and my family in Malaysia. Their unconditional love, unwavering encouragement, and profound support have been the cornerstone of my journey throughout my entire PhD program and indeed, my research career. This research work could not have been completed without their support and understanding.*

I would also like to extend my deepest appreciation to all the dedicated staff members in the ***Raw Material Preparation and Environmental Technologies.*** *Their invaluable advice, consistent technical support, continuous assistance, and ready cooperation were indispensable during the implementation of my experimental work throughout the past years. In particular, I wish to thank Dr. Ádám Rácz, Dr. Márton, Dr. Tamás, Fanni, Isabella, Maria, Tamás, Ildikó, Melinda, Cornelius, and many others whose contributions were vital. My sincere gratitude also goes to Professor Dr. Sandra Breitung and her research group, Sofiia, Alex, and Sebastian. Their insightful comments and valuable suggestions on several aspects of my work during my visiting research were immensely helpful.*

Furthermore, I express my sincere thanks to my colleagues from other departments, Dr. Jamal and Sarah, Mr Anuar from UTHM, and Professor Kenji from the University of Tokyo. I am profoundly grateful to all of them for the countless hours of engaging and productive discussions, experimental assistance, and collaboration, as well as for generously sharing their extensive and valuable practical skills and knowledge with me.

Finally, I wish to acknowledge the ***Hungarian Government*** *for generously providing me with a full scholarship, which made my PhD study possible during its entire duration.*

TABLE OF CONTENT

LIST OF FIGURES

LIST OF TABLES

LIST OF SYMBOLS AND ABBREVIATIONS

Symbols:

CF	Collision frequency (s^{-1})
d_{GM}	Grinding media size (mm)
E_m	Specific grinding energy (J g^{-1})
L/S	liquid-to-solid ratio
m_A	Active mass (g)
P_0	Power input (J)
P	Non-load power (J)
rpm	Revolution per minute
RS	Relative span [-]
S_{BET}	Specific surface area-Brunauer, Emmett and Teller
S_m	Geometric surface area
SI	Stress intensity
SE	Stress energy (J g^{-1})
t_G	Grinding time (min)
x_{10}	Particle size for cumulative 10 % finer (μm)
x_{50}	Particle size for cumulative 50 % finer (μm)
x_{90}	Particle size for cumulative 90 % finer (μm)
ρ_{GM}	Grinding media density (g/cm^3)

Abbreviations:

DoE	Design of Experiment
ATR/FT-IR	Attenuated total reflectance Fourier transform - infrared spectroscopy
NaOH	Sodium hydroxide
Na_2SiO_3	Sodium silicate
$Na_4P_2O_7$	Sodium pyrophosphate
PSA	Particle size analysis
SEM	Scanning electron microscope
XRD	X-ray diffraction
XRF	X-ray fluorescence

1. INTRODUCTION

1.1 Background

Mining and mineral processing represent a persistent and growing environmental challenge worldwide. Over the past century, the surge in global demand for metals, minerals, and energy resources has led to a dramatic increase in both active open-pit and underground mining operations [1,2]. Among these resources, coal remains a cornerstone of global power generation. Among these resources, coal remains a cornerstone of global power generation. However, its extraction produces substantial quantities of coal gangue, a solid waste by-product that typically accounts for approximately 10 - 25 % of total coal production, or roughly 0.15 tons per ton of coal mined [3]. The Bükkábrány opencast lignite mine in Borsod-Abaúj-Zemplén County, Hungary, produces significant quantities of coal waste as a by-product of mining, as shown in Fig 1.1 [4]. This waste material consists of sandy, muddy, and clay sediments that lie between the lignite, as well as overburden layers that must be removed. The coal gangue is composed of fine-grained clay and interbedded sediments within the lignite deposits. Large quantities of coal gangue are associated with environmental problems related to disposal, polluting soils and groundwater.

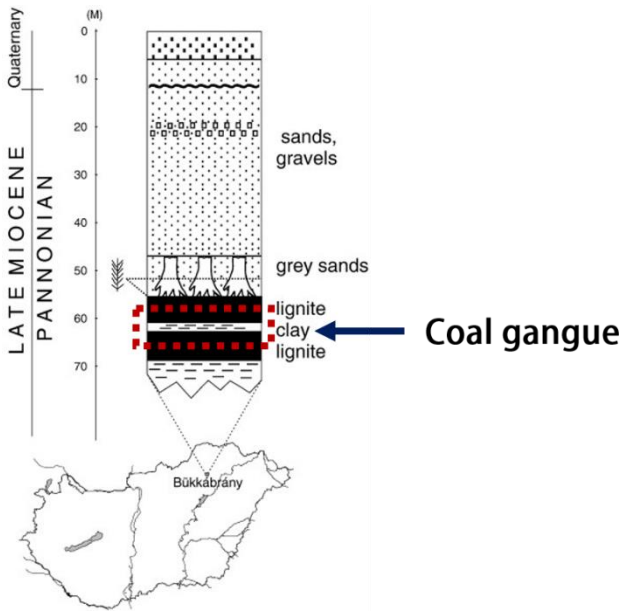

Fig 1.1: Location and sampling site of coal gangue

In recent years, the transition to a circular economy has emerged as the key sustainable alternative to the traditional linear economic model. This paradigm shift is driven by the need to optimize material recycling and repurpose industrial by-products for new, value-added

applications. Unlike primary raw materials, which are increasingly costly and resource-intensive to extract, secondary materials offer a viable solution. However, their heterogeneous composition often poses technical challenges that require innovative processing approaches. This shift directly aligns with the European Commission ambitious 2030 climate target plan, which aims to reduce greenhouse gas emissions by 2030 and achieve climate neutrality by 2050 [5]. Achieving these targets will require systemic changes in resource management, particularly in high environmental impact sectors such as mining, manufacturing, and energy, where waste recovery and circular economy principles can significantly reduce the carbon footprint. The principles of the circular economy have rapidly been adopted and implemented by most countries, fundamentally changing global economic perspectives and influencing national strategic plans [6]. To maximize the potential of recycling coal gangue and address the associated environmental concerns, it is crucial to explore recent advancements in processing techniques and gain a deeper understanding of the coal gangue properties.

Global research into waste-derived geopolymers as sustainable building materials has increased significantly. This emerging field has attracted great scientific and industrial interest because geopolymers represent a highly promising, environmentally friendly alternative to traditional Portland cement. Geopolymers not only exhibit exceptional mechanical properties, including high compressive strength and durability, but their manufacture also produces significantly lower carbon emissions [7]. These properties make geopolymer technology particularly attractive for sustainable construction applications, aligning with global efforts to reduce the environmental impact of building materials. Nevertheless, a major obstacle to using coal gangue in geopolymerization is its inherently low reactivity. This low reactivity means coal gangue particles frequently fail to achieve complete dissolution before the finalized hardened structure forms. This limitation presents substantial challenges in accurately quantifying reaction progression in coal gangue-based geopolymers [8],[9]. Methods such as mechanical activation [10],[11], calcination activation [12],[13], and chemical activation [14] represent alternative strategies to recycle coal gangue and significantly improve its reactivity for geopolymerization. Calcination activation, despite its effectiveness in enhancing the reactivity of certain materials, presents significant drawbacks that hinder its widespread industrial application. High energy consumption is the primary issue, as the process typically requires maintaining temperatures ranging from 650 - 900 °C extended durations. This energy demand directly contradicts the principles of sustainable resource utilization [15],[16]. In contrast, the mechanical activation process requires specialized high energy mills that employ

various working regimens, including compression, shear, and impact forces, to increase the material surface energy by inducing amorphization or defect into crystal lattice [17]. Mechanical activation represents a particularly promising approach as it modifies raw material reactivity through surface property alterations without fundamentally changing the overall chemical structure. This methodology is increasingly recognized as a pioneering and environmentally friendly processing technique, with applications extending across diverse technological fields, such as cement [18],[19], metal extraction [20], mineralization [21], and the extraction of rare earth elements [22]. Mechanical activation is a recognized strategy to enhance the reactivity of raw materials for geopolymer applications, a fact that has been consistently demonstrated in recent years. The underlying mechanisms include particle size reduction, increased specific surface area, the creation of crystal lattice defects, and higher amorphous content 25]. As a result, significant improvements in geopolymer properties for their utilization, such as compressive strength, setting time, and rheology characteristics, are now thoroughly reported [25-28].

1.2 Research objective

This research aims to investigate the mechanical activation of coal gangue through a dry grinding process, employing high-energy milling to enhance its reactivity. The primary objective is to determine the optimal grinding parameters to achieve the most favourable reactivity while also identifying limitation of specific grinding energy. Ultimately, this study seeks to establish a comprehensive understanding of both raw and mechanically activated coal gangue and effect on the performance characteristic of resulting geopolymer properties.

- **i.** To investigate a comprehensive analysis and characterization of raw coal gangue
- **ii.** To systematically optimize the key grinding parameters, grinding media size (d_{GM}), revolution per minute (rpm), and grinding time (t_g) for high-energy milling to achieve mechanically activated coal gangue properties while determine specific grinding energy (E_m) consumption. Furthermore, to critically compare the effectiveness of two distinct high-energy milling techniques (vibratory vs. planetary ball milling) on the resulting coal gangue reactivity
- **iii.** To conduct comprehensive analysis of the mechanically activated coal gangue to specifically examining changes in particle size distribution (PSD), aggregation/ agglomeration and deagglomeration, specific surface area (S_{BET}) and geometric surface area (S_m), powder morphology (SEM), functional groups via (FT-IR) that

cause its molecular bonds to vibrate (stretch and bend), and phase composition (XRD).

Characterization and optimization of raw and mechanically activated coal gangue for geopolymer applications.

- **i.** To experimentally synthesize geopolymers using both raw and optimized mechanically activated coal gangue as the primary precursor. This includes systematically optimizing the key geopolymerization parameters (liquid-to-solid ratio, NaOH molarity, sodium silicate percentage, and curing temperature) to evaluate and maximize the resulting mechanical strength and performance characteristics.
- **ii.** To develop a comprehensive matrix and establish a predictive correlation between the physicochemical properties of the mechanically activated coal gangue and the final geopolymer performance.

2. LITERATURE REVIEW

This chapter provides the theoretical background required to understand the scope and the main scientific questions of this research. In particular, aspects related to mechanically activated coal gangue and geopolymers are discussed.

2.1 Mining industry and waste

Critical raw materials are essential to the EU economy and a wide range of key technologies in strategic sectors such as renewable energy, digital technology, aerospace, and defence. The Critical Raw Materials Act (CRM Act) aims to ensure a secure and sustainable supply of these materials for the EU and to help Europe meet its 2030 climate and digital targets. For example, EU demand for rare earth metals is expected to increase six-fold by 2030 and seven-fold by 2050, while demand for lithium is projected to rise twelve-fold by 2030 and twenty-one-fold by 2050. Currently, Europe is highly dependent on imports, often from a single country, and recent crises have highlighted these strategic dependencies [27]. This dependence on imports and the growing demand for critical materials emphasises the importance of the mining industry. The expansion of the mining industry brings with it both opportunities and challenges. Navigating this complex landscape raises the pressing question of how the mining sector can simultaneously create new economic value, minimise its harmful social and environmental impacts and effectively reduce the long-term liability associated with mining waste [28]. While the active operation of open pit and underground mines to extract vital metal and energy resources is critical to global development, it also generates massive waste streams, particularly gangue and tailings, which require innovative management to reduce the significant environmental impacts. Gangue is the commercially valueless material that surrounds or is intimately mixed with a desired mineral in an ore deposit [29]. Tailings, a major waste stream from mineral processing, consists of fine-grained (1 - 600 μm) crushed rock left behind after the extraction of valuable minerals or ore processing [30]. Crucially, this waste is associated with process water, which may contain dissolved metals and residues of reagents from ore processing, posing a potential environmental risk [31,32]. By aligning with the principles of Sustainable Development Goal 12 and adopting sustainable practises, the mining sector can continue to meet global resource needs while reducing its environmental footprint and making a positive contribution to the Sustainable Development Goals [33,34]. To achieve a truly sustainable future, the mining industry must undergo a fundamental transformation. This requires the development and implementation of comprehensive, long-term strategies

aimed at achieving a zero environmental footprint. Despite recent advances in mining management, there is still a lack of optimal scenarios for mining waste that deliver overall sustainable benefits. Recycling is essential for the security and sustainability of the supply of critical minerals for the transition to clean energy. Recycling reduces the need for new mines and increases safety and sustainability. The Clean Industry Deal emphasises the circular economy, which aims to reduce waste and extend the life of materials by promoting recycling, reuse and sustainable production. Maximising the EU limited resources and reducing over-reliance on third country raw material suppliers is crucial for a competitive and resilient market [35]. The circular economy model emphasises the importance of closed loops that reduce the need to extract and process new resources. With this in mind, a Circular Economy Act is planned for 2026 to accelerate this transition. The aim of this law is to ensure that scarce materials are used and reused efficiently, reduce global dependencies and create quality jobs, with the aim of making 24 % of materials circular by 2030. Globally recognized as one of the most abundant and widely distributed energy resources, coal remains a critical cornerstone of power generation, steelmaking, and cement production. Its pivotal role continues to underpin the world's economic infrastructure, significantly supporting the escalating energy demands of a developing human society [36]. Consequently, the imperative to meet these energy needs through extensive open-cast mining operations inevitably generates substantial volumes of waste materials, encompassing rock, soil, and a diverse suite of mineral constituents. This discarded material, commonly termed overburden or gangue [37], represents a considerable yet largely unexploited of potential resources. Specifically, coal gangue, a mineral-rich byproduct generated during coal extraction processes accounting for a substantial 10 % to 25 % of total coal mining production [34]. The indiscriminate disposal of this gangue poses a significant dual threat to environmental sustainability such as occupation of valuable land resources, and it frequently precipitates severe environmental pollution and engenders critical health risks for local populations. Despite increasing efforts towards the utilization of coal gangue, its generation volume continues to be substantial, presenting a persistent environmental challenge. Recognizing its inherent mineralogical composition, primarily comprising SiO_2 and Al_2O_3, coal gangue can be strategically re-envisioned as a valuable resource rather than waste product, provided appropriate beneficiation strategies are implemented. The dominant mineralogical phases typically include 1:1 kaolinite and other 2:1 clay mineral such as illite, alongside non-clay minerals like quartz, sodium feldspar, and calcite, often reported as impurity phases within these complex structures [38]. The mineralogical of coal gangue exhibits a striking resemblance to that commonly observed in mine tailings, which are predominantly composed

of quartz, feldspar, albite, and muscovite [39,40]. The chemical composition of mine tailing or gangue, on the other hand, formation predominantly of silicon, aluminium and calcium oxides, with content ranging from 60 % and 90 % [41]. In the purpose of reducing the environmental construction impact, the aluminosilicate inorganic polymers, also called geopolymers present attractive alternative materials [42]. The escalating global demand for coal, evidenced by China leading production of 4940 Mt and India 1363 Mt annually, alongside the European Commission projection of over 293 Mt consumption in 2025, underscores the continued significance of coal as an energy source as shown in Fig 2.1 [43].

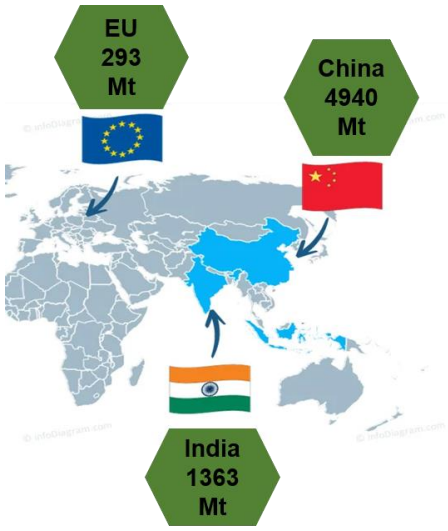

Fig 2.1: Global coal consumption, sources International Energy Agency (IEA) data from 2000-2026

2.2 Reaction mechanism of geopolymer formation

This groundbreaking work paved the way for the complete substitution of ordinary Portland cement (OPC) with innovative binders called alkaline cements. These alternative materials, which include both alkali-activated materials (AAM) and geopolymer, are synthesized through the alkaline activation of various industrial byproducts and natural minerals rich in alumina and silica. The term alkali-activated material (AAM) is often used interchangeably with geopolymer, particularly when emphasizing the alkali activation of an aluminosilicate source material derived from industrial waste [44,45]. In the 1940s, the Belgian scholar A. O. Purdon discovered that combining alkali and slag produced a new, rapidly hardening binder. By the early 1950s, the use of alkali-activated slag cement became widespread, with V. D. Glukhovsky playing a pivotal role in the development of AAM [46]. Despite their similar origins, AAM and geopolymer have fundamental differences in their chemistry. AAM are defined by their hydration process and are not polymers as its harden and

gain strength through chemical reaction with water. The solid binding phase formed is also disordered, but in the presence of sufficient calcium, its nanostructure is based on the calcium silicate hydrate (C-S-H) or C-(A)-S-H) binder phases which form in traditional Portland-type or pozzolanic hydraulic cements. This distinction makes terms like N-A-S-H or K-A-S-H (which describe hydrated gel phases) irrelevant in the context of geopolymer [47]. Therefore, they cannot be classified as geopolymers [48]. Geopolymers, conversely, are polymers, not hydrates.

In the 1970s, the French scientist Joseph Davidovits introduced the term geopolymer. He revolutionized the field of cementitious materials by explaining the mechanism of geopolymerization, a process that creates compounds with remarkable cementitious properties. Geopolymers are a type of inorganic polymer with a 3D cross-linked polysialate chain structure. This structure forms through the hydroxylation and polycondensation of natural minerals like clay, slag, and fly ash when activated by a highly alkaline solution at temperatures below 160 °C. This inorganic polymer was first named polysialate in 1976, Davidovits later coined the term geopolymer. Geopolymers are fundamentally composed of an aluminosilicate framework characterized by a cross-linked structure of tetrahedral AlO_4 and SiO_4 units, for which the chemical designation poly(sialate) has been proposed. Aluminosilicate source materials abundant in alumina (Al_2O_3) and silica (SiO_2) are essential for initiating the geopolymerization reaction, typically requiring a highly alkaline environment to facilitate the dissolution and subsequent polycondensation of these precursors [49]. These source materials play a pivotal role in geopolymer formation by providing the crucial Al^{3+} and Si^{4+} ions that constitute the structural backbone of the binding system. Geopolymers are synthesized by activating solid aluminosilicates with alkaline activator such as sodium hydroxide and sodium silicate through a series of dissolution. The OH ions attack the silicon-oxygen (Si-O) and aluminium-oxygen (Al-O) bonds within the alumina-silicate framework, and the detailed mechanism of Al and Si dissolution can be understood from Fig 2.2 [50].

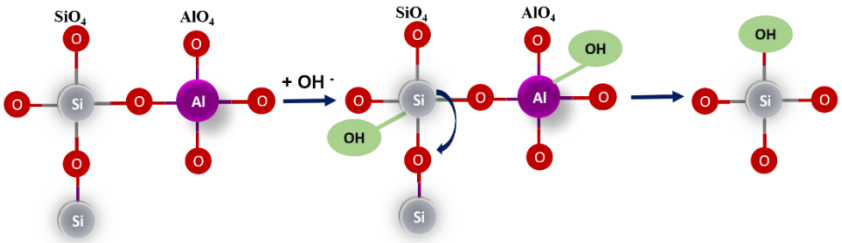

Fig 2.2: Schematic representation of the mechanism of dissolution of Si and Al

It is assumed that a highly reactive intermediate gel phase is formed by co-polymerization of individual alumino and silicate species, from which the geopolymer gel is formed. The binding property of the geopolymer results from the amorphous alkali aluminosilicate gels, which have a general formula as eq. (1):

$$M_n[-(Si-O_2)_Z-Al-O]_n wH_2O \quad (1)$$

wherein M represents one or more alkali metals and z is 1, 2 or 3 and n is degree of polymerization. Positive ions (Na^+, K^+, Li^+, Ca^{2+}, Ba^{2+}, NH_4^+, H_3O^+) must present in the framework cavities to balance the negative charge of Al^{3+} in IV-fold coordination. The final product has Si-O-Al backbone. Davidovits classified the geopolymer structure into three types with a Si/Al ratio of 1:1, poly(sialate-siloxo) with a Si/Al ratio of 1:2 and poly(sialate-disiloxo), with a Si/Al ratio of 1:3 as shown in Fig 2.3 [51] [52].

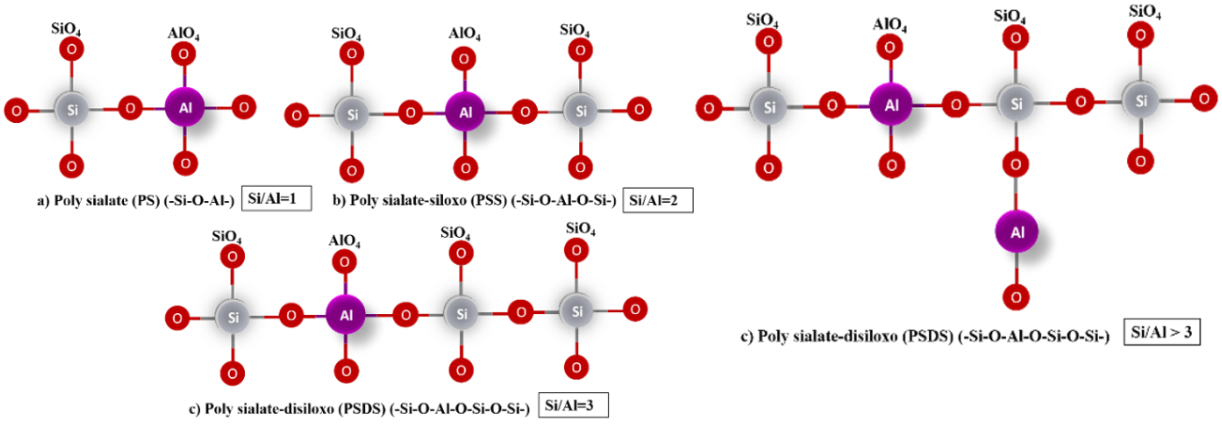

Fig 2.3: Type of polysialate

Under a high concentration of alkali activator and complicated mechanism, polymerization happen when reactive alumina silicates are dissolved and free [SiO^4]- and [AlO^4]- tetrahedral ions are released in solution consequently produce polymeric Si-O-Al bonds [53]. The released $[SiO(OH)_3]^-$ and $Al(OH)_4^-$ polycondense into amorphous or semicrystalline oligomers by attractions between OH groups as eq. (2), eq. (3) and eq. (4).

$$Al_2O_3 + 3H_2O_3 + 2OH^- \rightarrow 2Al(OH)_4^- \quad (2)$$

$$SiO_2 + H_2O + OH^- \rightarrow [SiO(OH)_3]^- \quad (3)$$

$$SiO_2 + 2OH^- \rightarrow [SiO_2(OH)_2]^{2-} \quad (4)$$

Reorganization and diffusion of dissolved ions with formation of small coagulated structures as eq. (5). Bonding of the solid particles into the polymeric framework and hardening of the whole system into a final solid polymeric structure. Since the geopolymer framework is developed in the aqueous phase, it comes across the active surface sites of the solid particles, where it is possible to react bonding the undissolved particles in the final geopolymer structure.

$$NaOH(aq) + NaAl(OH)_4(aq) \rightarrow Na_2(SiO)_3(aq) \quad (5)$$

The ultimate properties of geopolymers are critically dependent on the physicochemical characteristics of the precursor materials. Specifically, materials exhibiting a predominantly amorphous state, a high density of microstructural defects, or significant crystal lattice distortions demonstrate enhanced reactivity in the geopolymerization process. Singh et al. [54] further elucidated that the activation and reactivity of the precursor are intricately influenced by its chemical and mineralogical composition, morphology, fineness (particle size distribution), and the proportion of the amorphous phase. Consequently, the complex process of geopolymerization is governed by a multitude of interacting factors, as schematically illustrated in Fig 2.4 [55][56,57]. Indeed, the amorphous phase is crucial for facilitating structural reorganization within the bonding network, as it constitutes the primary reactive material that undergoes dissolution and transformation during the initial depolymerization stage of geopolymerization. The reactivity of the precursor is typically characterized by its solubility in the alkaline activation solution, which represents the critical first step in the geopolymerization mechanism. Elevated reactivity of the source material promotes rapid gel formation, leading to a densification of the microstructure and reduction in porosity, ultimately enhancing the mechanical properties of the geopolymer matrix [58,59].

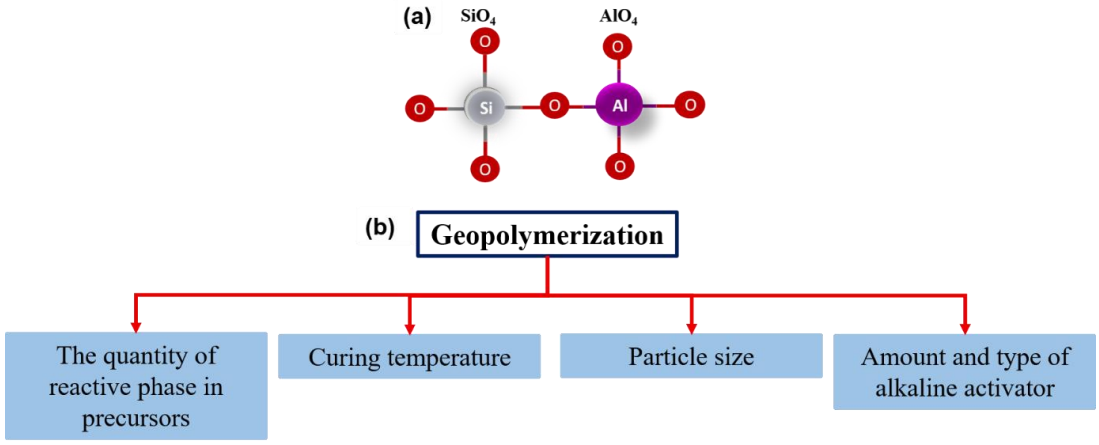

Fig 2.4: (a) Structure of AlO_4 crosslink with SiO_4 (b) Factor influencing geopolymer process

2.3 Mechanical activation

In the pursuit of sustainable material production with enhanced technical performance, significant research efforts are directed towards developing processes that minimize environmental impact. Among these, mechanical activation has garnered considerable attention as a promising strategy. The foundational concept of mechanical activation, or grinding, was initially defined by Smekal et al. [60] as a process driven by mechanical energy input, resulting in chemical reactivity of the system without inducing alterations in its bulk chemical composition. Building upon this, Butylating [61] the mechanical activation is defined as an increase in reaction ability due to change in solid structure by sudden impact between particles or grinding media. The primary objective of mechanical activation is the liberation of inherently intergrown mineral grains through a sequence of four principal stress-related events, compression, shear (attrition), impact, and collision [62,63]. In other words, under the synergistic influence of frictional forces, particle collisions, shear stresses, and other mechanical interactions within the milling environment, a portion of the imparted mechanical energy is transduced into increased entropy and internal energy within the solid structure, particularly in the near surface region of the particles [64]. This energy accumulation at the surface level is a key driver for enhanced reactivity. Expanding on this, P. Baláž [17] due to that mechanical activation typically induces an increase in the entropy of the material's structure, often accompanied by generation of defects or other metastable forms can be registered. Further elaborating on the mechanistic aspects, Juhász [65] proposed a subdivision of processes occurring under mechanical activation into primary and secondary phenomena, as schematically illustrated in Fig 2.5.

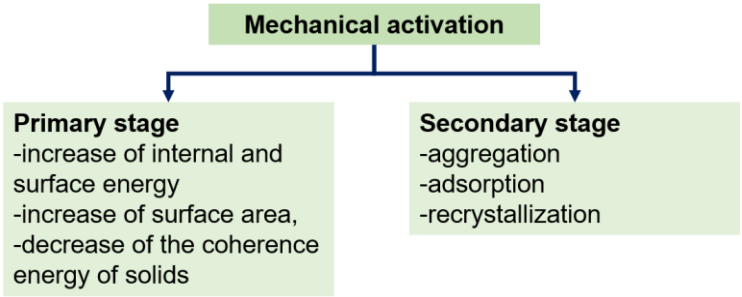

Fig 2.5: Mechanical activation can be subdivided into primary and secondary stages

Within solid materials, structural units are typically arranged in geometrically close-packed or tightly interconnected network structures, dictated by the nature of the interatomic chemical bonds. Consequently, the migration of ions or other chemical species is contingent upon their ability to disrupt these ordered arrangements, often facilitated by the generation of structural

defects. The formation and propagation of micro and nano cracks (typically below 30 µm) along grain boundaries during mechanical activation produce selective comminution effects [66], as visually depicted in Fig 2.6. In crystalline materials, specific defects such as amorphous regions, point defects, and dislocations can induce significant local strain concentrations, potentially leading to the rupture of atomic bonds and transcrystalline cleavage fracture, as illustrated in Fig 2.7.

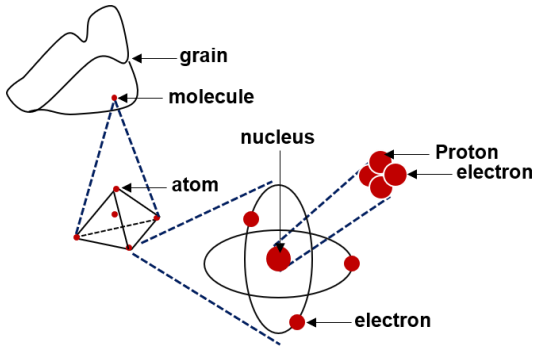

Fig 2.6: Element of component

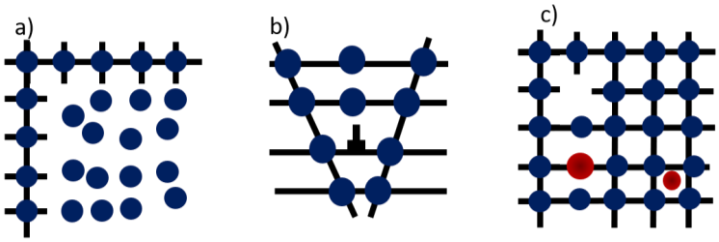

Fig 2.7: Defect during mechanical (a) amorphous region; (b) dislocations; (c) point defect

Dislocations are a prevalent type of linear defect commonly observed in crystalline solid substances. Furthermore, the formation and characteristics of defect phases can be modulated by the overall chemical composition of the material and the applied processing parameters [67,68] [69]. Currently, the most widely accepted theory explaining the phenomenon is that of mechanical activation. This theory posits that mechanical forces induce a metastable state in solids by displacing atoms from their equilibrium lattice positions and distorting chemical bonds, thereby accumulating significant potential energy [70]. It claims that mechanical forces produce a metastable state in solids, atoms are shifted from their lattice positions and the distorted chemical bonds accumulate potential energy. Initially, this stored energy is dissipated through localized heating and particle fragmentation. However, as particles are progressively reduced to a critical size, additional processes become increasingly prominent including amorphization, the accumulation of lattice defects, and the initiation of solid-state chemical reactions, as illustrated in Fig 2.8 [71].

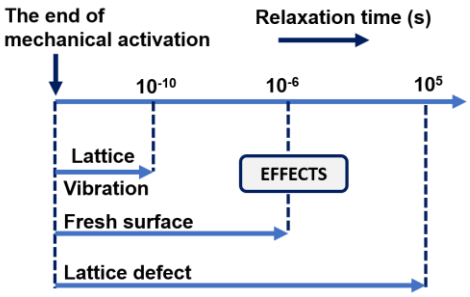

Fig 2.8: The period and duration of excitation states effects

The comminution process in is usually determined by stress model. Therefore, in order to reduce the experimental expenditure and to improve the optimization result, a physical grinding model should be developed, which describes the effect of the different operating parameters by characteristic numbers in a combined form [72].

Stress model of product [73]:

a) SN_F = how often each feed particle and its resulting fragments are stressed and thus by the number of stress events of a feed particle
b) SI = how high the specific energy or specific force at each stress event

Stress model of mill:

a) SF_M = the number of stress events which are supplied by the mill per unit time
b) SE = the energy which can be supplied to the product particles by the mill at each stress event

The stress energy *SE* is determined by the energy dissipated in each ball contact. The contacts can occur as collisions between two balls or a ball and the beaker and as a gliding contact of balls along the wall [74].

2.3.1. Mechanical activation of waste material and coal gangue in geopolymer

In recent years, mechanical activation has emerged as a route to gain increasing interest for geopolymer applications, capturing growing interest from both academic researchers and industrial practitioners. This surge in attention stems from its potential as a clean and energy-efficient alternative to traditional thermal treatment methods for activation of raw and waste material as in Table 2.1 Mechanical activation offers a compelling approach to precisely tailor

the reactivity of raw materials by specifically modifying such as increasing specific surface area and introducing structural defects at the particle level without altering the bulk chemical composition of the material. A key principle in achieving higher reactivity for geopolymer synthesis through mechanical activation is the production of finer particles, as this increases the surface area available for reaction and enhances the dissolution kinetics of the precursors [75,76]. The dry grinding appeared to be more effective in imposing significant structural changes, even despite problems related to high temperature or agglomeration. At the same time, wet grinding can intensify shrinkage, cracking and deformations of the material exposed to the subsequent drying.

Table 2.1. A comparison mechanical activation (MA) of waste material

Main raw material	MA	Grinding time	rpm	Method of grinding	Application	Ref
Low grade clay	Ring mill	4 and 8 hours	-	Dry	Geo	[77]
Waste clay from marine	Planetary ball mill	5 and 30 min	650	Dry	Geo	[78]
Gold ore tailing	Planetary ball mill	40 and 80 min	-	Dry	Cement	[79]
CDW	Stirred media mill	1,3,5,10	5 m/s	Dry	Cement	[80]
Nickel-laterite mine waste	RJM-102 benchtop ball mill.	30 and 200 min	200 and 500	Dry	Geo	[81]
Blas furnace slag	Planetary ball mill	1-9 hours	50 rpm	Dry	Cement	[82]

*MA = Mechanical activation, Geo= geopolymer, rpm =rotational per minute

Utilization of mechanically activated coal gangue as a supplementary cementitious material is also well discussed in previous research [83]. Figiela et al. [84] have shown that by grinding coal gangue to a size of less than 200 μm, improved strength properties of geopolymers can be achieved while saving energy without the need to further grind the particles to a size of less than 200 μm, with the proportion of quartz being 42.5 %, muscovite 12.5 % and kaolinite 36.5 %. However, a crucial aspect of their methodology that combined mechanical grinding with a thermal treatment in a chamotte furnace at 700 °C for 24 h. Meanwhile, a study by Li et al. [85] has shown that mechanical activation with an optimum particle size of 200 mesh in coal gangue-based geopolymers and the increase in compressive strength. Zhao et al. [86], the reactivity of coal gangue was significantly enhanced by the proposed mechanical activation and thermal treatment which could be employed as primary cementitious materials. Frasson et al. [87], demonstrated that a composite activation 5 min mechanical activation as pre-grinding step followed by a substantial 24-hour thermal pre-treatment at 700 °C effectively enhanced

the reactivity of coal gangue. However, despite these promising laboratory-scale results, the reliance on prolonged high-temperature thermal treatment presents significant challenges for large-scale industrial implementation. These limitations, as highlighted by Yang et al. [16] include substantial energy consumption, the generation of considerable waste residues associated with the thermal process, and the often narrow temperature window within which the desired calcination reactions optimally occur. Consequently, while the combination of mechanical activation and thermal activation offers a route to improved coal gangue reactivity, its practical applicability is severely constrained by inherent economic and environmental sustainability concerns.

2.3.2. Grinding process parameter

Mechanical activation is usually carried out using devices depending on the type of mill, the stresses occurring during milling may include compression, shear (attrition), stroke impact and collision impact. From reported data, the geopolymer reactivity of mechanically activated materials depends on factors such as type of mill and grinding time. The different mill parameter as well as mill types lead to characteristic change of the crystal lattice of solids. The type of reaction is not only determined by type of reaction but also kind and intensity of applied mechanical energy, since the factor also determine the formation of defects mainly responsible for reactivity of powder as the phase transformation of a solid material strongly depends on the process and device utilized for that purpose [88]. A number of various types of high energy density milling equipment can be used for the mechanical activation for geopolymer application including vibratory ball mill, planetary ball mills or stirred media mill as shown in Fig 2.9.

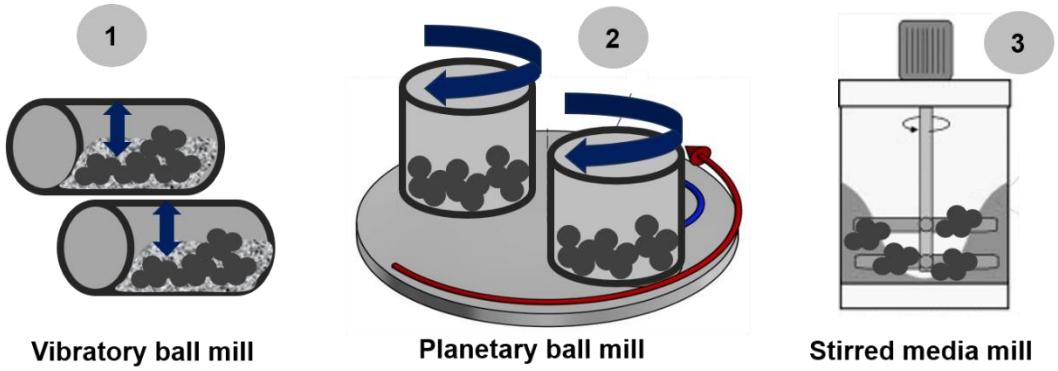

Fig 2.9: Types of high energy milling equipment: (1) vibratory ball mill (2) planetary ball mill (3) stirred media mill used to enhance reactivity of raw material

Economic benefits generally come from the good mechanical properties of the geopolymer concretes or pastes, these benefits must balance the energy consumed for milling. In practical terms, the milling needs to be carried out with the lowest possible energy consumption that gives the best outcome, as judged by the particle size reduction and crystalline structure distortion. The same mill may be operated either under continuous dynamic or batch static conditions [89]. Planetary ball mills, a widely employed mechanism in mechanical activation research, generate high dynamic energies through the differential rotation of grinding jars and balls, resulting in both significant shear and impact forces. Numerous studies have demonstrated the effectiveness of this technique in enhancing geopolymer reactivity by facilitating faster dissolution and reaction kinetics due to decreased particle sizes, increased specific surface area (SSA), the formation of a reactive amorphous layer on grain surfaces, and the introduction of structural defects through raw material disordering [90–93]. Nevertheless, despite their well-established benefits at the laboratory scale, the suitability of planetary ball mills for larger-scale industrial production is questionable, particularly regarding their ability to consistently meet the accuracy, consistency, and reliability requirements needed for continuous industrial processes, often facing challenges related to energy consumption, throughput limitations, and maintaining uniform milling quality at larger volumes. In contrast to planetary ball mills, the vibratory ball mill represents another type of mill that has found successful as continuous industrial application [94]. It has been reported that the use of high-energy vibratory mills can induce significant changes in the structure and surface properties of solid phases, such as increased defects and enhanced surface energy [95]. In this type of mill, the drum containing the balls and powder is subjected to high-frequency, low-amplitude vibrations, generating substantial milling forces to promote effective mechanical activation [96,97]. Building upon the successful industrial application of vibratory ball mills, several studies have investigated their specific impact on the mechanical activation of precursors for geopolymer synthesis. For instance, Kumar [98] demonstrated the importance of selecting the activation duration in an eccentric vibratory ball mill for fly ash, highlighting that optimal activation is material-dependent. Similarly, Chu et al. [99] found that vibratory milling of fly ash can trigger mechanochemical reactions, leading to the formation of new chemical bonds relevant for geopolymer application. Takumi Sangu et al. [100] reported that the specific surface areas of coal ash particles increased after two hours of mechanochemical treatment and surface decreased due to particle agglomeration after prolonged grinding time of four and six hours. Recent studies on mechanical activation that employ grinding times ranging from 1 to 240 min, exploring their efficacy and implications in enhancing reactivity and material

properties. Nana et al. reported where despite a reduction in specific surface area after 90 min of pegmatite grinding in an eccentric vibratory ball mill, compressive strength continued to increase. Recent studies on mechanical activation employ grinding times ranging from 1 to 240 min exploring their efficacy and implications in enhancing reactivity and material properties. For example, Nana et al. [101], reported that despite a reduction in specific surface area after 90 min of pegmatite grinding in an eccentric vibratory ball mill, the geopolymer compressive strength continued to increase. Niu et al. [102], mechanical activation phlogopite mica mining tailing via vibratory ball mill for geopolymer between 1-16 min grinding time show altered minerology, enhanced alkaline reactivity and larger specific surface are. Souri et al. [103] in previous results showed that the increased specific surface area of the mechanochemically kaolin enhanced the early age hydration speed and the strength development of blended cements. Wang et al. [91] have studied the effect of mechanically activated kaolin combination with the calcination method for geopolymer. The specific surface area of powder and compressive strength geopolymer increases according to grinding time. A similar result was reported by Kumar and Kumar [104]. Meanwhile Gao et al. [105] investigated the different reactivity of fly ash in terms of specific surface area in geopolymer and found that a higher specific surface area 476.5 m^2/g does not contribute to higher compressive strength. It is undeniable, although milling plays a crucial role in the production of coal gangue as precursors, it should be highlighted that a prolonged milling time may significantly reduce the economic and environmental benefits of recycling coal gangue in geopolymer production. Many studied have investigated the mechanical activation of coal gangue as shown in Table 2.2.

Table 2.2. A comparison mechanical activation (MA) coal gangue

Main raw material	MA	Grinding time	Rpm/grinding media size d_{GM}	Method	Application	Ref
Coal gangue	Ball milling	0.5,1, 1.5 hours	400 rpm/1,2,4 mm	dry	-	[106]
Coal gangue	Drum tank	18 and 8 hours	450 rpm/8-25 mm	dry/wet	cement	[107]
Coal gangue + lime	Laboratory grinder	-	600 rpm/-	dry	geopolymer	[108]
Coal gangue	Vertical stirred mill	0,30,60,120 min	450 rpm/2-10 mm	wet	cement	[109]
Coal gangue	Planetary ball mill	2,10,20 hours	400 rpm/-	dry	geopolymer	[110]
Coal gangue + red mud	Planetary ball mill	5 min	-	dry	geopolymer	[111]

Furthermore, prior to using a starting material as a geopolymer, it seems essential that this optimum fineness should be determined to avoid potential adverse effects of over-grinding. Balczár et al. [112] point out in their study of kaolin for geopolymer mortar that the maximum compressive strength decreases slightly after 240 min of grinding due to possible agglomeration with an amorphous content of 60 %. This trend is consistent with the findings of Szabó et al. [76], who reported similar fluctuations in compressive strength during the mechanical activation of perlite, where variations were closely linked to changes in the geometric surface area (cm^2/g) due to agglomeration. Although grinding plays a crucial role in improving the reactivity of coal gangue as precursors, prolonged grinding time may significantly diminish the economic and environmental benefits of recycling coal gangue for geopolymer production. Therefore, increased grinding kinetics may lead to a more efficient process. The efficiency of the grinding process depends on several parameters, such as grinding time, grinding media size, and grinding speed (Hz or rpm). Optimising these parameters is crucial for achieving higher reactivity rates of the raw material within shorter processing times. While the literature predominantly focuses on longer grinding or activation durations for coal gangue [106] [107] [108]. For example, Tole et al. [113] investigated the process parameters of clay for cementitious properties between 400 and 600 rpm and grinding times of 15 to 60 minutes, and found that 600 rpm produced a high degree of amorphous content. Previous work by Balczár et al. [112], using mechanochemical activation of kaolinite (500 rpm rotation speed and 75 min grinding time), showed that a compressive strength of 44.5 MPa can be achieved, which is comparable to the result (43.0 MPa) obtained by thermal activation (700 °C and 1 hour heat treatment) of geopolymer mortar. The most important parameters controlling the reactivity of raw material process are the rate of stress and the efficiency of the energy transfer in the mill. Several collisions occur in a ball mill within the specified milling time. Each collision transfers energy to the total mass of the treated powder. The transferred energy and number of collisions are directly dependent on the number and mass of the used balls. The evaluation of the specific grinding energy of the mechanical treatment can be defined by the following eq. (6)

$$E_m \left[\frac{\mathrm{J}}{\mathrm{g}}\right] = \int_0^t \frac{(P - P_o)}{m}\, dt \tag{6}$$

According to industrial data, the energy required for the calcination or thermal treatment of kaolinite is approximately 1600 kWh/t. Mechanical activation was found to have the required energy for the mechanical treatment of kaolinite, is expected to be in the range of 200-

1000 kWh/t [103]. The data obtained by Mucsi et al. [114] revealed a relationship between grinding operating parameters (specific grinding energy) and material characteristics for fly ash such as phase change.

2.3.3. Reactivity of mechanically activated raw material

Optimizing the properties of raw materials through mechanical grinding stands as a pivotal step in enhancing the performance of geopolymers. It has been found that mechanical activation leads to structural changes accompanies higher specific surface area that led to more reactive sites [115,116]. A higher specific surface area provides a greater interfacial area for the alkaline activator to interact with the precursor material, thereby accelerating the leaching of Si and Al and fostering the formation of the aluminosilicate gel network. During mechanical activation, the mechanism induces two primary mechanistic effects, as conceptualized by as Juhász and Opoczky [117] shown in Fig 2.10, how mechanical activation effect on particle is primary involved mechanical dispersion (size reduction) and surface activation [117,118].

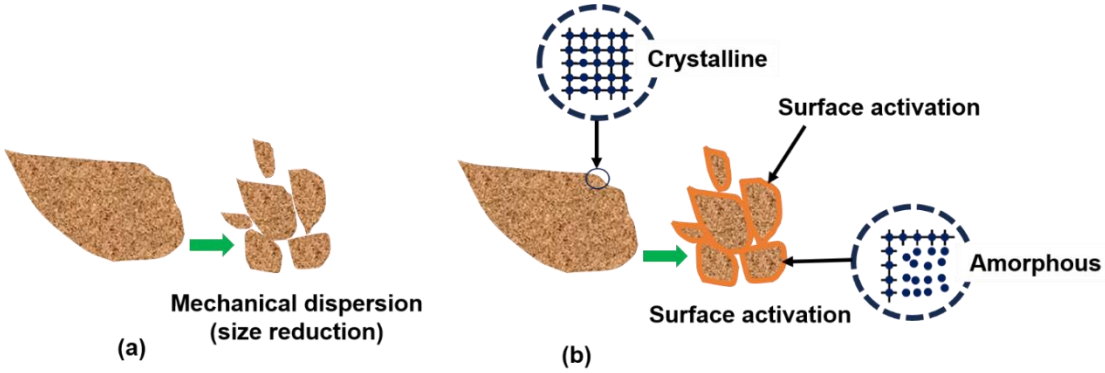

Fig 2.10: Schematic various states of mechanical activation: (a) mechanical dispersion, (b) surface activation

Research by Temuujin [119] and others indicates that mechanical activation of fly ash can reduce particle size, alter its morphology, and enhance its reactivity when used to prepare geopolymer cement. The resulting geopolymer material showed an 80 % increase in strength compared to geopolymer made from non-mechanically activated fly ash. Kumar [104] study further suggests that mechanical activation significantly improves the reactivity of fly ash, as its activity is directly proportional to its particle size. When the particle size of fly ash is less than 5 - 7 µm, it has sufficient reactivity for polymerization reactions to occur at room temperature. At ambient temperature, the rate of geological polymerization is very slow. The use of ultrafine metakaolin with smaller particle sizes will also increase the reactivity of the

geopolymer [120]. Other researchers have investigated the effects of mechanical grinding to elucidate the surface modifications induced by through various instrumental techniques such as XRD, Fourier Transform Infrared Spectroscopy (FT-IR), pozzolanic reactivity, leaching test, and physical properties. For example, Cristelo et al. [121] observed changes in fly ash powder during mechanical activation. Their study, which used a ceramic bowl at 300 rpm for 15 - 240 min, noted a darkening of the fly ash after 240 min. This colour change was attributed to the physical alteration of unburned carbon (coal) content, which became more prominent after different milling time as shown Fig 2.11.

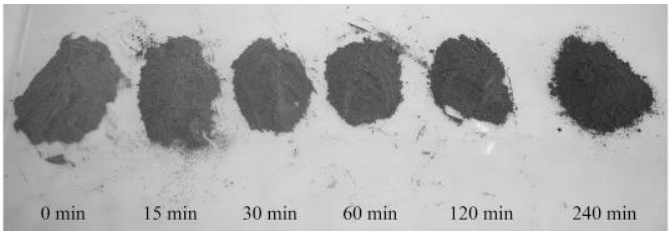

Fig 2.11: General view of the fly ash after different milling time

FT-IR method offers the capability to probe alterations in the vibrational modes of surface functional groups, the potential formation of new chemical bonds, and shifts in the structural arrangement of the precursor material with grinding time. In previous study, Frost et al. [122] reported on clay minerals that were ground for 1-10 hours. In their study, the band at 1103 cm^{-1} shifted to lower wavenumbers, indicating lattice distortion in kaolinite, while the bands at 1034 cm^{-1} and 1056 cm^{-1} shifted to higher wavenumbers due to the removal of hydroxyl groups and the onset of amorphization. In a study by Guo et al [123] it was reported that the Si-O-T peaks shifted from 1033 cm^{-1} to 1095 cm^{-1} after grinding gangue in a planetary ball mill for 20 hours. Likewise, Tan et al. [124] explained that the main Si-O-T asymmetric stretching bond vibrations, initially cantered at around 1028 cm^{-1} in raw construction demolition waste, shifted to a higher wavenumber of 1036 cm^{-1} and became broader after 4 hours of milling. In the study by Yankwa Djobo et al. [125] investigated the mechanical activation of volcanic ash in an eccentric vibratory ball mill for 120 min. Due to the glassy nature of the raw material, the Si-O-T wavenumber shifted from 1006 cm^{-1} to 1057 cm^{-1}. A reported by Rescic et al. [126], who found that the concentration of silica (Si) extracted from kaolin for geopolymer applications decreased after 40 minutes of grinding in a planetary ball mill at 720 rpm. However, the study did not explicitly attribute this decline to aggregation or agglomeration. Additionally, previous studies [127],[128] have consistently reported that silica (Si) and alumina (Al) leaching generally increases with grinding time.

3. MATERIAL AND METHODS

3.1. Raw material and properties

Coal gangue, the primary material for these experiments, was sourced from the Bükkábrány coal mine in Hungary. During the initial exploratory phase of this study, three representative samples were collected from this single mining site. The purpose of analysing these initial samples was to conduct a preliminary characterization of the coal gangue properties before subjecting it to further mechanical activation processes. Additionally, a characterization was performed to assess the coal gangue suitability as a geopolymer precursor. The step-by-step methodological framework of this study is illustrated in the schematic outline in Fig 3.1.

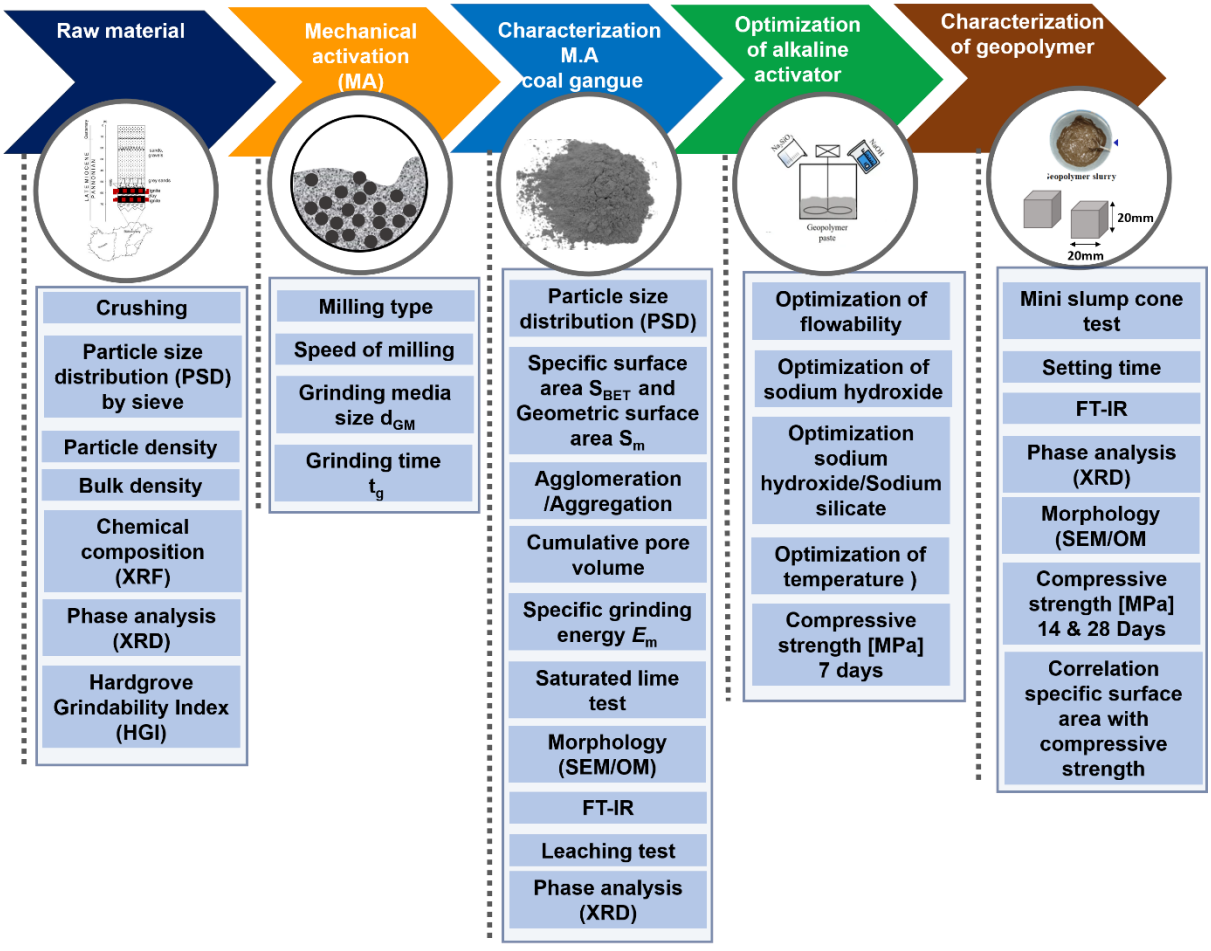

Fig 3.1: Schematic outlining the study methodological approach.

As a next step in the sample preparation, the collected coal gangue samples underwent a drying process in an oven at 105 °C for 24 hours until a constant mass was recorded, ensuring the removal of any free water. Initially, the particle size distribution of the raw coal gangue was

determined through sieving, and the results are depicted in Fig 3.2. The characteristic x_{10} value for particle size ranged from 0.078 to 0.079 mm across the different coal gangue samples. The median particle size x_{50} showed a wider range of values, from 1.262 to 1.849 mm, as shown in Table 3.1.

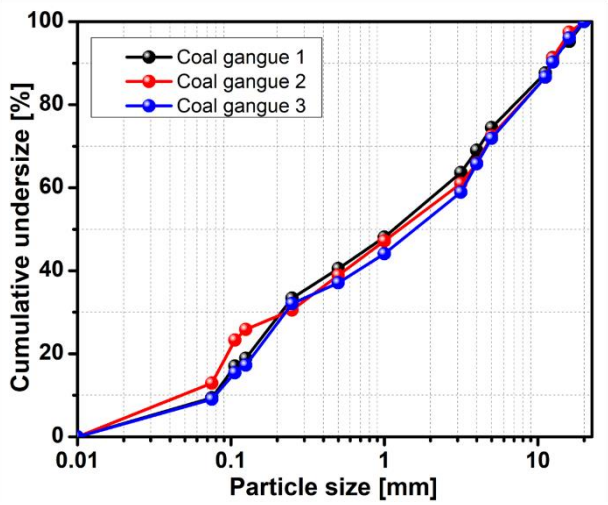

Fig 3.2: Raw material of coal gangue

Table 3.1: Characteristic particle size of raw material after crushing

Coal gangue	**x_{10} (mm)**	**x_{50} (mm)**	**x_{90} (mm)**
Coal gangue 1	0.078	1.262	12.029
Coal gangue 2	0.066	1.435	12.147
Coal gangue 3	0.079	1.152	12.397

As an initial step, the coal gangue sample was crushed using a hammer crusher for quantitative sample preparation to approach required particle size. This preliminary crushing was performed to reduce the size of the raw coal gangue, which was deemed too large for direct analysis of particle density and for chemical composition. Furthermore, to ensure effective mechanical activation, the median particle x_{50} size was targeted to be less than 1000 μm for further investigations. The particle density of the crushed coal gangue was then determined using the pycnometer method, with alcohol as the liquid medium, following eq. (1). The bulk density was also subsequently measured. The results for moisture content, bulk density, and particle density of the raw coal gangue after crushing are summarized in Table 3.2.

$$\rho\ \text{Particle} = \frac{M_2 - M_1}{(M_4 - M_3) + (M_2 - M_1)}\ \text{x}\ \rho\ \text{Alcohol}\ (0.79 \frac{g}{cm^3}) \qquad (1)$$

M_1 = Measure the clean empty pycnometer

M_2 = The mass of the pycnometer, now containing the coal gangue and sealed with its cap, was measured

M_3 = Alcohol was then carefully added to the pycnometer containing the material. The mass of the pycnometer, including the material, alcohol, and cap, was measured

M_4 = The mass of the pycnometer, now filled solely with alcohol, was measured

Table 3.2: Coal gangue characterization

Type of coal gangue	Moisture content (%)	Particle density (g/cm^3)	Bulk density (g/cm^3)
Coal gangue 1	1.37	2.28	0.73
Coal gangue 2	0.94	2.62	0.89
Coal gangue 3	1.09	2.26	1.16

Chemical composition analysis of all coal gangue samples revealed a substantial combined content of SiO_2, Al_2O_3, and Fe_2O_3, ranging from 84.03 % to 89.33 %, as detailed in Table 3.3. This determined value significantly exceeded the minimum requirement of 70 wt% stipulated by ASTM C618 for Class N pozzolans. Trace elements were also detected, including Cu (36 ppm), Zn (127 ppm), Pb (12 ppm), Rb (118 ppm), Sr (102 ppm), Ba (526 ppm), As (12 ppm), Cr (100 ppm), Ni (52 ppm), and Zr (244 ppm). The concentrations of these metals were found to be much smaller than permissible [129]. Consequently, based on the criteria outlined in ASTM C618 [130], the investigated coal gangue samples were determined to possess pozzolanic activity and certain cementitious characteristics. In addition to their favourable oxide composition, all coal gangue samples exhibited relatively low loss on ignition (LOI) values, which ranged from 4.5 % to 7.9 %. These measurements fell well below the maximum allowable limit of 10 % as outlined in ASTM C618 standards. Loss on ignition was identified as a critical parameter in assessing the geopolymerization potential of the samples, as research indicates that the presence of unburned carbon in such materials can significantly impact performance by absorbing the activator solution during the geopolymerization process [131]. The phase analysis of the coal gangue samples (1-3) indicated that the primary mineral components were kaolinite 1:1 clay mineral and illite 2:1 clay mineral, with quartz being the dominant mineral phase. Based on the phase analysis presented in Table 3.4, the amorphous content was determined to be less than 20 %.

Table 3.3: Chemical composition of raw coal gangue

Component	Coal gangue 1	Coal gangue 2	Coal gangue 3
SiO_2	59.2	61.1	72.1
Al_2O_3	20.8	17.8	13.4
MgO	2.30	1.92	1.07
CaO	0.68	0.67	0.65
Na_2O	0.55	0.69	0.86
K_2O	3.50	2.99	2.20
Fe_2O_3	7.08	5.67	4.33
MnO	0.127	0.104	0.123
TiO_2	1.076	0.959	0.624
P_2O_5	0.093	0.103	0.084
S	0.14	0.13	0.02
F	<0.3	<0.3	<0.3
Total	95.5	92.1	95.5
$SiO_2 + Al_2O_3 + Fe_2O_3$	87.08	84.57	89.33
LOI	4.5	7.9	4.5

Table 3.4: Phase analysis of raw coal gangue

Type of minerals	Coal gangue 1 wt%	Coal gangue 2 wt%	Coal gangue 3 wt%
Kaolinite	6.2	4.5	6.3
Illite	22.5	16.2	12.6
Quartz	30.7	45.2	56.3
Muscovite	14.1	9.6	5.6
Albite	4.5	5.7	6.1
Microcline	2.8	2.6	2.1
Amorphous	**16.3**	**13.8**	**8.8**

For characterization of the grindability, 3 samples of 50 g coal gangue were used for Hardgrove Grindability Index (HGI) and calculated Bond - Work Index. HGI measurement as eq. (2)

$$HGI = 13 + 6.9\, m_{75} \tag{2}$$

where:

HGI – Hardgrove Grindability Index,

m_{75} – mass of the product which below 75 μm (g).

Using the result of HGI the Bond – Work Index can be calculated by eq. (3) which is the Csőke [132] empirical formula:

$$W_{I,B}^{H} = \frac{468}{HGI^{0.82}} \tag{3}$$

The grindability of the coal gangue samples was characterized using the Hardgrove Grindability Index (HGI), and the results were presented in Table 3.5. The determined HGI values exhibited a significant range, from 91 to 237. It is crucial to note that a lower HGI value signifies a greater resistance to grinding, implying that coal gangue with a lower HGI is harder and would necessitate a considerably higher energy input to achieve the desired level of fineness. Specifically, coal gangue 3, with its notably low HGI of 91.309 indicated a particularly challenging material to grind. This challenge can be primarily attributed to its chemical composition, which features a dominant SiO_2 content (71.2 wt %) and a high quartz content (56.3 %) identified via phase analysis. Considering the impracticality and energy intensity and amorphous content, no additional mechanical activation steps were undertaken to modify the properties of coal gangue 3. As mentioned above, since the physical and chemical properties of coal gangue from different location vary, this research preliminarily focused only the coal gangue 1 and 2 as precursor material.

Table 3.5: Hardgrove grindability index (HGI)

Type of coal gangue	**Hardgrove Grindability Index [-]**	**HGI derived bond-Work Index [kWh/t]**
Coal gangue 1	217.851	5.732
Coal gangue 2	222.721	5.520
Coal gangue 3	91.309	11.542

3.2. Geopolymerization of raw coal gangue and test procedures

The raw coal gangue was investigated to optimize the alkaline solution. The optimization of the alkaline activator in this study is schematically represented in Fig 3.3. The alkaline solution used in the geopolymerization process was a combination of sodium hydroxide (NaOH) and sodium silicate (Na_2SiO_3). The molarity of the alkaline activator was crucial for establishing the environment necessary for the dissolution of aluminium (Al) and silicon (Si) species. For the alkaline solution, laboratory-grade sodium hydroxide (NaOH) and sodium silicate were used as activators. An 8 – 14 M (NaOH) solution was prepared by dissolving sodium hydroxide pellets in double-distilled water. The sodium silicate solution used in this stage had a composition of Na_2O (14.2 %), SiO_2 (31.12 %), and H_2O (54.68 %) by mass.

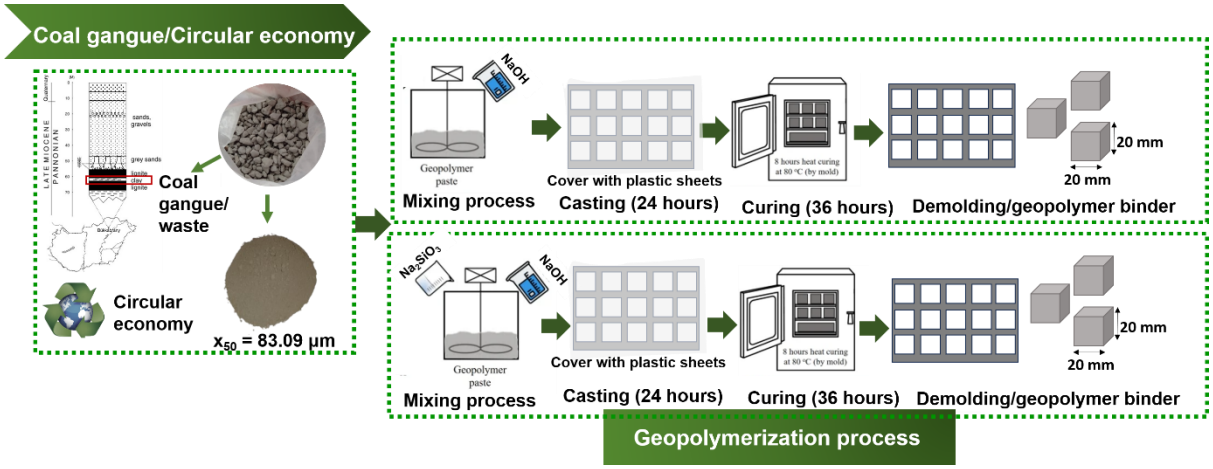

Fig 3.3: A systematic preliminary of geopolymerization of raw coal gangue

Firstly, the raw material with a median particle size x_{50} of 83.09 µm was used without mechanical activation. The geopolymer samples, with a liquid-to-solid (L/S) ratio ranging from 0.63 to 0.80, were prepared and tested for 7 days compressive strength and flowability. Next, after optimizing the liquid-to-solid ratio, initial mixtures excluded sodium silicate to allow for a focused investigation of the effects of NaOH concentration on the geopolymerization process, as detailed in Table 3.6. Following the selection of the optimized NaOH concentration, the next step involved incorporating sodium silicate (Na_2SiO_3) solution into the mixture. To ensure a homogeneous geopolymer paste, the coal gangue and alkaline solution were thoroughly mixed using a mechanical mixer for five minutes. The geopolymer paste was placed into pre-oiled 20 mm × 20 mm × 20 mm plastic molds, followed by compaction via vibration to remove any entrapped air and ensure a uniform density. To prevent premature drying and moisture loss, the samples were immediately covered with plastic sheets and left to cure at ambient room temperature (20 ± 1 °C) for the first 24 hours. Following this initial stage, the final curing was performed in a drying oven at a different temperature for 36 hours. After this period, the samples were allowed to cool naturally to room temperature before being carefully demoulded. The samples of geopolymer were then stored until they were tested for compressive strength at 7 days.

Table 3.6: Mixture compositions and sample numbers

Median particle size x_{50}	Curing time	Compressive strength
83.09 μm	36 hours	7 days

Samples	Coal gangue (g)	NaOH (g)	NaOH (mol/L)	Na_2SiO_3 (L)	L/S
Liquid-to-solid ratio (L/S)					
0.80	33.33	26.67	8	0	0.80
0.67	35.92	24.08	8	0	0.67
0.63	36.81	23.19	8	0	0.63
Sodium hydroxide (NaOH)					
8 M	36.81	23.19	8	0	0.63
10 M	36.81	23.19	10	0	0.63
12 M	36.81	23.19	12	0	0.63
14 M	36.81	23.19	14	0	0.63
Sodium hydroxide (NaOH): Sodium silicate (Na_2SiO_3)					
NH100:SS0	36.81	23.19	8	0	0.63
NH75:SS25	36.81	17.4	8	5.79	0.63
NH50:SS50	36.81	16.2	8	16.2	0.63
NH25:SS75	36.81	5.79	8	17.4	0.63
NH0:SS100	36.81	0	8	23.19	0.63
Drying temperature °C					
60	36.81	5.79	8	17.4	0.63
70	36.81	5.79	8	17.4	0.63
80	36.81	5.79	8	17.4	0.63

3.3. Mechanical activation and geopolymerization

3.3.1. Mechanical activation in vibratory ball mill

Mechanical activation was achieved using a vibratory ball mill operating in parallel mode under dry grinding conditions, as depicted in Fig 3.4. The mill was equipped with two 1000 mL steel bowls; each charged with 2542.5 g of 15 mm diameter steel grinding media. Detailed process parameters are provided in Table 3.7. The grinding media filling ratio was maintained at 70% (v/v), while the material filling ratio relative to the media pore volume was set at 110% (v/v), based on optimized conditions according to the methodology used previous works by Musci et al. [114]. The electrical power consumption was cumulatively recorded using a digital energy meter, enabling the calculation of the specific grinding energy based on the difference between the initial and final meter readings.

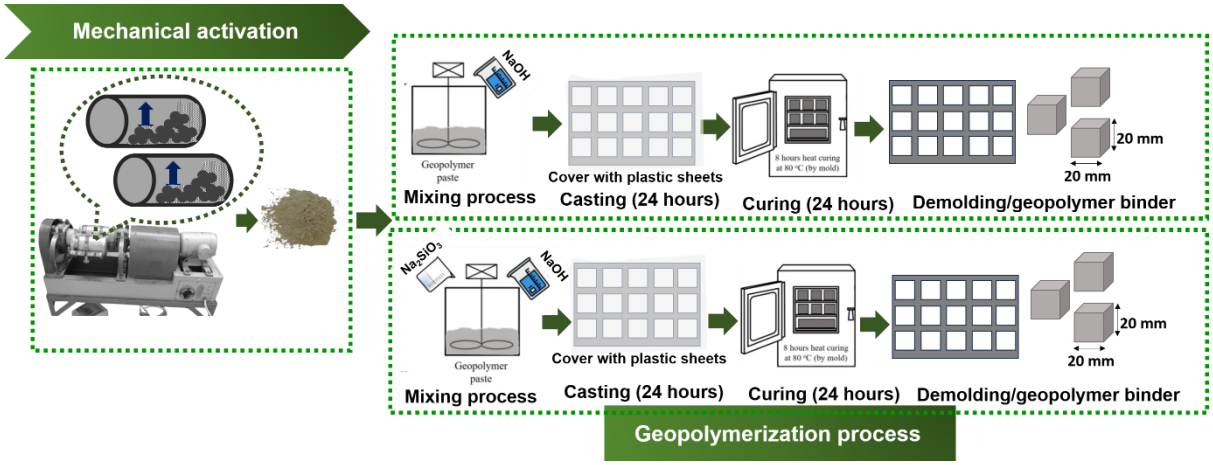

Fig 3.4: Schematic diagram of M.A coal gangue in vibratory ball mill for geopolymerization

Table 3.7: Investigated parameters of mechanical activation

Parameters	Value	Unit
Frequency	50	Hz
Volume of grinding chamber V_{GC}	1000	mL
Grinding media size (steel) d_{GM}	15	mm
Density grinding media d_{GM} = 15 mm, ρ_{GM}	7.87	g/cm^3
Grinding time	1, 5, 10, 15, 30, 60, 120	min

3.3.2. Mechanical activation in planetary ball mill

The schematic diagram for the mechanical activation of coal gangue in a planetary ball mill for geopolymer applications was illustrated in Fig 3.5. A material to ball ratio of 1:10 was

maintained, following the manufacturer technical data. Grinding was performed at 450, 600, 650, and 700 rpm for durations of 1, 5, 10, 15, 30, 60, and 120 min, as shown in Table 3.8. To mitigate the high temperatures generated by long-term grinding, the operation was paused after every 20 min for a 20 min cooling period.

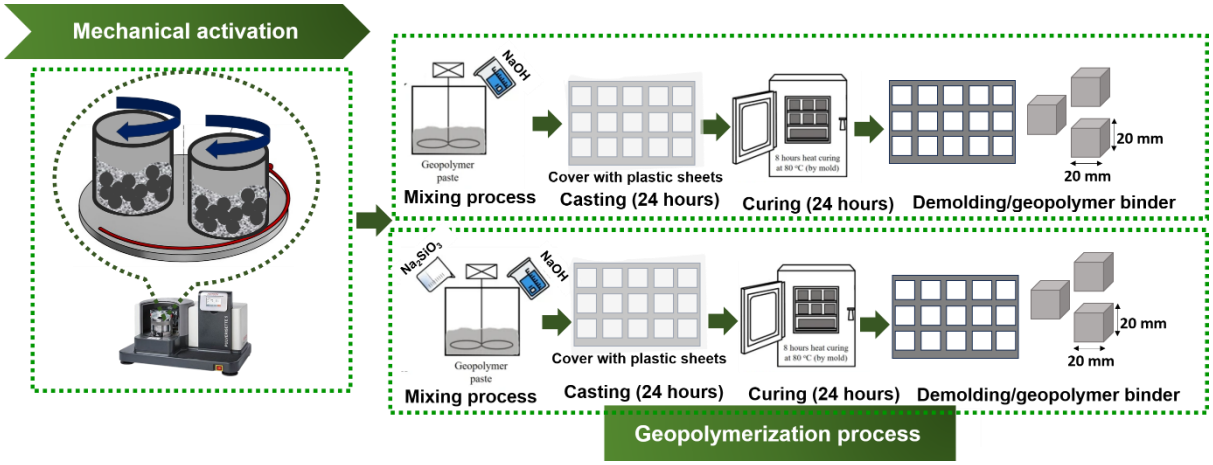

Fig 3.5: Schematic diagram of M.A process coal gangue in planetary ball mill

Table 3.8: Investigated process parameters

Parameters	**Value**	**Unit**
Rotational speed	450, 600, 650, 700	rpm
Grinding media size (steel) d_{GM}	5, 10	mm
Density grinding media d_{GM} = 5 mm, ρ_{GM}	0.956	g/cm^3
Density grinding media d_{GM} = 10 mm, ρ_{GM}	1.332	g/cm^3
Grinding media filling ratio φ_{GM}	2.662, 2.773	-
Grinding media size (steel) d_{GM}	5, 10	mm

3.3.2.1. Stressing conditions

The specific grinding energy E_m was determined according to Burmeister et al. [133], who established the relationship between the stress energy *SE* and the grinding media size d_{GM}, rotational speed rpm, and filling ratio. These parameters were modelled with the discrete element method using the software package EDEM 2.5 for a planetary ball mill. The stress energy was given by eq. (4). The calculated collision frequency *CF*, as a function of the process parameters, was given by eq. (5). The constants c1 and c2, which were unknown in this case and therefore neglected, accounted for factors such as the friction generated by the product. This calculation was based on the assumption that the stress energy was proportional to the kinetic energy of the grinding media transferred per collision. The material-related stressing was described by the stressing intensity *SI*, which considered the active mass (m_A) captured

between colliding media and, therefore, received the dissipated energy. This approach assumed that stress energy was proportional to the kinetic energy transferred per collision. The stressing intensity *SI*, given by eq. (6), further characterized the material stressing by considering the active mass (m_A) captured between colliding media and thus receiving the dissipated energy.

$$\overline{SE} = c1.n_{SUN}^{2.67}.\ d_{GM}^{3.85}.\varphi_{GM}^{0.5} \quad (4)$$

$$CF = c2.n_{SUN}^{0.42}.\ d_{GM}^{-3.93}.\varphi_{GM}^{1.18} \quad (5)$$

$$SI = \frac{SE}{M_A} \quad (6)$$

The power consumption (P) of a planetary ball mill was the sum of the stress energy and collision frequency, as shown in eq. (7). The specific grinding energy E_m was dependent on power and grinding time, as seen in eq. (8). To calculate Po, the grinding media and grinding media filling ratio were neglected.

$$P = \overline{SE}.CF = \text{kJ} \quad (7)$$

$$E_m = \frac{\int(P - P_O)}{m_{feed}}.\ t_g = \text{kJ g}^{-1} \quad (8)$$

3.3.3. Geopolymerization of mechanically activated coal gangue

The mechanically activated coal gangue was investigated for the optimization of an alkaline solution. For geopolymer preparation, the process followed a methodology similar to that previously discussed in **Section 3.2**. However, the study adjusted the liquid-to-solid (l/s) ratio to a range of 0.87-1.0 and utilized a finer median particle size as detail in Table 3.9. The molarity of the alkaline solution was also varied between 8 - 12 M. To optimize the liquid-to-solid ratio, the molarity of the sodium hydroxide (NaOH) solution, and the ratio of sodium hydroxide to sodium silicate (Na_2SiO_3) solution, the compressive strength was tested after 7 days. Once the systematic approach was established, the compressive strength was further tested for durations of 14 and 28 days for all samples of mechanically activated coal gangue and three replicate samples were tested to ensure statistical reliability

Table 3.9: Mixture compositions and sample numbers

Parameter	Unit
Raw material	x_{50} = 83.09 μm
Vibratory ball mill	x_{50} = 6.56 μm
Planetary ball mill	x_{50} = 6.17 μm
Vibratory ball mill, liquid-to-solid ratio (L/S)	0.87
Planetary ball mill, liquid-to-solid ratio (L/S)	1.0
Sodium hydroxide (NaOH)	8, 10, 12 M
Sodium hydroxide (NaOH): Sodium silicate (Na_2SiO_3)	100:0, 75:25, 50:50, 25:75
Drying temperature °C	60, 70, 80
Curing time	24 hours
Compressive strength (optimization)	7 days
Compressive strength	14, 28 days

3.4. Test procedures

3.4.1. Particle size distribution and geometric surface area of coal gangue powder

The particle size distribution (PSD) of both the raw and mechanically activated coal gangue was determined using a HORIBA LA-950V2 laser particle size analyser and deionized water (H_2O) served as the dispersion medium. The PSD was estimated from the measured data using Fraunhofer's approximate method. The geometric surface area, a parameter related to the external or relative surface area, was obtained by software-based calculation from the PSD data, assuming a spherical particle surface S_m [134]. To evaluate the potential for particle aggregation or agglomeration, selected samples were tested with sodium pyrophosphate ($Na_4P_2O_7$) as a dispersing medium. This specific test was performed on samples ground for 60 and 120 min.

3.4.2. Morphology of coal gangue powder and geopolymer samples

Powder coal gangue and geopolymer samples morphology was assessed via scanning electron microscopy (SEM) using a JEOL JCM-7000NeoScope™ Benchtop. Secondary electron (SE) imaging was performed at an accelerating voltage of 30 kV. Samples were sputter-coated with a gold layer to facilitate electron conduction and improve signal detection.

3.4.3. Specific surface area of coal gangue powder

For the measurement of the total specific surface area S_{BET}, Tristar 3000 from Micrometrics Corporation was used. Before each measurement, the sample was degassed. From the adsorbed gas, the surface area of the particle is determined. The BET (Brunauer, Emmett, and Teller) method is used to determine the specific surface area of the particles including meso- and

micropores. To degas the powder, the samples were dried at 90 °C for 30 min and additionally at 300 °C for 180 min in flowing nitrogen gas in the Micrometrics Smart prep before the adsorption measurements were taken. The gas used for adsorption was nitrogen, and the adsorption temperature were 190 °C. The complete adsorption isotherms were recorded. The specific surface area was calculated by a five-point BET method. The weight of each sample was approximately 1 g.

3.4.4. Saturated lime test of coal gangue powder

The saturated lime test was conducted to assess the pozzolanic reactivity of both raw and mechanically activated coal gangue. For each material, 2 g was placed into separate plastic bottle containers, followed by the addition of 100 mL of a saturated lime solution $Ca(OH)_2$. The containers were then sealed and thoroughly shaken. To ensure continuous interaction, the containers were manually shaken once daily. At 2-day intervals, a 50 mL of the solution was extracted for titration with a 0.05 mol/L hydrochloric acid solution, using methylene orange as an indicator. Immediately after each sampling, 50 mL of fresh saturated lime solution was added back to the respective plastic container to maintain a consistent. Based on the titration results, the amount of CaO uptake by the 2 g of each material was subsequently calculated to evaluate its pozzolanic activity.

3.4.5. Alkaline leaching test of coal gangue powder

The reactivity of both raw and mechanically activated coal gangue was evaluated by quantifying the release of alumina (Al) and silica (Si) during leaching in 8 M sodium hydroxide (NaOH) solution. Specifically, one gram of each material was stirred at 400 rpm in 40 mL of the NaOH solution, maintained at a temperature of 60 °C for a duration of 2 hours. Following leaching, the resulting suspensions were subjected to centrifugation at 5000 rpm for 3 min and subsequently acidified using 37 % HCl. The concentrations of the leached Al and Si were then determined using microwave plasma atomic emission spectrometry (MP-AES).

3.4.6. Phase composition analysis of coal gangue powder

The crystalline phases of both raw and mechanically activated coal gangue samples were identified using X-ray diffraction (XRD) with a Rigaku Mini flex II diffractometer with CuKα radiation and a monochromator, scanned at 1°/min and matched against the ICDD database.

3.4.7. Fourier transform-infrared spectroscopy (FT-IR)

The vibrational characteristics of molecular structure (stretching and bending) in the raw, mechanically activated coal gangue and geopolymer samples were determined by Fourier transform - infrared spectroscopy (FT-IR) using a JASCO FTIR 4200 system equipped with a diamond ATR for reflection measurements. To ensure reproducibility, three parallel measurements were carried out for each sample with each spectrum were recorded in the absorbance range of 4000 - 400 cm^{-1} at a resolution of 4 cm^{-1}.

3.4.8. Mini slump cone test geopolymer paste

A mini-cone mould made of poly(tetrafluoroethylene) was selected to assess slump according to liquid to solid ratio (L/S). The mini-slump test setup used in this study was a downscaled cone with the following geometry: a 19 mm top diameter, a 38 mm bottom diameter, and a 57 mm height, as illustrated in **Fig.3.6**. Before the test, the interior surface of the mould was lubricated with mould oil. The fresh mixture was then agitated ten times using a glass stick. The excess material was slowly scraped off with a trowel, and the cone was lifted as slowly as possible. After one minute, the spread diameter was measured in two perpendicular directions. Three repetitions were conducted.

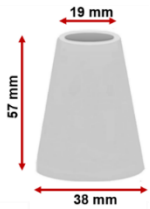

Fig.3.6: Mini slump cone mould

3.4.9. Optical microscopic of geopolymer samples

Optical microscopy using a Carl Zeiss Primo Star Light Microscope was employed to investigate the microstructure of coal gangue geopolymer samples.

3.4.10. Setting time of geopolymer paste

The setting time of the fresh geopolymer paste was determined in accordance with ASTM C191 [135]. The initial setting time was identified using a Vicat apparatus, where a penetration depth of 25 mm was taken as the benchmark. The penetration depth was recorded over time for geopolymer pastes produced with mechanically activated coal gangue that was subjected to varying grinding times. The results were then plotted to illustrate the relationship between penetration depth and grinding time.

3.4.11. Compressive strength

The compressive strength of the 20 mm x 20 mm x 20 mm hardened geopolymer samples was evaluated at the ages of 7 days. A Controls Automax5 universal testing machine was used to apply a compressive load, with a consistent loading rate applied to all specimens. For each testing age, three replicate samples were tested to ensure statistical reliability. The maximum load at failure for each sample was recorded and subsequently divided by the specimen cross-sectional area to calculate the compressive strength. The average compressive strength for each testing age was determined from the three replicate tests, and the standard deviation was calculated to represent the dispersion of the data.

4. RESULTS AND DISCUSSION

4.1. Preliminary investigation of raw coal gangue, grinding parameter and geopolymerization

4.1.1 Preliminary investigation of coal gangue properties

Coal gangue can be utilized as a source material for producing geopolymer because the geopolymerization process is fundamentally based on an aluminosilicate chain. In this study, coal gangue 2 was used across all experimental results. The median particle size x_{50} of the raw coal gangue was 83.09 µm, which is consistent with the cumulative undersize curves shown in Fig 4.1(a). This raw coal gangue had a corresponding specific surface area S_{BET} of 6.69 m^2/g and geometric surface area of 1738 cm^2/g. Furthermore, its morphology, shown in Fig 4.1(b), was composed exclusively of coarser and irregular particles. The phase analysis of the raw coal gangue exhibits a complex crystalline structure with distinct peaks associated with kaolinite, microcline, and albite, as seen in Fig 4.1(c).

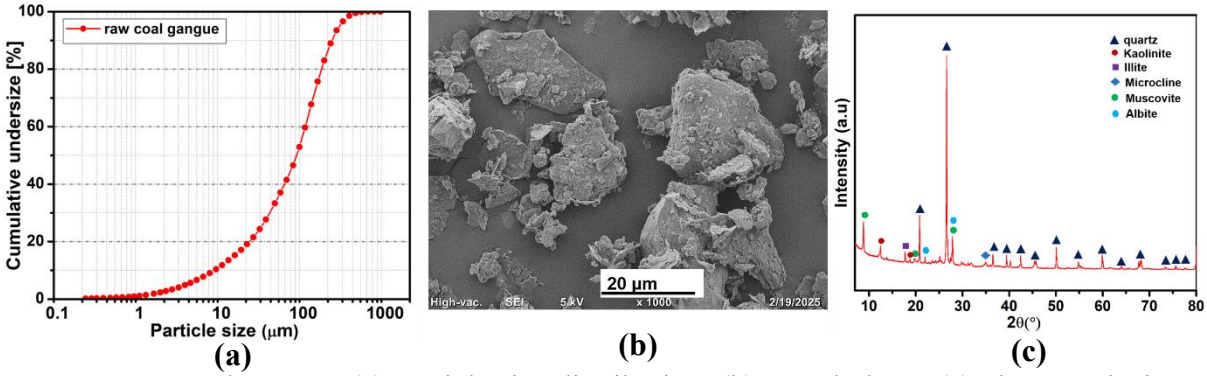

(a) (b) (c)

Fig 4.1: Raw coal gangue, (a) particle size distribution, (b) morphology, (c) phase analysis

4.1.2 Preliminary investigation of grinding process

A systematic preliminary mechanical activation was designed and conducted to achieve an optimal particle size distribution and high specific surface area, a critical factor for enhancing the reactivity of coal gangue. A planetary ball mill was used to determine precisely the most effective grinding media size for maximising the geometric surface area (S_m). Three grinding media sizes (10, 20, and 30 mm) were tested, consistently maintaining a grinding time of 5 min and 450 revolutions per minute (rpm), to investigate specifically the effect of grinding media size. The resulting cumulative undersize was analysed via laser particle size distribution, as illustrated in Fig 4.2(a). A comparative analysis of the results presented in Table 4.1 clearly demonstrates that the smallest grinding media size, 10 mm, yielded the most significant increase in geometric surface area. After determining the optimal grinding media size, the

effect of rotational speed on the mechanical activation of coal gangue was systematically studied. Three revolutions per minute (300, 325, 400 and 450 rpm) were used, while the grinding time was kept constant at 5 min and the optimal 10 mm grinding media was employed. Fig 4.2(b) and Table 4.1 reveal a direct relationship, the highest rotational speed resulted in a greater increase in geometric surface area. Specifically, 450 rpm speed produced the most significant increase in specific surface area, highlighting the importance of this parameter for optimizing mechanical activation processes.

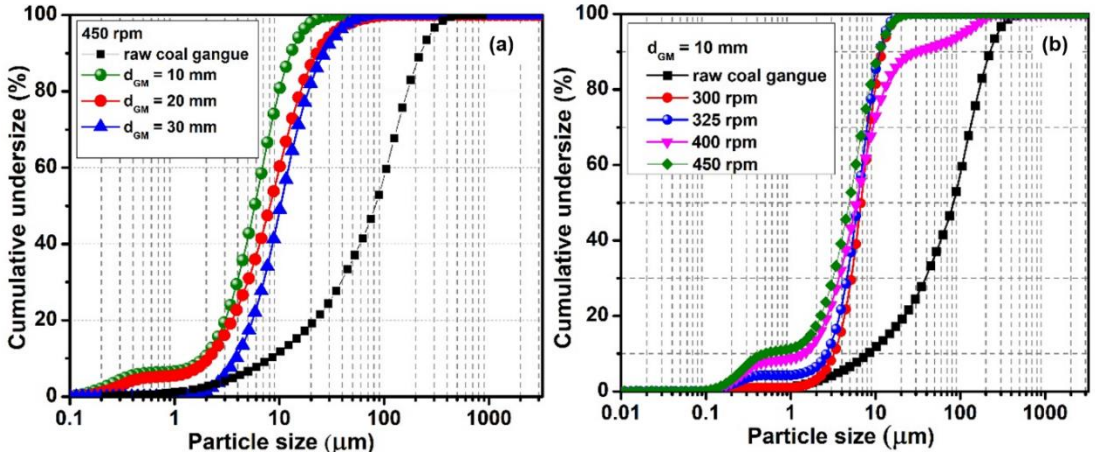

Fig 4.2: Cumulative undersize with (a) different grinding media size (b) rpm

Table 4.1: Characteristic particle size of coal gangue with different grinding media size

Grinding media size (mm)/ revolutions per minute (rpm)	**x_{10} (μm)**	**x_{50} (μm)**	**x_{90} (μm)**	**Geometric surface area S_m (cm^2/g)**
raw coal gangue	8.22	83.09	224.08	1738.05
d_{GM} 10 mm	1.87	5.87	12.89	7638.26
d_{GM} 20 mm	2.08	8.12	22.97	6351.74
d_{GM} 30 mm	3.86	10.26	26.80	4001.80
300 rpm	3.21	6.72	11.69	2021.30
325 rpm	2.62	6.13	11.18	3526.01
400 rpm	1.39	5.93	30.57	5415.07
450 rpm	1.87	5.87	12.89	7638.26

Given the utilization of the vibratory ball mill maximum operating frequency of 50 Hz and grinding media size d_{GM} 15 mm, a preliminary investigation to determine optimal frequency was deemed unnecessary. Furthermore, the applicability and performance characteristics of this specific vibratory ball mill have been previously established by Mucsi et al. [114], who conducted a comprehensive study on the mechanical activation of fly ash using the same equipment and a grinding media size 15 mm.

4.1.3 Preliminary investigation of geopolymerization of raw material

Fig 4.3(a) shows the 7 days compressive strengths of the geopolymer samples as affected by the liquid-to-solid (L/S) ratio. The liquid-to-solid (L/S) ratio in geopolymer is a critical mixing parameter that defines the mass ratio of the alkaline activating solution (the liquid) to the mass of the coal gangue (the solid). From Fig 4.3(a), it can be observed that the highest compressive strength 0.48 MPa was achieved with a geopolymer sample at liquid-to-solid ratio of 0.63. It is apparent, therefore, that there is an optimum liquid-to-solid ratio that is favourable for producing geopolymer with good compressive strength. Fig 4.3(b) presents the compressive strength of coal gangue geopolymer using NaOH at various concentrations (8 to 14 M). The results show that the compressive strength reached a maximum of 0.415 MPa at 8 M NaOH. Excessive molarity beyond the ideal range can negatively impact geopolymerization, potentially leaving unreacted sodium hydroxides within the matrix. This was evidenced by the reduced compressive strength observed at 10 M NaOH. Visual inspection of these geopolymer samples indicated deterioration, suggesting inadequate bonding between the gel matrix and the coal gangue particles.

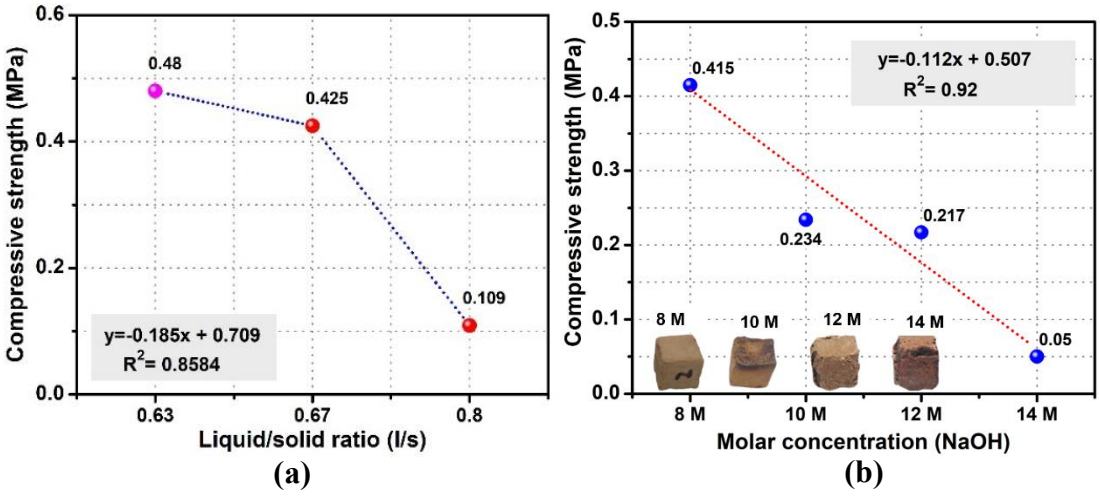

Fig 4.3: Compressive strength of geopolymer as a function of (a) liquid-to-solid ratio (L/S) (b) NaOH concentration

Subsequently, when the alkaline activator comprised a NaOH: Na_2SiO_3 concentration ratio of 25:75, the resulting geopolymer exhibited a compressive strength of 2.31 MPa. This sodium silicate (Na_2SiO_3) appears to offer favourable conditions for the geopolymerization process. Conversely, the geopolymer binder composed of 100 sodium silicate failed to set, resulting in a sticky and dense paste. This complication made controlling the geopolymer paste difficult, as illustrated in Fig 4.4(a), highlighting the importance of balanced activator components for successful binder development. Fig 4.4(b) illustrates the influence of elevated temperature on

compressive strength. The increase in temperature from 60 °C to 80 °C appears to enhance the dissolution of reactive components within the raw coal gangue by the alkaline solution. The highest compressive strength of 2.31 MPa was achieved in the sample cured at 80 °C for curing 36 hours. This elevated temperature likely accelerated the geopolymerization process, specifically the dissolution mechanism of the precursor materials, leading to improved strength development.

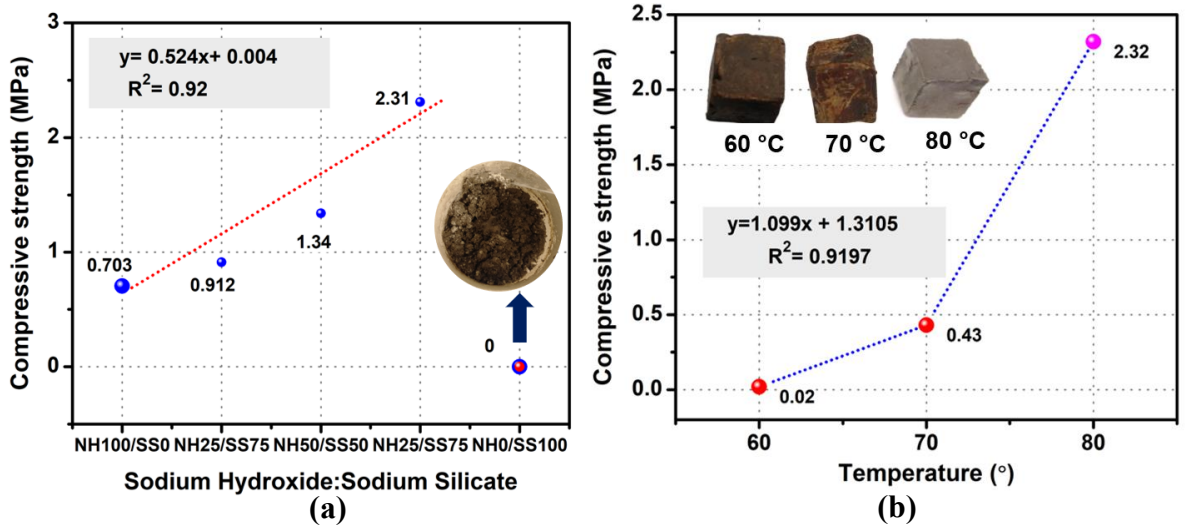

Fig 4.4: Compressive strength of geopolymer as a function of (a) sodium hydroxide: sodium silicate (b) elevated temperature

4.2. Mechanical activation of coal gangue in vibratory ball mill

4.2.1 The effect of mechanical activation on particle size distribution

The aim of mechanical activation by grinding was to increase and activate the particle surfaces on which the polymerization reactions take place. Thus, particle size measurements were carried out to observe how particle sizes with grinding media size 15 mm varies depending on the grinding time. Based on the determined particle size distribution, the relative span (RS) was calculated, which is a measure of the width of the particle size distribution. The relative span (RS) is defined, where x_{10}, x_{50}, and x_{90} represent the proportion of particles below 10%, 50% and 90% of all particles. From the perspective of different grinding time, the variation of particle size led to a narrower distribution as shown in Fig 4.5. Broader distributions were observed when the grinding time was varied and resulting in the production of particles of varying fineness.

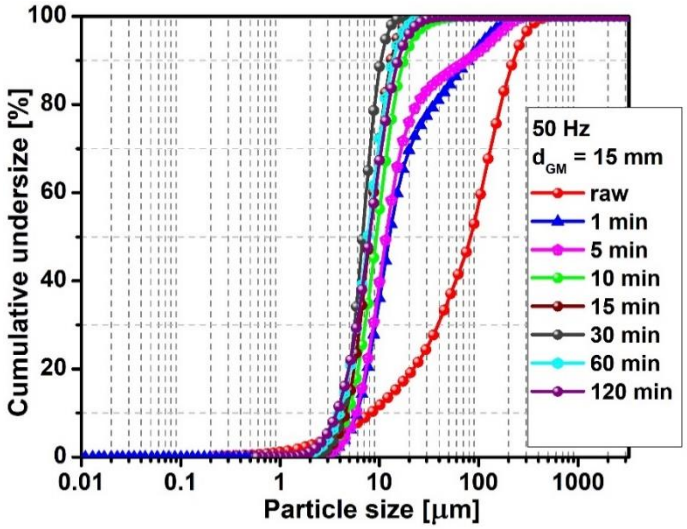

Fig 4.5: Cumulative undersize of raw and mechanically activated coal gangue

To elucidate the impact of mechanical activation on particle granulometry, the characteristic particle diameters x_{10}, x_{50} and x_{90} were meticulously tracked as a function of grinding time, as visually represented in Fig 4.6. This analysis provides critical insights into the evolution of coal gangue particle sizes across varying fineness levels achieved through mechanical activation process. The median particle size x_{50}, a key indicator of the overall particle size distribution, was observed to range from 7.95 µm to 12.93 µm after mechanical activation. The decrease in particle diameter x_{50} and x_{90} continued up to 30 min grinding time respectively and then increased. The particle size decreases were most significant during the first 30 min of grinding. There, it can be observed from 4.20 µm and 6.56 µm for x_{10} and x_{50}.

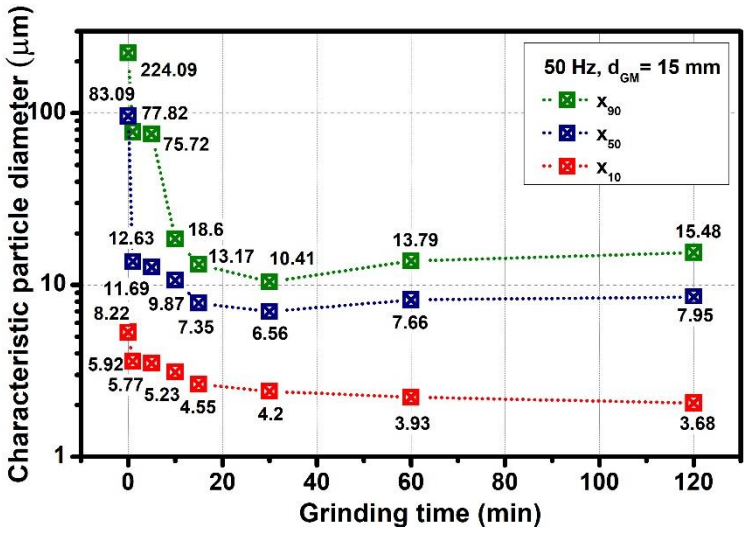

Fig 4.6: Characteristic particle size of x_{10}, x_{50}, and x_{90} with grinding time

The median particle size x_{50} exhibited a notable increase in fineness from 6.56 µm to 7.66 µm after 30 min of grinding likely due to the initiation of particle agglomeration or aggregation by weak Van der Waals forces [136]. The broadening of the particle size distribution curve during the 60 min of grinding further suggests the formation of aggregation or agglomeration. The relative span (RS), a measure of particle size uniformity, provides key insights into the mechanical activation process. Initially, for shorter grinding times (1 to 5 min), the relative span remained remarkably consistent, ranging from (RS = 5.69 - 5.98). This high RS value indicates a broad particle size distribution with a significant presence of coarser particles. This observation is further supported by the x_{90} values for mechanically activated coal gangue, which ranged from 77.82 to 75.72 initially as illustrated in Fig 4.6. A notable reduction in particle size is evident when comparing the raw material median particle size x_{50} of 83.09 µm to the median particle sizes x_{50} after 1 to 5 min of grinding, which fell between 11.69 and 12.63 µm. Grinding of mechanically activated coal gangue for 30 min resulted in the most uniform particle size distribution, characterized by a relative span of (RS = 0.94) as depicted in Fig 4.7. These finding highlights 30 min as the optimal grinding time for producing a narrow and uniformity particle size. In addition to uniformity, maximizing the fineness of particles is critical for enhancing specific surface area (SSA). The observed broadness in particle size distribution, indicating the co-existence of both fine and coarser particles, strongly suggests a significant role of grinding time in determining the final particle characteristics that enhance specific surface area. The grinding in the beginning can be correlated to Rittinger stage. The second is attributed to aggregation led to decreased in particle size [137],[138]. This inherent tendency of fine particles to agglomerate through adhesive forces is a critical consideration

when processing particulate solids, as it can impact their overall characteristics and behaviour [139].

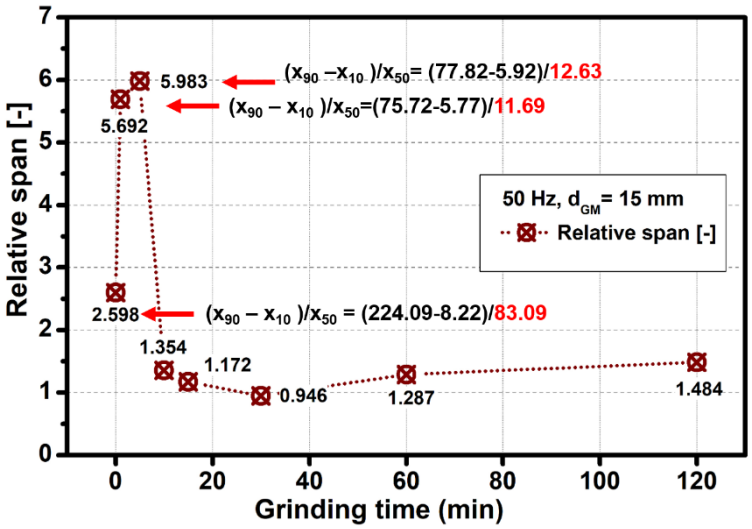

Fig 4.7: Relative span [-] as function of grinding time

Notably, investigation shows that sodium pyrophosphate ($N_2P_4O_7$) as chemical dispersant in overcoming these strong bonds and achieving better dispersion as shown in Fig 4.8. Furthermore, observations indicate that in the absence of this dispersant, the primary mechanism behind the increase in particle size is aggregation driven by weak van der Waals forces, which provide minimal resistance against dispersion. A significant analysis and discussion on particle size and agglomeration was present by Guzzo et al. [140] by comparing water and alkaline solution in particle size distribution.

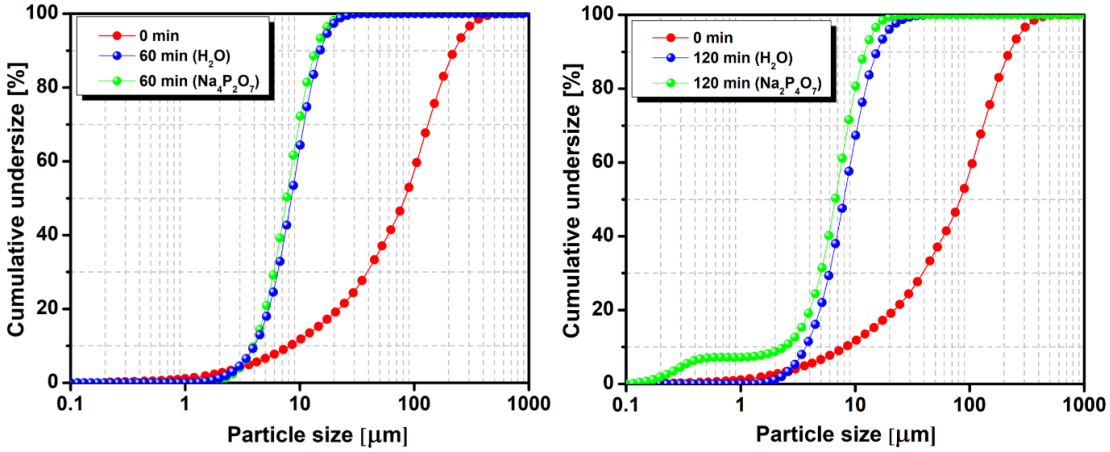

Fig 4.8: Cumulative undersize measured by laser scattering in water (H_2O) and sodium pyrophosphate ($N_2P_4O_7$) of grinding time 60 and 120 min

4.2.2 Correlation between specific surface area and specific grinding energy

Mechanical activation significantly increases the surface energy, primarily by enlarging its specific surface area (SSA). This enhanced SSA is vital for promoting effective contact and subsequent reaction with alkaline activators. Consequently, accurate evaluation of the specific surface area throughout the process becomes crucial. Optimizing the grinding process is paramount for achieving maximal energy efficiency and minimizing high grinding costs, as it directly controls the kinetics of particle aggregation and agglomeration, phenomena which can undesirably reduce the final specific surface area (SSA) of the mechanically activated coal gangue. The influence of specific grinding energy on both the specific surface area measured by nitrogen physisorption S_{BET} and the geometric surface area derived from laser scattering is illustrated in Fig 4.9.

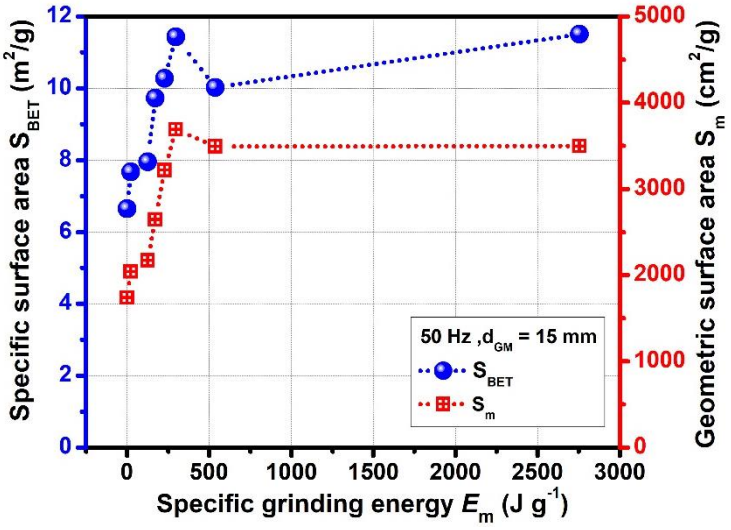

Fig 4.9: Specific surface area S_{BET} and geometric surface area S_m as function of grinding time

Notably, the geometric surface area minimal change between 60 and 120 min of grinding (3493 and 3496 cm^2/g, respectively), with the highest value observed at 30 min of grinding (3690 cm^2/g). This contrasts significantly with the specific surface area S_{BET} results, where the maximum specific surface area S_{BET} was obtained after 120 min of mechanical activation. This is because the magnitude of specific surface area S_{BET} depends on the morphology of the absorbent, or more precisely on the size of its internal pores and cracks, and on the shape and curvature of the external surface. It seems that the internal surface of aggregates remains accessible to the molecules of nitrogen gas. However, the granulometric surface values are markedly affected by the presence of the finest size fractions [141]. During the initial Rittinger stage (up to 30 min of grinding), a high rate of specific surface area increase was observed, and the relationship between specific grinding energy and specific surface area was linear. After

this period, specifically around 60 min, the particle of mechanically activated coal gangue entered an aggregation stage. At this point, the accumulated specific surface area and specific grinding energy became high enough to facilitate the attachment of particles through Van der Waals forces. This aggregation phenomenon signifies the attainment of an apparent specific grinding limit, where further energy input no longer yields significant benefits in surface area enlargement.

4.2.3 Specific surface area and cumulative pore volume

The coal gangue specific surface area S_{BET} and median particle size x_{50} as a function of grinding time of the raw and mechanically activated coal gangue are shown in Fig 4.10. Fig 4.11 displays the relationship between specific surface area S_{BET} and cumulative pore volume as a function of grinding time. Mechanical activation enhances the reactivity of coal gangue particles by simultaneously decreasing particle size, increasing specific surface area, and altering the inter-pore distribution [142]. The significant difference between the values of the various specific surface area S_{BET} with cumulative pore volume can be explained by the porous structure of the coal gangue particles [143]. In the 120 min mechanically activated coal gangue, the cumulative pore volumes increased even more than those in the 30 min mechanically activated sample. This non-linear trend for cumulative pore volume in study differs from the consistent linear relationship between specific surface area and cumulative pore volume cm^3/g reported by Huo et al. [14] in their investigation of combined chemical and mechanical activation of coal gangue.

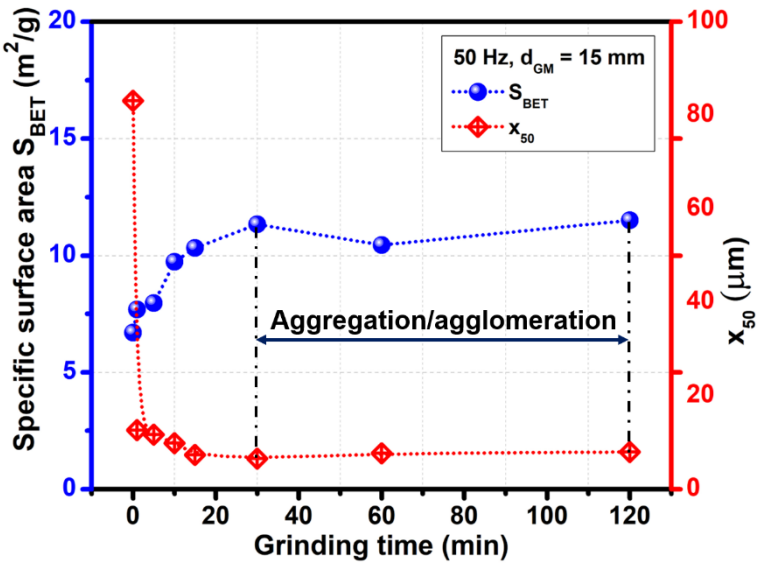

Fig 4.10: Specific surface area S_{BET} with x_{50} as a function of grinding time (min)

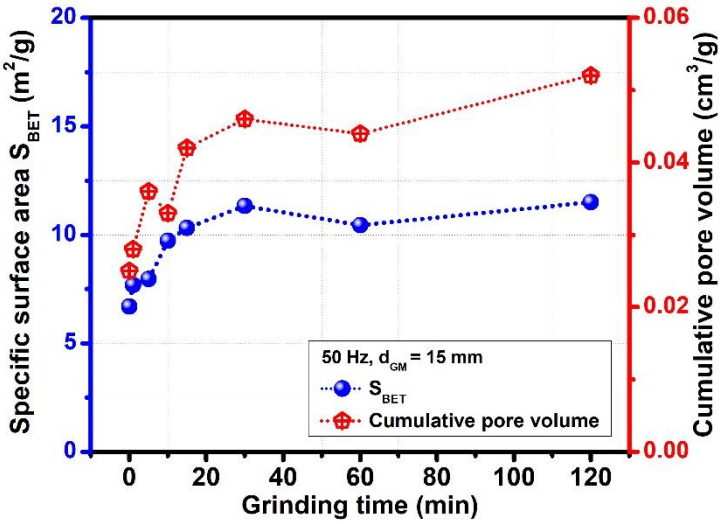

Fig 4.11: Specific surface area S_{BET} with cumulative pore volume as function of grinding time

4.2.4 The effect of specific grinding energy on morphology coal gangue

Coal gangue is characterized by a complex mineralogical composition. A significant fraction of this material comprises clay minerals, which are often present as distinct mineral particles within the gangue matrix. These clay particles are typically held together by relatively weak Van der Waals forces making them susceptible to disaggregation under mechanical stress including compression, impact, shear, and attrition [144]. These forces are crucial in inducing various fracture mechanisms within the coal gangue structure. Within the investigated specific grinding energy range 2.286E+01 - 2.754E+03 J g^{-1}, particle breakage events were consistently observed as anticipated leading to particle size reduction in Fig 4.12.

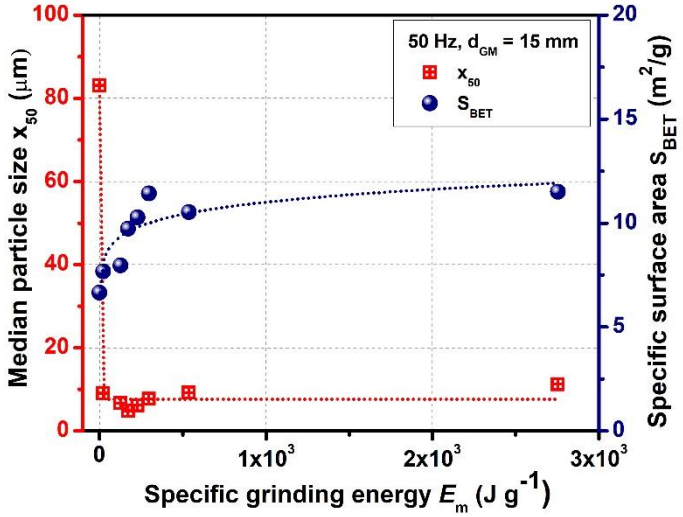

Fig 4.12: Grinding kinetics of mechanically activated coal gangue

The weak interlayer bonding attributed to Van der Waals forces in clay minerals renders them particularly vulnerable to inter-particle fracture that breaking of bonds between individual mineral particles, leading to liberation. Intra-particle fracture, cracking and fragmentation within the individual mineral grains themselves [63]. These mechanisms collectively lead to particle breakage, where larger particles are reduced into smaller ones. As the result, the physical properties of the mechanically activated coal gangue exhibited remarkable stability across this broad energy range as clearly illustrated in Fig 4.13(A). This preservation of physical characteristics despite substantial specific grinding energy input and demonstrable particle size reduction prompted further detailed microstructural investigation by scanning electron microscopy (SEM). Particle size analysis, supported by SEM was conducted at selected step of mechanical activation process in Fig 4.13(B). The morphology of raw coal gangue is characterized by plate-like, pseudohexagonal particles as shown Fig 4.13B (a). SEM images of mechanically activated coal gangue after 30 and 120 min of grinding Fig 4.13B (b-c) distinctly show the formation of smaller particles. These observations indicate the presence of fine particles adhering to the surface of larger, partially fractured particles, as well as weak aggregation of fine particles on coarser surfaces. The evolution of particle morphology during grinding has been investigated in previous studies which reported that the type of material being ground, the mill type, as well as the mode of breakage may have a large impact on the particles produced [145].

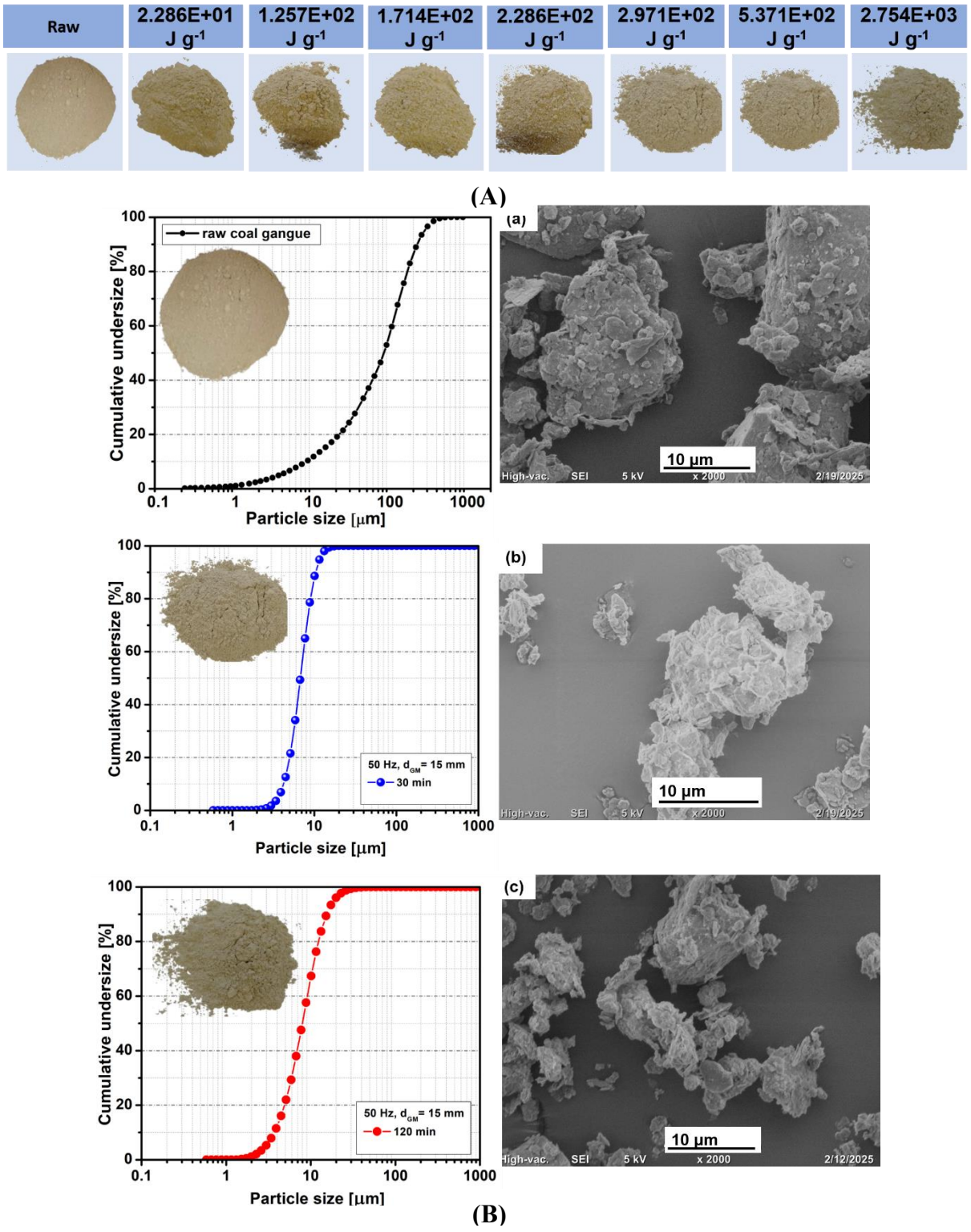

Fig 4.13: (A) Photograph of raw and mechanically activated coal gangue. (B) Cumulative undersize and SEM images of (a) raw and mechanically activated (b) 30 min and (c) 120 min

4.2.5 The FT-IR of raw and mechanically activated coal gangue

Fourier Transform Infrared (FT-IR) spectroscopy was employed to identify and characterize the key functional groups in coal gangue that cause its molecular bonds to vibrate (stretch and bend), as shown in Fig 4.14. This analysis allowed for the revelation of structural defects induced on the particle surfaces as a direct consequence of the grinding process. For crystalline solid materials, the characteristics of absorption bands are closely related to the degree of crystallinity, well-crystallized materials typically exhibit sharp and intense bands, whereas poorly crystallized or disordered structures yield broader and weaker bands. This well-documented correlation is further detailed in the Handbook of Inorganic Non-metallic Materials [146].

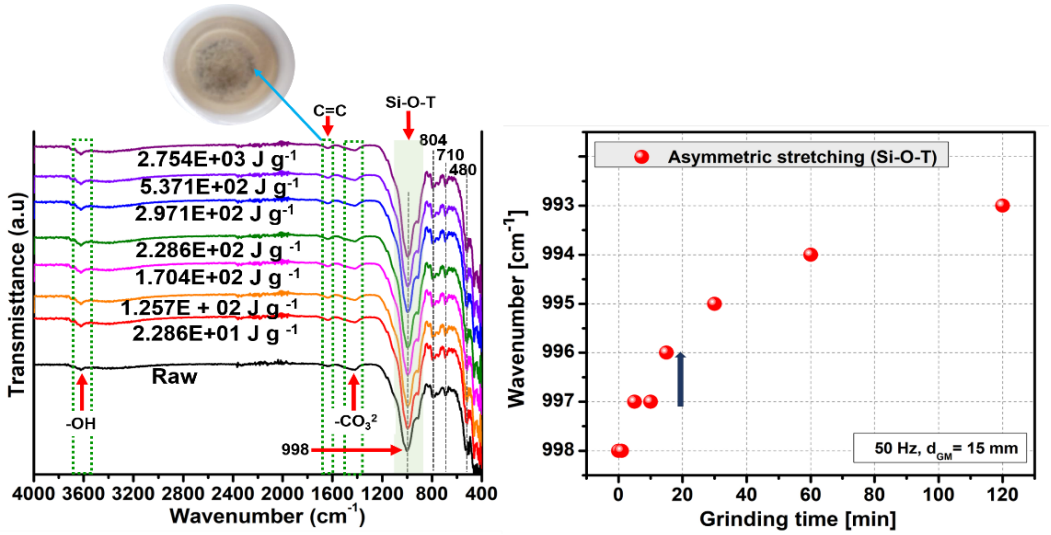

Fig 4.14: FT-IR of raw and mechanically activated coal gangue with different grinding time

The absence of significant absorption in the 3000 - 3700 cm^{-1} indicates minimal hydroxyl -OH stretching, reflecting a relatively low content of free water [147]. The absorption peaks between 1000 and 1200 cm^{-1} and 900 - 1100 cm^{-1} correspond to the stretching of the T-O bond and the asymmetric stretching vibration of the Si-O-T bond (T = Si or Al), respectively [78]. Further analysis of the asymmetric stretching vibration peaks of Si-O-T (T = Si or Al) revealed a shift wavenumber from 998 cm^{-1} in the raw coal gangue to 996 cm^{-1} after short duration grinding (1-15 min). With prolonged grinding in the range of 30 - 120 min, the mechanically activated coal gangue exhibits a progressive shift in the characteristic absorption band toward 993 cm^{-1}. This shift reflects due to decreasing particle size. It is evidently clear from the findings that that the increasing grinding time resulted in lower wavenumber number of finesse particle [110]. In previous research by Mucsi et al. [148] grinding construction demolition waste (CDW), the wavenumber increased with increasing grinding time as the particles become smaller, and more

vibrations can be observed from more tiny particles. The band at 473 cm^{-1} produced by Si-O vibration which indicate asymmetrical bending vibration has no obvious change, indicating that the quartz structure remains unchanged [149]. This similar report by Delogu et al. [150].

4.2.6 Phase analysis raw and mechanically activated coal gangue

Phase analysis of the raw and mechanically activated coal gangue, conducted using X-ray diffraction XRD and presented in Fig 4.15. The major crystalline phases detected are kaolinite type 1:1 clay ($Al_2Si_2O_5(OH)_4$), illite type 2:1 clay ($(K, H_3O)Al_2Si_3AlO_{10}(OH)_2$), albite a mineral from feldspar group ($NaAlSiO_8$), muscovite $KAl_2(Si,Al)_4O_{10}(OH)_2$ and quartz (SiO_2). Phase analysis revealed the absence of any new crystalline phases in the mechanically activated coal gangue. Coal gangue is a heterogeneous particle composed of multiple crystallites and mechanical activation breaks down the particle, which will either expose smaller crystallites [151],[152]. Consequently, the intensity of diffraction peaks for the mineral phases, specifically kaolinite, illite, albite, and muscovite, decreased as the grinding time increased (30, 60 and 120 min).

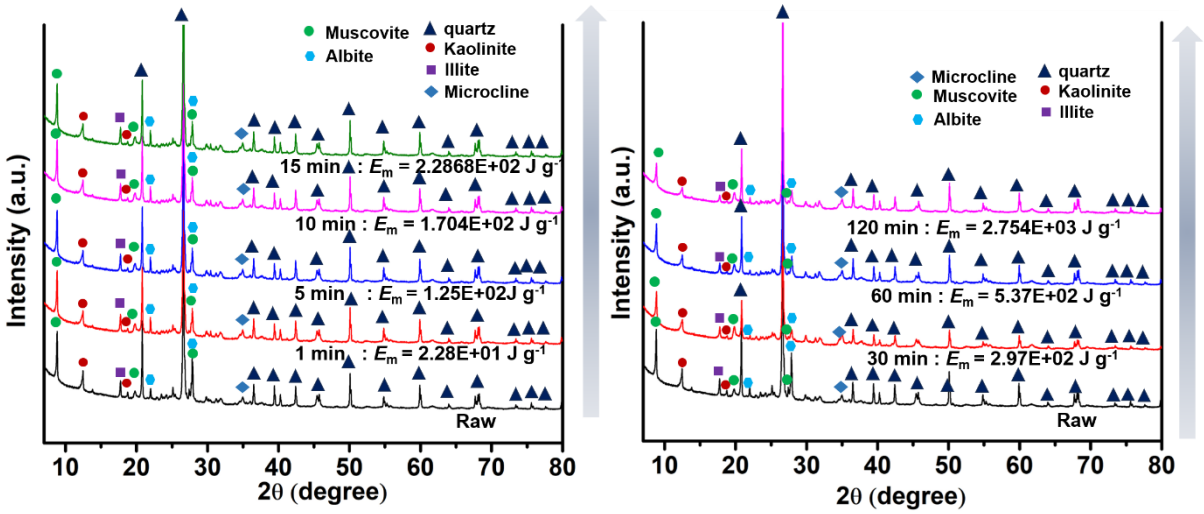

Fig 4.15: Phase analysis of raw and in vibratory ball mill mechanically activated coal gangue

However, the results showed that a specific grinding energy of 2.754E+03 J g^{-1} (120 min of grinding), the albite peak exhibited a greater reduction in diffraction peak intensity in contrast to other mineral phases such as kaolinite and illite. The differential peak reduction among the individual mineral phases within the coal gangue was likely attributable to variations in their hardness and the relative stability of their crystalline lattice structures [153]. Moreover, the mechanical activation occurred due to complex motions within the jar, involving four contact types, impact, torsion, shearing, and rolling between the coal gangue, grinding media, and the

mill wall [154]. Despite the resilience of quartz to mechanical activation, several studies indicate that its presence can enhance the process of amorphization [155]. This is often due to the higher hardness of quartz particles allowing them to act as effective grinding media for softer minerals like kaolinite, thereby accelerating the grinding process [156]. However, in this study, the quartz did not affect the softer minerals. Consequently, the primary effect of this grinding process was mechanical dispersion (particle size reduction). This outcome is consistent with the findings of Mucsi et al. [114] and Sanjay et al. [104] who similarly observed limited structural transformation in mechanically activated fly ash under vibratory milling conditions.

4.2.7 Leaching of raw and in vibratory ball mill mechanically activated coal gangue

Unlike cement, which is structurally strengthened through the hydration of calcite and C-S-H gels, the strength of geopolymers is dependent on the dissolution and condensation of silica-alumina precursors in an alkaline solution to create geopolymerization [157]. To investigate the effects of mechanical activation at different grinding times (1 - 120 min) and the corresponding changes in specific surface area S_{BET} and the leaching rates of silica (Si) and alumina (Al) from both raw and mechanically activated coal gangue in an 8 M NaOH solution presented in Fig 4.16.

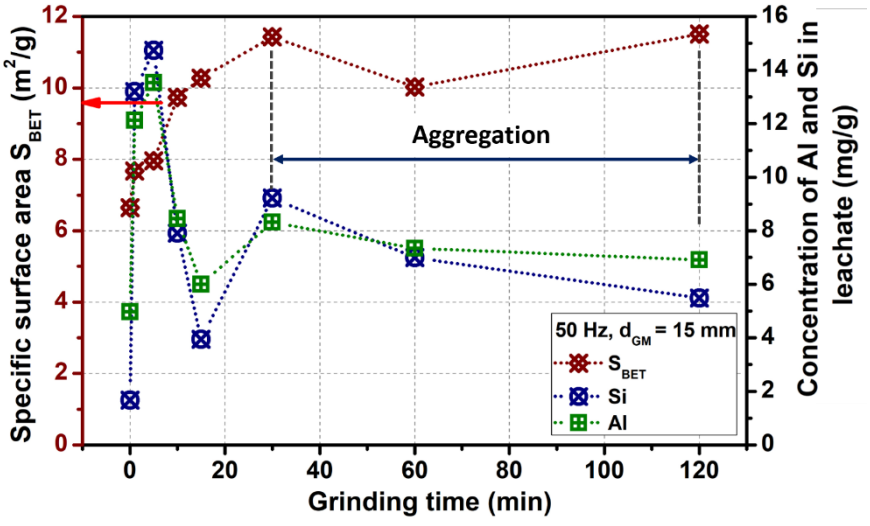

Fig 4.16: Concentration of Si and Al with specific surface area as function of grinding time

The results are essential for the estimation of alumina (Al) and silica (Si) and how the decrease in specific surface area S_{BET} leads to aggregation of the mechanically activated coal gangue may affect the properties of the geopolymer. Lower concentrations of Si and Al elements were released from the mechanically activated coal gangue into the alkaline solution. The increase

in concentration became less apparent when the grinding time exceeded 30 min. Although it was initially speculated that Si and Al concentrations might decrease after aggregation (60 and 120 min), the results showed a different trend. Despite the mechanically activated coal gangue of 30 min exhibiting the lowest median particle size x_{50} and most uniform particle size distribution, characterized by a relative span of (RS = 0.94), higher concentrations of Si and Al were actually observed at 1 and 5 min of grinding, Si range between 10.36 - 10.98 mg/g and Al range between 12.12 - 13.53 mg/g. Thus, it is speculated that other fine particles may adhere to the surfaces of the mechanically activated coal gangue between 30 and 120 min, thereby preventing further Si and Al release [160].

4.2.8 Saturated lime test of raw and mechanically activated coal gangue

The saturated lime test is a specific laboratory method used to evaluate a pozzolanic reactivity. This test directly measures the amount of calcium oxide (CaO) that raw and mechanically activated coal gangue consumes over a set period when mixed in a saturated lime solution, $Ca(OH)_2$. The amount of CaO consumed is then used to determine the material reactivity. Mechanical activation facilitates this reaction by disrupting the crystal structure at the particle surface and increasing the specific surface area of the coal gangue, thereby making more reactive sites available for interaction with the lime solution. Fig 4.17(a) illustrates the swelling of raw and mechanically activated coal gangue. It's clear that the mechanically activated coal gangue had a slightly swelling than the raw material at the end of the saturated lime test. This swelling is a visual indicator of the pozzolanic activity taking place. Based on Fig 4.17(b), the CaO uptake for the 60 min and 120 min of mechanically activated coal gangue decreased over the measurement period, with values recorded up to the 30 days (15 titration).

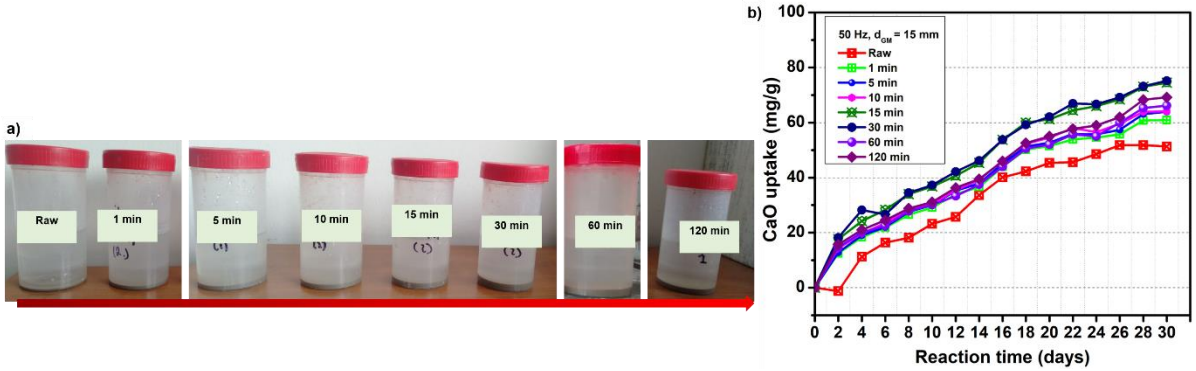

Fig 4.17: (a) Swelling of raw and mechanically activated coal gangue from 1 to 120 min (b) CaO uptake of samples with reaction time (days)

The raw control sample showed the lowest CaO uptake at both 15 days (33.6 mg/g) and 30 days (51.3 mg/g) (Fig 4.18). The results indicated that increasing the geometric surface area led to higher CaO uptake compared to the raw control values. For mechanically activated coal gangue (30 min), CaO uptake ranged from 46.2 mg/g at 15 days to 75.2 mg/g at 30 days, representing increases of 27.2 % and 31.7 %, respectively, with the highest geometric surface area of 3690 cm^2/g. Conversely, CaO uptake decreased as the geometric surface area decreased (3493 - 3496 cm^2/g).

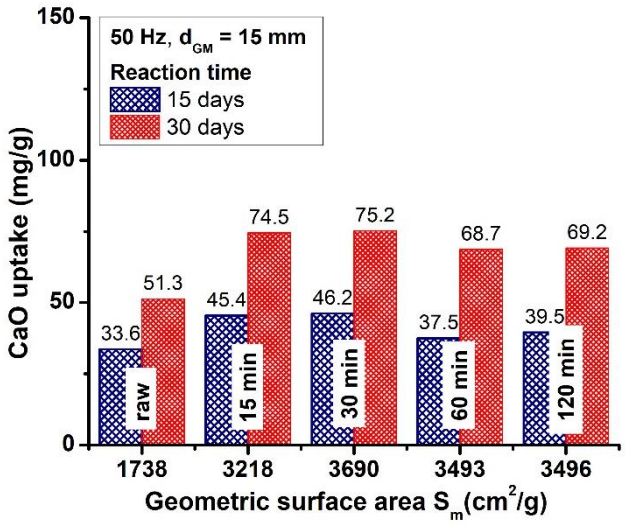

Fig 4.18: Relationship amount of CaO uptake at reaction time of 15 and 30 days with geometric surface area

This finding suggests that, under the specific griding energy conditions, the mechanical activation process may not have effectively enhanced the pozzolanic reactivity of the coal gangue. This observation is consistent with the XRD analysis (as discussed in Section 4.2.6), which indicated the persistent presence of less reactive mineral phases within the mechanically activated coal gangue, thereby limiting the generation of highly reactive amorphous phases. In parallel, other studies, such as that by Tuğluca et al.[158], who investigated the grinding of construction and demolition waste (CDW) from roof tile, hollow brick, and red clay brick, similarly measured reduced CaO consumption over grinding durations of 60 - 180 min, suggesting a comparable limitation in pozzolanic activity.

4.3. Performance of geopolymer produced using mechanically activated coal gangue by a vibratory ball mill

4.3.1 Effect of NaOH concentration on geopolymerization

To evaluate the optimization of the NaOH concentration ranging from 8 - 12 M for mechanically activated coal gangue, the compressive strength was tested at 7 days using a median particle size x_{50} of 6.56 µm as illustrated in Fig 4.19. This median particle size was selected based on the mechanically activated coal gangue 30 min of grinding. Raw coal gangue geopolymer was also included for comparison purposes. The use of a median particle size of x_{50} of 6.56 µm resulted in an overall increase in compressive strength to 0.73 MPa compared to the raw coal gangue, which exhibited a strength of only 0.0415 MPa. In this case, no NaOH concentration optimization was required for the raw material, as detailed results were presented in the previous section (Section 4.1.3).

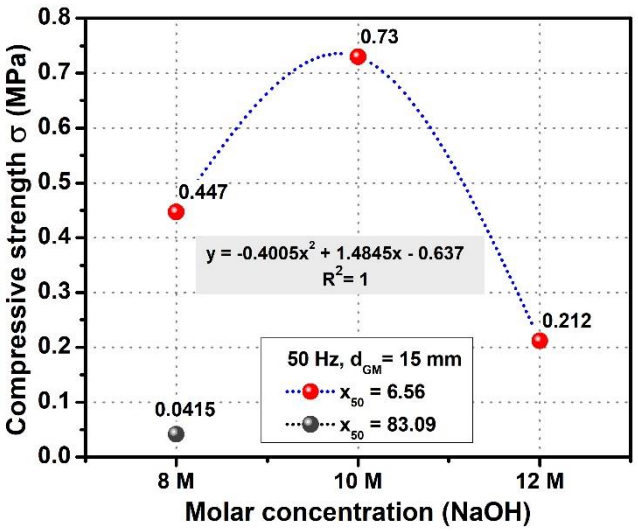

Fig 4.19: Effects of NaOH concentrations on the compressive strength of the geopolymer.

The highest compressive strength in the geopolymer was achieved with a 10 M NaOH solution. It should be noted that the reaction tends to occur more effectively at higher NaOH concentrations. Nevertheless, the reactivity of the coal gangue is also an important factor that explains the decrease in compressive strength. It is also noteworthy that the rate of geopolymerization was considerably slow, even though mechanical activation effectively reduced particle size and generated finer particles, thereby increasing surface-active sites [159]. This suggests that a single alkaline activator system using 10 molar NaOH leaches more Si and Al, which enhances the geopolymerization process. These results are consistent with those of Cheng et al. [12], who also found that increasing NaOH concentration from 8 M - 16 M NaOH

increased the strength of coal gangue geopolymer. It is also shown that, in this study, mechanically activated coal gangue tested with 12 M NaOH beyond the identified optimum caused a substantial decrease in strength 0.212 MPa, highlighting the importance of optimization between NaOH concentration.

4.3.2 Effect of NaOH: Na_2SiO_3 concentration

As the next step in optimizing the alkaline activator, the effect of median particle size x_{50} of 6.56 µm on the ratio of sodium hydroxide NaOH to sodium silicate Na_2SiO_3 was investigated (NH100/SS0), (NH75/SS25),(NH50/SS50) (NH25/SS75) as shown in Fig 4.20. This is due to the fact that NaOH acts as a dissolvent that breaks down the Si-O-Si and Al-O-Si bonds on the coal gangue surface, while sodium silicate acts as a binder, providing additional soluble silicate and helping to form the gel in the geopolymerization reaction [160]. The highest compressive strength value was observed when ratio of sodium hydroxide: sodium silicate was NH25/SS75 used in geopolymer the compressive strength 1.31 MPa highest than raw with median particle size x_{50} 83.09 (0.061 MPa). In overall, an increase in the alkali reactant ratio increases the strength of geopolymers. Increasing Na_2SiO_3 content favours the polymerization process which leads to reaction product with higher compressive strength [161]. Furthermore, Na^+ released from Na_2SiO_3 accelerates the geopolymerization process by acting as charged-balanced ion the system and increasing the amount of soluble silicate present [162].

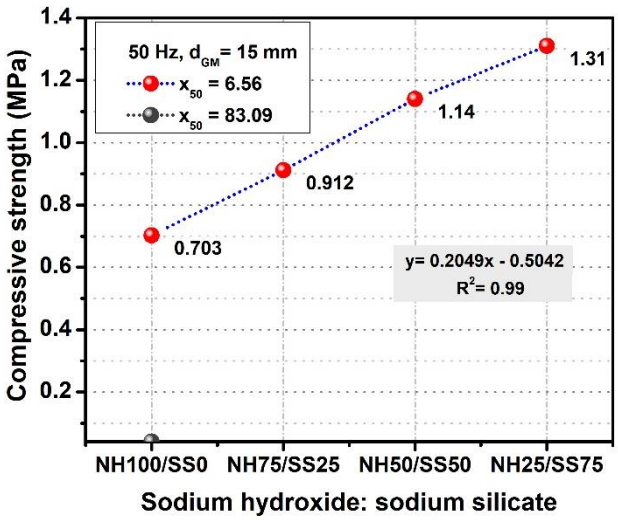

Fig 4.20: Effects of ratio NaOH:Na_2SiO_3 on the compressive strength of the geopolymer

4.3.3 Effect on temperatures series of geopolymerization

On the other hand, the compressive strength of geopolymer samples with a median particle size x_{50} of 6.56 µm was evaluated under different elevated curing temperatures (60, 70, 80 °C for 24 hours). These samples were activated using the optimal alkaline activator concentration identified in Section 4.3.2, which was NH SS75. The optimal compressive strength, reaching 1.01 MPa at 7 days, was achieved with a curing temperature of 70 °C Fig 4.21. The hardening occurs at room temperature or at moderate temperatures below 100 °C depending on the reactivity of the raw material [163]. Furthermore, prolonged exposure to high curing temperatures can lead to the immediate and excessive loss of water incorporated in the geopolymer paste, causing the rate of geopolymer gel formation to surpass and incomplete reactions [164].

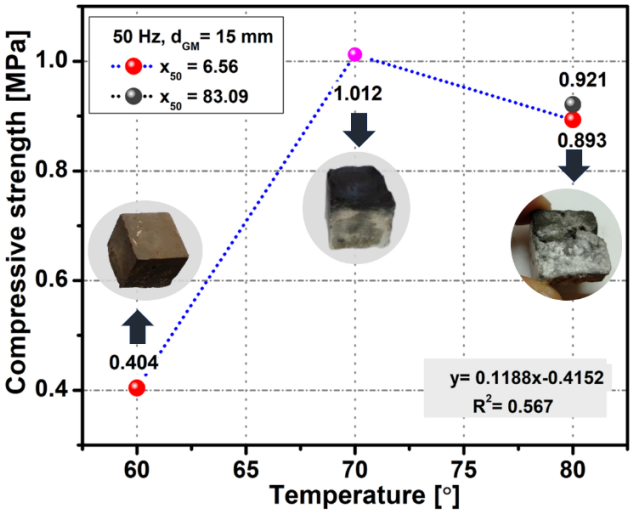

Fig 4.21: Compressive strength test of geopolymer with different curing temperature

As a result, elevating the curing temperature to 80 °C led to a significant decline in compressive strength to 0.893 MPa, likely due to crack propagation within the geopolymer sample, which is clearly observed in Fig 4.21. Although the ratio of sodium hydroxide NaOH and sodium silicate (Na_2SiO_3) was used in the sample, the limitation of the more amorphous phase from the mechanically activated coal gangue hindered the geopolymerization process. The dissolution of aluminosilicate materials in the alkaline medium occurs through the severing of covalent Si-O-Si and Al-O-Al bonds and the formation of silicate and aluminate species. Alkaline silicate solutions with alkaline hydroxide are usually used for producing geopolymers referred to as poly(sialate-siloxo) and poly(sialate-disiloxo) [52].

4.3.4 Visual observation of geopolymer samples

Fig 4.22 provides visual evidence of the relationship between the mechanical activation of coal gangue and the microstructure properties of the resulting geopolymers. The photographs depict both the prepared geopolymer and their fracture samples, clearly illustrating a significant change in colour depending on the specific grinding energy employed during the mechanical activation process. This distinct colour variation, apparent after 28 days, highlights the sensitivity of the geopolymer formation to the fineness and potentially the reactivity of the mechanically activated coal gangue. The findings align with those reported by Marjanović et al. [165] in their study on geopolymer mortar, where mechanical activation of fly ash through varying grinding times resulted in distinct colour changes, suggesting a correlation between mechanical activation, material reactivity.

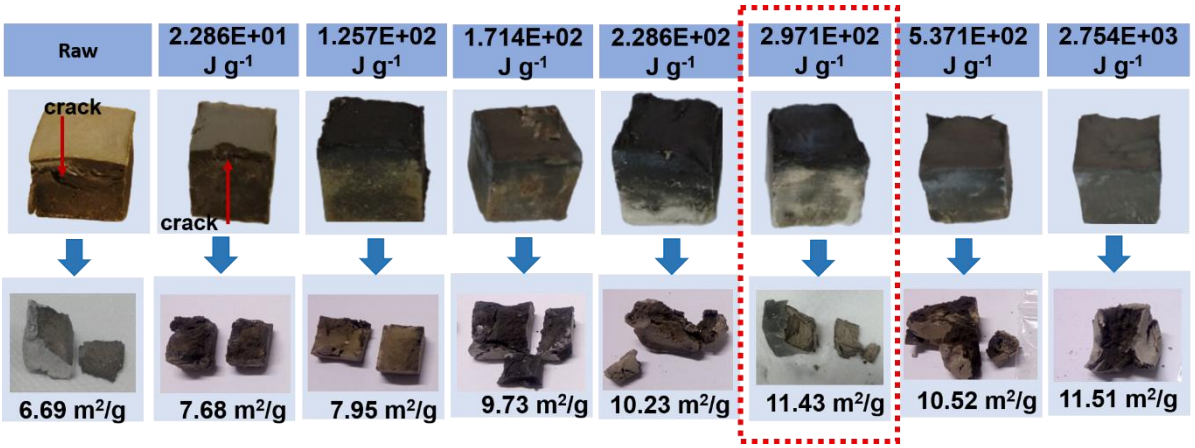

Fig 4.22: A photograph of geopolymer sample with different specific grinding energy and specific surface area

The colour of geopolymer samples exhibited a noticeable variation depending on the specific grinding energy and specific surface area. Samples prepared with specific surface area S_{BET} of 7.68, 7.95, 9.73, 10.52, and 11.52 m^2/g appeared darker. Mechanically activated coal gangue geopolymer 10.23 - 11.43 m^2/g, corresponding to specific grinding energy between 2.286E+02 - 2.97E+02 J g^{-1} were brighter in colour. This phenomenon is particularly pronounced in mechanically activated coal gangue geopolymers subjected to specific surface area S_{BET} 10.52 -11.51 m^2/g where specific grinding energy ranged from 5.37E+02 - 2.754E+03 J g^{-1}. Fig 4.22 visually represents these observed colour changes. This finding suggests a link between the mechanical activation process and the resulting colour, likely attributable to alterations in the reactivity and aggregation of the coal gangue samples. The geopolymer specimens in the compression tests displayed a viscous/ductile failure, deviating from typical brittle fracture.

This can be explained by the diffusion of Si^{4+} and Al^{3+} species into the solution, as reported which reduced their availability for forming a rigid network [166]. The resulting excessively alkaline solution promoted the formation of a gel layer on the surface of both raw and mechanically activated coal gangue particles. This gel layer effectively hindered the further release of reactive Si^{4+} and Al^{3+} ultimately contributing to the observed ductile behaviour under compression. Similarly, Rattanasak et al. [167] observed the formation of a gel layer, characterized by spherical units (0.5 - 2.0 μm), on the surface of fly ash particles treated with varying NaOH concentrations. The consistently lower strength observed in the geopolymers across the 1 - 120 min mechanical activation range suggests that full geopolymerization was not achieved. This is likely due to the limited reactivity of the mechanically activated coal gangue, even with specific grinding energy between 2.286E+01 - 2.754E+03 J g^{-1}. A critical factor contributing to this reduced reactivity might be that the specific grinding energy required to enhance the coal gangue's surface reactivity also makes it more susceptible to alkali frosting. This phenomenon, characterized by the loss of the alkaline activator, directly hinders the geopolymerization process. The findings align with Zheng et al. [168]. Furthermore, as Duxson et al. [169] pointed out, a greater amount of unreacted material leads to increased material defects, which are detrimental to the overall strength of the geopolymer specimens.

4.3.5 Morphology analysis of geopolymer samples

Microstructure analysis of selected geopolymer samples as shown in Fig 4.23(a-d). The images clearly exhibit unreacted raw coal gangue particles still present on the surface of the geopolymer samples, which did not participate in the geopolymerization reaction, even at 28 days. In geopolymers prepared with mechanically activated coal gangue (30 min, 60 min and 120 min grinding), the microstructure showed no significant changes, as illustrated in Fig 4.23(b-d). This resulted in weak adhesion between the gels and the matrixes, which were full of loosely packed, unreactive particles with median particle range x_{50} of 6.96 - 7.95 μm. Silva et al. [170] reported similar effects with different particle sizes (5 - 15 μm). While previous research emphasizes that the improvement of reactivity of geopolymers is observed with the reduction of particle size distribution [171] [172] [76]. It has been reported that the mechanical activation does not alter the chemical composition of the raw material but physically disrupts the structure, particularly weakening specific bonds such as Si-O-Si and Si-O-Al within the surface of the particles and releasing previously inaccessible reactive components and increasing the surface area available for reaction [148],[173]. These weakened bonds within

the particles are more susceptible react with alkali activators and form a denser microstructure of geopolymer.

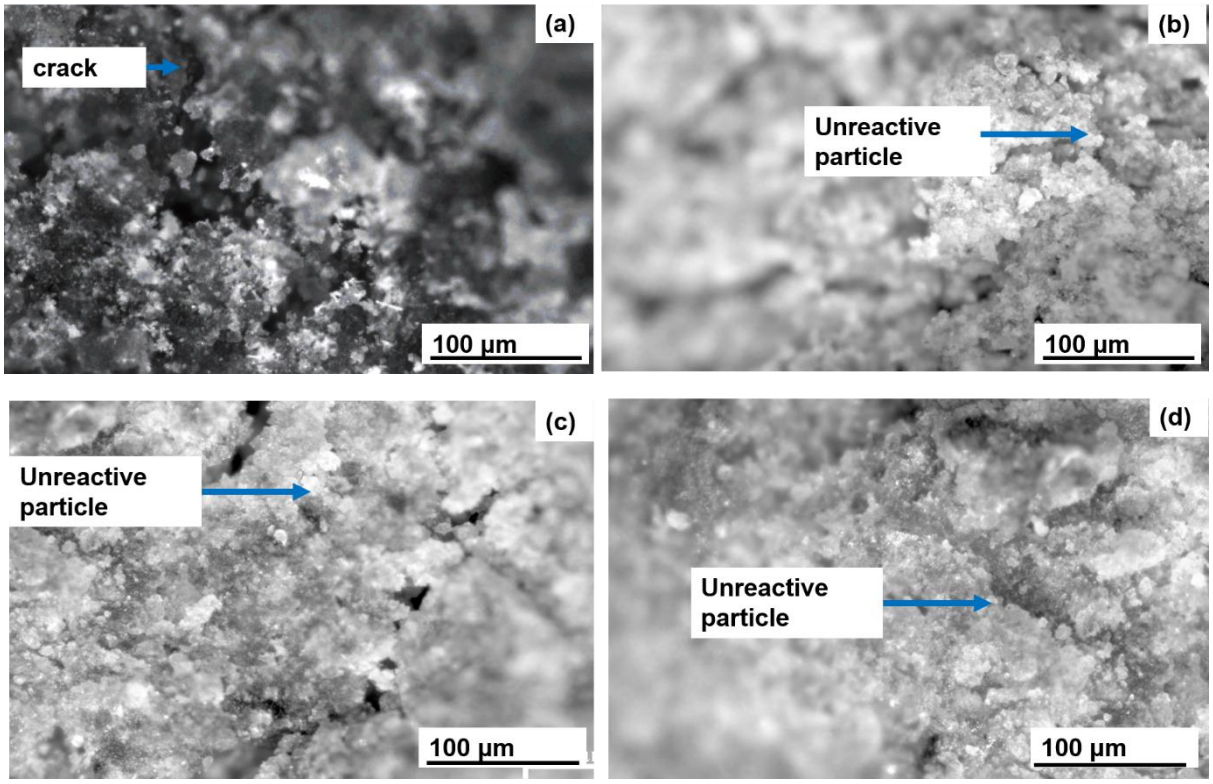

Fig 4.23: Optical image of geopolymer: (a) raw, (b-d) mechanically activated coal gangue 30, 60 and 120 min

4.3.6 Relationship between specific surface area and compressive strength

The compressive strengths of geopolymer binder after 14 and 28 days are shown in Fig 4.24. The results show that there is an optimum grinding time for the activation of coal gangue with mechanical activation, beyond which the compressive strength decreases. The compressive strength of geopolymer binder improved from 0.072 MPa to 0.109 MPa for geopolymer binder based on the raw coal gangue and mechanically activated coal gangue (1 min grinding) respectively after curing 14 days. This trend continued over 28 days curing period, where compressive strength values rose to 0.008 MPa and 0.210 MPa, respectively. The mechanically activated coal gangue 1 to15 min exhibit compressive strength less than 1.00 MPa.

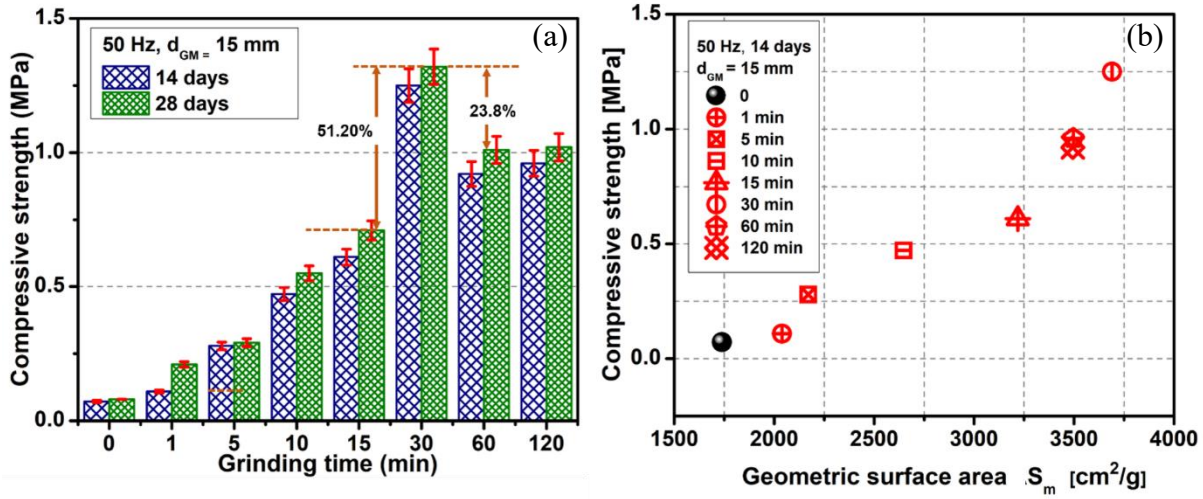

Fig 4.24: Compressive strength of geopolymer as function (a) grinding time (b) geometric surface area

This is attributed to the fact that aluminosilicate minerals in mechanically activated coal gangue are present in crystalline state, which has low reactivity and is only partially able to dissolve under alkaline solution, so that the increase in strength is not significant. The mechanically activated coal gangue 30 min show a significant improvement in compressive strength value 1.25 MPa after 14 days, and 1.32 MPa after 28 days of curing. The significant increase observed at 30 min of mechanically activated coal gangue, particularly the 51.20 % improvement over the 15 min grinding, suggests that prolonged grinding enhances the reactivity of coal gangue by increasing specific surface area and inducing limited structural disorder, which facilitates dissolution of aluminosilicate phases during geopolymerization. Comparing the different geopolymer series, it can be seen that the compressive strength decreases with a value of 0.92 to 0.96 MPa (14 days) and 1.01 to 1.02 MPa (28 days) with mechanically activated coal gangue 60 and 120 min. From this data, it can be interpreted that the geopolymer sample prepared from mechanically activated coal gangue shows a better compressive strength value as compared to the sample prepared from raw coal gangue. Dry grinding induced high stresses in the particles, resulting in mechanically activated layer on the particle coal gangue surfaces, and the aggregation of particles could affect the geopolymer properties.

In order to compare the geopolymer properties and mechanically activated coal gangue characteristics, the specific surface area S_{BET} and compressive strength was determined in Fig 4.25.

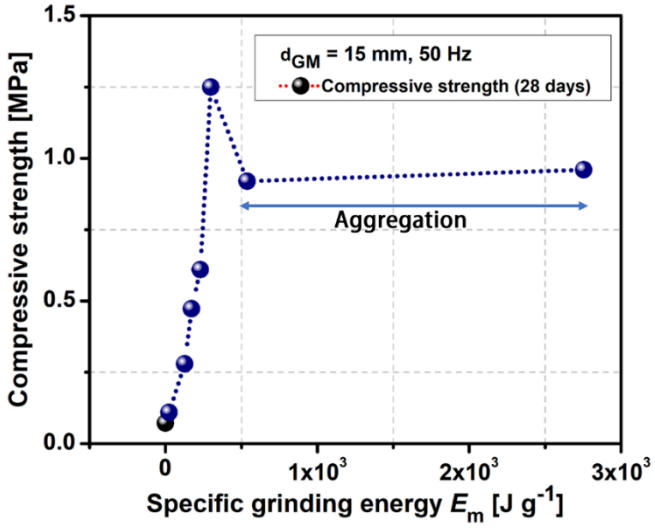

Fig 4.25: Compressive strength as a function of specific grinding energy

The highest compressive strength of 1.25 MPa (after 28 days of curing) was achieved using coal gangue mechanically activated for 30 min, which also exhibited the highest specific surface area S_{BET} of 11.43 m^2/g. As expected, the increase in specific surface area contributed positively to the compressive strength due to enhanced particle reactivity and dissolution during geopolymerization. Finer particles provide a larger reactive surface, which accelerates the dissolution of aluminosilicate phases, thereby promoting a denser and more cohesive geopolymer matrix. However, beyond the optimal grinding time, particularly after 30 min, the compressive strength began to decline despite further mechanical activation as, agglomeration and aggregation had a negative effect on the compressive strength. This phenomenon is clearly reflected in the observed inflection point, where both the specific surface area S_{BET} 10.54 m^2/g and the compressive strength 0.92 MPa (14 days) and 1.01 MPa (28 days) show a parallel decrease after 60 min of grinding. This indicates that excessive mechanical activation leads to a reduction in effective reactivity rather than further improvement. The improved reactivity of mechanically activated coal gangue can be attributed to the effects of reduced particle size, increased surface modification by grinding [98]. Research has shown that micro and nanoparticles can serve as effective nucleation sites for alkaline reaction with surface of mechanically activated powder thus enhance geopolymerization process [174],[175]. These results are similar to those reported by Nana et al. [101], where despite a reduction in specific surface area after 90 min of pegmatite grinding in an eccentric vibratory ball mill, compressive

strength continued to increase. The increase in specific surface area S_{BET} facilitated the higher dissolution of the coal gangue particles, thereby resulting in better compressive strength specimens. In this study demonstrates that the reactivity and the resulting development of compressive strength in geopolymer binders are strongly correlated with the specific surface area S_{BET} and geometric surface area attained through mechanical activation. This trend is consistent with the findings of Szabó et al. [76], who reported similar fluctuations in compressive.

4.3.7 FT-IR characterization of coal gangue geopolymer samples

FT-IR analyses of raw and mechanically coal gangue for selected samples were carried out to study the evolution of chemical bonding as shown in Fig 4.26 at 28 days.

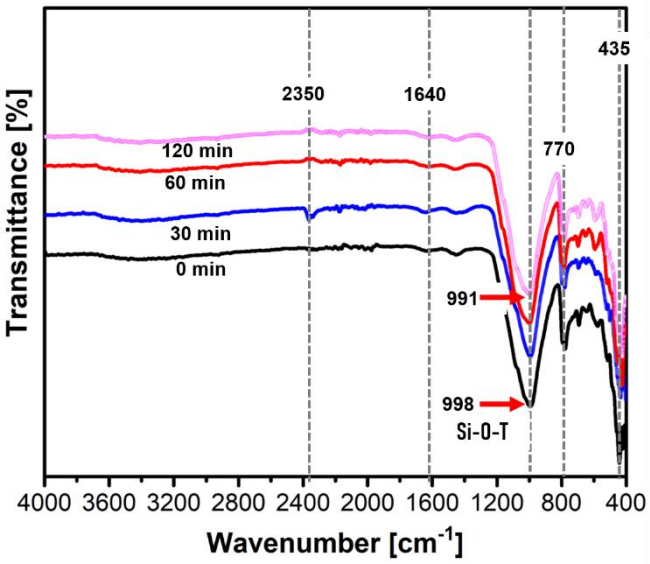

Fig 4.26: Geopolymer reaction

Based on the data, the frequency values for different raw mechanically activated geopolymer are as follows 998, 992, 991 and 991 cm^{-1} correspond to asymmetric stretching vibrations which represent the formation of geopolymer structural backbone after alkaline reaction, and suggested the formation of inorganic polymer [176],[177]. These results are in agreement with previous research by Ozyer at al. [178], the frequency shift around 998 - 980 for less reactivity material. A decline in the frequency number is indicated by a shift of the Si-O-T stretching bands to smaller numbers. The shift of frequency toward the lowest frequency suggests it is an indication of a reaction product related to the alkaline activator in other words, increases in the polymerization reaction between the Si-O-Al bonds, resulting in the formation of aluminosilicate gel.

4.4. Discussion

This study reveals that the mechanical activation of coal gangue via vibratory ball milling proceeds through two primary mechanisms that dictate reactivity, a fundamental reduction in particle size, directly increasing the specific surface area, and less significant alterations in the internal structure (specifically stretching and bending) of the mechanically activated coal gangue. By comparing the results shown in Fig 4.5 and Fig 4.6, it is evident that beyond 30 min, aggregation occurs, resulting in an increasing median particle size x_{50} and a reduced specific surface area. In addition, as the result, based on the combined evidence from persistence of well-defined, high-intensity peaks in both XRD patterns and FT-IR, only minor shifts in characteristic wavenumbers (FT-IR). This suggests that the mechanical activation process, with a specific grinding energy ranging from 2.2860E+02 to 2.754E+03 J g^{-1}, resulted in limited reduction to improve the surface activation and decreased activation energy stored in the non-equilibrium and disordered crystal lattice of coal gangue. Consistent with the mechanism of mechanical activation described by Juhász and Opoczky [117], the study demonstrates that the primary effect on coal gangue is mechanical dispersion (size reduction), resulting in a greater specific surface area as shown in Fig 4.27 [117,118].

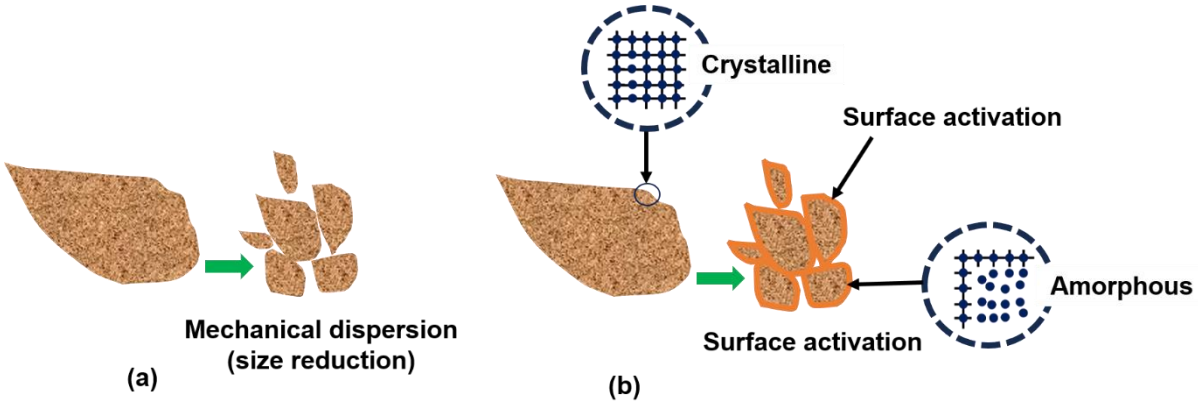

Fig 4.27: Schematic various states of mechanical activation: (a) mechanical dispersion, (b) surface activation

The results of the geopolymer properties, presented in Fig 4.19 - Fig 4.21, underline that the median particle size x_{50} significantly impacted the selection of the sodium hydroxide NaOH concentration, the sodium hydroxide: sodium silicate ratio, and the curing temperature. Although mechanical activation enhanced the specific surface area (SSA), the alkaline activator showed limited reactivity with the mechanically activated coal gangue particles when the grinding time was in the 1-120 min range. This limited reactivity suggests insufficient changes in surface activation and structural disorder of mechanically activated coal gangue,

both of which play a critical role in the development of geopolymer matrix [179]. Consequently, aggregation of the mechanically activated coal gangue restricts geopolymerization reaction, causing a decline in compressive strength after 30 min of grinding. These findings suggest that optimizing the grinding time is crucial as insufficient activation (1-120 min) fails to generate adequately reactive surfaces, while excessive grinding could lead to particle aggregation or agglomeration, which hinders further reactivity and results in high energy consumption.

4.5. Mechanical activation of coal gangue in planetary ball mill

4.5.1 The effect of mechanical activation on particle size distribution

The impact of grinding on the particle size distribution of raw and mechanically activated coal gangue for a chosen grinding time (1, 5, 10, 15, 30, 60, and 120 min) is shown in Fig 4.28 (a-b). Obviously, a significant reduction in particle size was observed. The increase in material fineness was clearly illustrated by the variation of the characteristic particle sizes (x_{10}, x_{50} and x_{90}) as a function of grinding time. Specifically, mechanical activation of the coal gangue in a planetary ball mill 450 rpm resulted in a rapid decrease in the median particle size x_{50}, dropping from 83.09 µm (raw) to 9.06 µm within the initial minute of grinding.

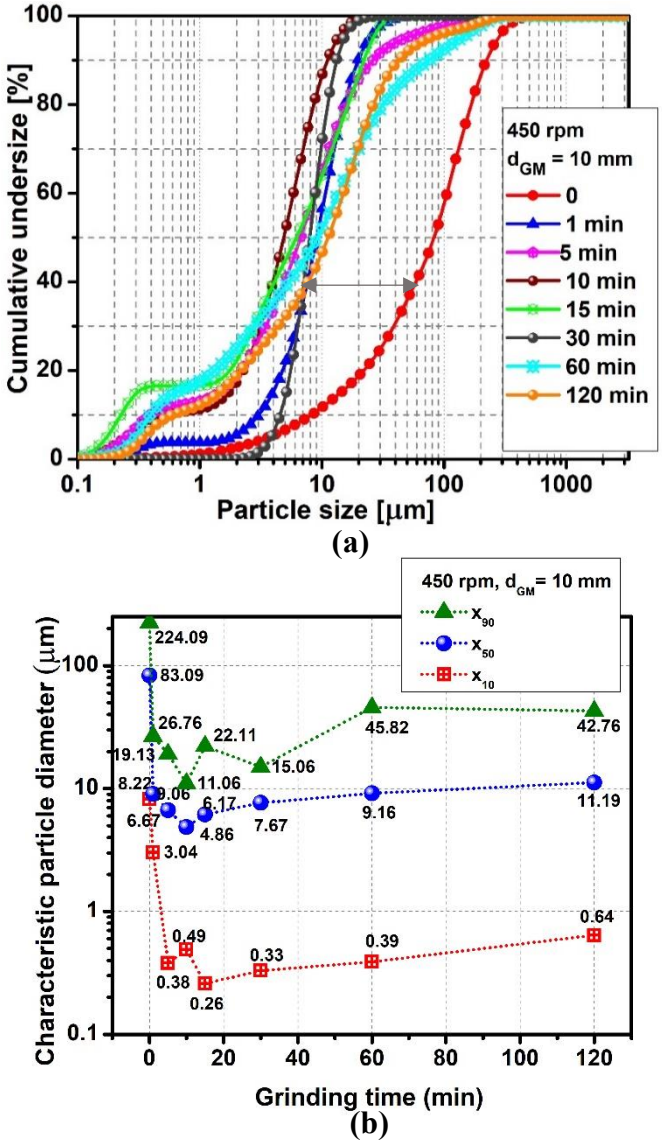

Fig 4.28: Raw and mechanically activated coal gangue, (a) cumulative undersize (b) characteristic particle size

Over the first 10 min, the particle size distribution continued shifting towards finer particles, with x_{50} reaching of 4.86 µm, indicating effective particle breakage. However, with prolonged grinding (15 to 120 min), the x_{50} increased to 6.17 µm and 11.19 µm, respectively. This reversal in particle size reduction suggests the occurrence of aggregation or agglomeration, where increased interparticle binding forces lead to particle clustering and a subsequent rise in median particle size [180],[181]. In addition to the experimental parameters, the relative span (RS) was a crucial factor for enabling a comprehensive comparison of results obtained for particles with varying size. The relative span value provided a more reliable representation of the width of the particle size distribution, independent of the median particle size, as shown in Fig 4.29. The relative span was calculated using eq (1):

$$RS = \frac{x_{90} - x_{10}}{x_{50}} \quad (1)$$

Investigation of variation of characteristic particle size of x_{10}, x_{50}, and x_{90} with grinding time as a function of grinding time revealed broadening of the relative span (RS = 4.95 - 3.85) for mechanically activated coal gangue after 60 - 120 min of grinding as illustrates in Fig 4.29. This wider distribution reflects the simultaneous presence of both fine and coarse particles, with x_{90} values recorded at 45.82 µm (60 min) and 42.76 µm (120 min) as shown in Fig 4.28(b). Conversely, mechanically activated coal gangue 30 min of grinding yielded the narrowest relative span (RS = 1.91), indicating a highly homogeneous distribution dominated by finer particles. It is critical to highlight that extending grinding beyond 30 min led to a significant increase in x_{90} to 45.82 µm, representing a 63.13 %.

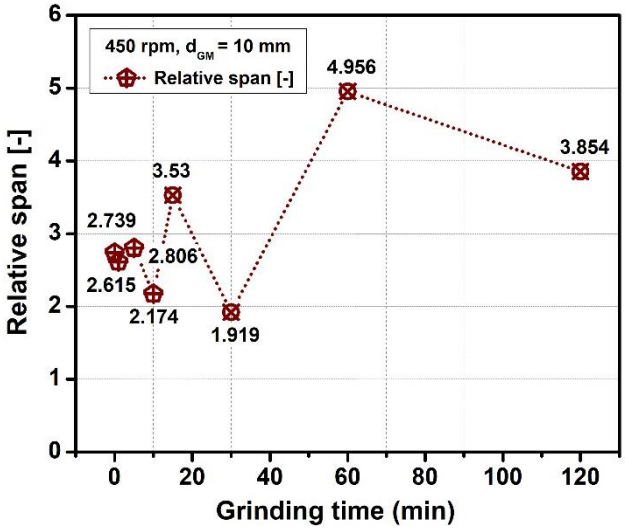

Fig 4.29: Relative span [-] as a function of grinding time (min)

Next, for the Design of Experiment (DoE), the resulting particle size distributions, characterized by the x_{10}, x_{50}, and x_{90} percentiles, are presented in Fig 4.30(a-c) via corresponding bar graphs. Mechanical activation of coal gangue was performed using a planetary ball mill with grinding times ranging from 15 to 120 min, at rotational speeds of 600 - 700 rpm, and employing grinding media sizes of 5 and 10 mm. A significant reduction in particle size was observed across all mechanically activated coal gangue samples, with all x_{50} values dropping substantially below that of the raw coal gangue x_{50} of 83.09 µm, and indeed falling below 10 µm. Specifically, at 120 min of grinding, the lowest x_{50} value 3.61 - 3.75 µm was achieved with 5 mm grinding media at 600 -700 rpm. These results clearly demonstrate a strong dependence on the process parameters, particularly concerning the x_{10}, x_{50}, and x_{90} values. In a planetary ball mill, the centrifugal force generated by the rotational speed is critical for effective grinding, as it directly influences the impact energy and movement of the grinding media, thereby governing particle size reduction. An increase in the x_{50} and x_{90} particle size values was observed for mechanically activated coal gangue after 15 min of grinding across most Design of Experiment (DoE), indicating the formation of aggregation or agglomeration. An exception was noted for the design utilizing 10 mm grinding media at 600 rpm, where this increase was not apparent. Furthermore, for the 10 mm grinding media at 600 rpm, continued grinding for 60 and 120 min did not result in a reduction of these larger x_{50} and x_{90} values, suggesting persistent agglomeration or a lack of deagglomeration under these specific conditions. The experimental design revealed that 5 mm grinding media consistently produced a finer particle size distribution compared to 10 mm grinding media, under identical rotational speed and grinding time conditions. This enhanced comminution efficiency is directly attributable to the higher frequency of collisions and a greater number of grinding media per unit volume achieved with the smaller media. This relationship is quantitatively supported by the constant powder filling ratio and calculations presented in Table 4.2. This observation was highly consistent with the foundational principles of the findings of Stenger et al. [182] who emphasized that the achievable optimal median particle size x_{50} was critically dependent on the stress intensity *SI* generated by the grinding media size.

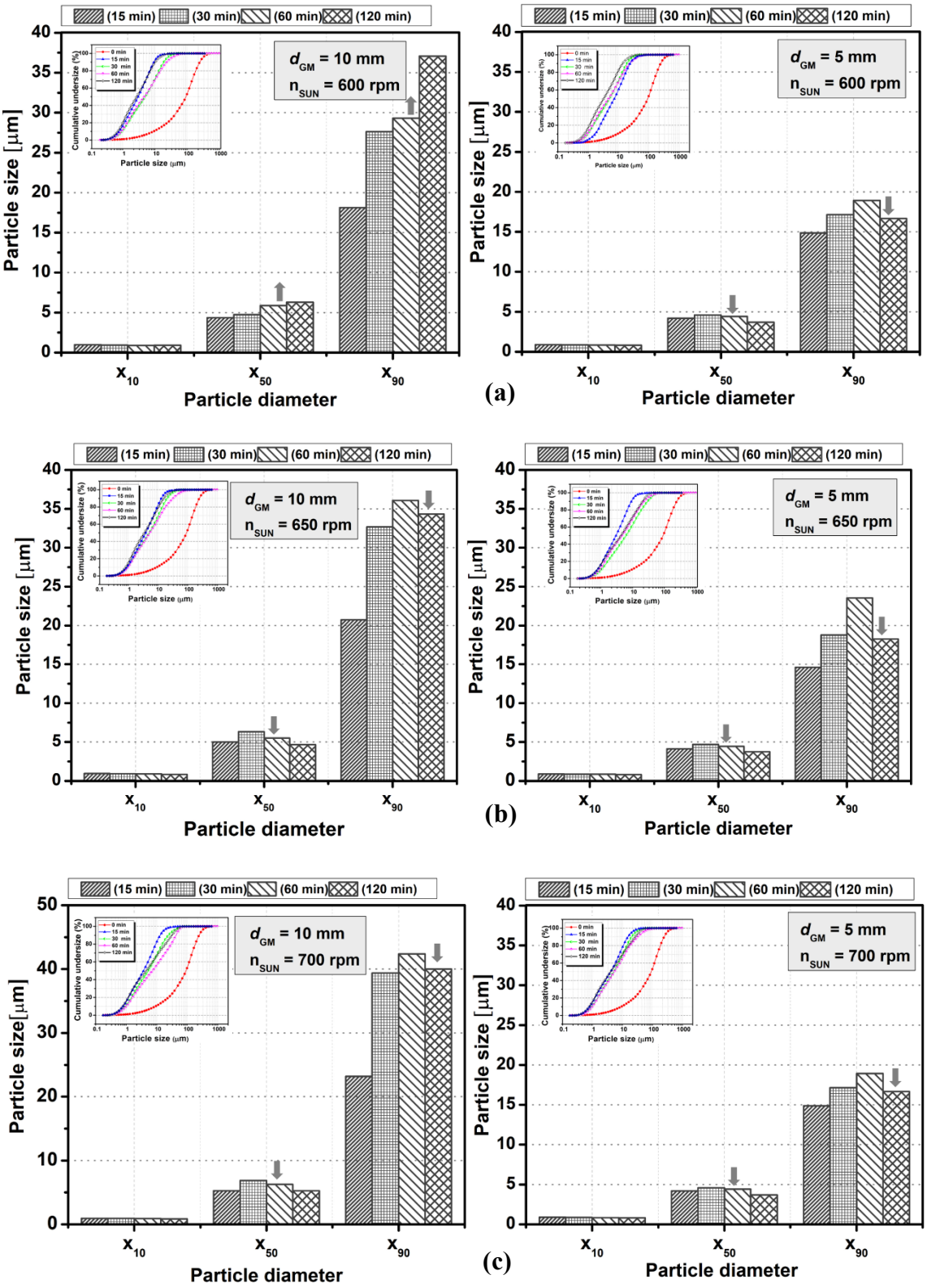

Fig 4.30: Characteristic particle size d_{GM} = 5-10 mm (a) 600 rpm, (b) 650 rpm, (c) 700 rpm

Table 4.2: Calculated collision frequency and stress energy for grinding media size 5 - 10 mm and revolution per minute 600 - 700 rpm

Revolution per minute [rpm]	d_{GM} [mm]	Collision frequency CF [s^{-1}]	Stress energy SE [J g^{-1}]
600	5	9.68E +09	1.08E-06
650	5	1.00E+10	1.33E-06
700	5	1.03E+10	1.63E-06
600	10	6.05E+08	1.52E-05
650	10	6.26E+08	1.89E-05
700	10	6.46E+08	2.30E-05

4.5.2 The effect of mechanical activation on morphology of coal gangue

Coal gangue is a heterogeneous material susceptible to aggregation and agglomeration, making the study of these phenomena essential for distinguishing between different particle size growth mechanisms during grinding. The increase in particle size observed during mechanical activation must be carefully analysed to differentiate between aggregation and agglomeration. According to Juhász and Opoczky [183], modifications in specific surface area (SSA) and median particle size x_{50} can be used to identify distinct phases of the grinding process, including Rittinger's stage, aggregation, and agglomeration. As illustrated in Fig 4.31(a-b), the particle size distribution and grinding time (60 and 120 min) was examined using deionized water (H_2O) and sodium pyrophosphate ($Na_4P_2O_7$) as dispersing mediums, alongside morphological analysis. The results indicate that after 120 min of grinding, the particle size distribution of mechanically activated coal gangue exhibits similarities in both dispersing mediums. Moreover, scanning electron microscopy (SEM) confirms significant agglomeration, suggesting that agglomeration at this stage involves strong, irreversible interparticle interactions, where chemical bonding plays a crucial role. This finding is further supported by the observation that agglomerates remain intact despite treatment with sodium pyrophosphate ($Na_4P_2O_7$) as chemical dispersion or ultrasound, indicating that the bonds formed are resistant to conventional dispersion methods. The increased formation of amorphized agglomerates might be responsible for the decreases in measured specific surface areas, as the high energy milling process can result in bonds between agglomerates that are difficult to be separated by chemical dispersant or ultrasound [116]. In comparison to the aggregation process, the SEM image reveals that after 60 minutes of grinding, significant amounts of fine powder and coarse grains are present. Consequently, the particle size distribution shifts toward finer particles when

sodium pyrophosphate ($Na_4P_2O_7$) is used as the dispersing medium. This suggests that aggregation at this stage is reversible, where primary particles are loosely connected with secondary particles through surface forces, primarily due to van der Waals interactions [184]. The results align well with the observed particle size distribution, confirming the presence of aggregation. For clarity, the values for specific surface area S_{BET} and median particle size x_{50} are presented, with particle size distribution measurements taken in a suspension of deionized water (H_2O). These findings are consistent with those reported by Tole et al. [185] and Manosa et al. [186] in their studies on mechanically activated clay for cement production, further validating the relationship between surface area and particle size.

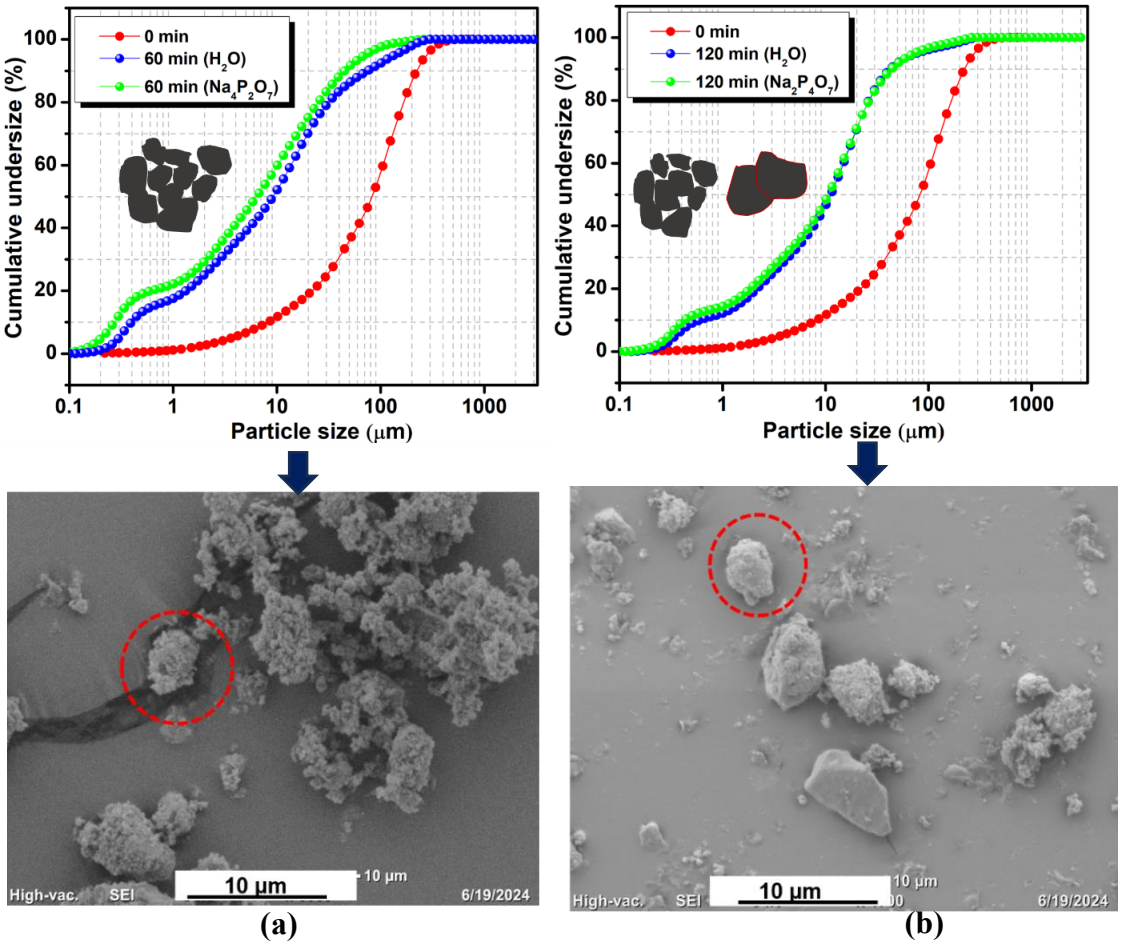

(a) (b)

Fig 4.31: Cumulative undersize of mechanically activated coal gangue using H_2O and $Na_2P_4O_7$ as dispersion solution with morphology analysis: (a) 60 min (b) 120 min

For Design of Experiment (DoE), the morphology of raw and mechanically activated coal gangue with grinding media of size d_{GM} =10 mm, 700 rpm, 120 min was examined as shown in Fig 4.32(a-b). It was clearly seen that the morphology of the raw and mechanically activated coal gangue changed after grinding. Initially, the morphology of the raw coal is irregular and

plate-like, as shown in Fig 4.32a. Since the experimental setup for grinding media with a size of 10 mm has a higher density, more energy could be transferred to the coal gangue particles compared to grinding media with a size of 5 mm, as calculated in according to eq. (6). However, the SEM image clearly shows that the morphology of the mechanically activated coal gangue could be seen in the form of flakes and coarse particles at a grinding media size of 10 mm, 700 rpm and 120 min Fig 4.32b. This indicates that when using 10 mm grinding media, the mechanically activated coal gangue is less susceptible to aggregation because it is more exposed to mechanical stress and less likely to be trapped. Conversely, when milled using 5 mm grinding media (120 min, 600 - 700 rpm), the mechanically activated coal gangue shows a pronounced tendency toward aggregation/agglomeration. The particles become noticeably more rounded and lose their initial hexagonal shape, a phenomenon clearly confirmed by the SEM images in Fig 4.33(a-d). The morphology results in Fig 4.33(b-d) are not fully consistent with the results of particle sizes x_{10}, x_{50} and x_{90} in Fig 4.30, which decrease after 120 min. This inconsistency could be a consequence of the sample preparation in particle size distribution, as the mechanically activated coal gangue were dispersed in water as a dispersion medium, which could lead to a separation of the aggregation seen in the SEM image. This result is consistent with the explanations of Baláž and M. Achimovičová [187]. In a previous study, Vdovic et al. [188] reported a similar change in morphology, where the plate-like pseudohexagonal particle structure of the clay had become a polydisperse powder with irregularly shaped particles modified by intensive dry milling via planetary ball mill.

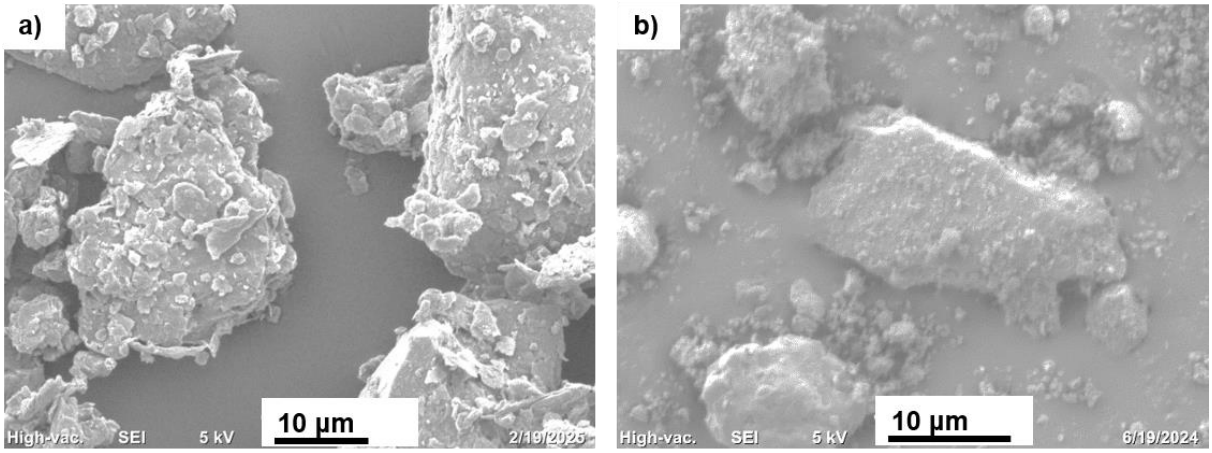

Fig 4.32: Morphology of (a) raw (b) d_{GM}=10 mm, 120 min,700 rpm

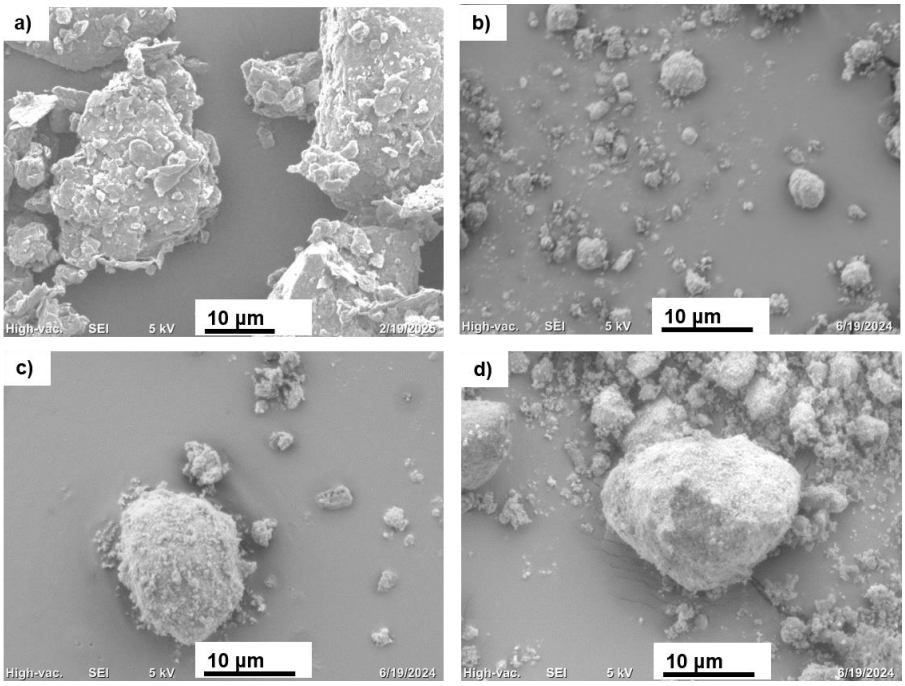

Fig 4.33: Morphology (a) raw, d_{GM} = 5 mm, 120 min (b) 600 rpm, (c) 650 rpm (d) 700 rpm

4.5.3 Specific surface area and cumulative pore volume

The coal gangue specific surface area S_{BET} and median particle size x_{50} as a function of grinding time of the raw and mechanically activated coal gangue are shown in Fig 4.34. The S_{BET} values were significantly higher for all mechanically activated coal gangue than for the raw coal gangue, 6.65 m^2/g. With a grinding time of 1 - 5 min, the specific surface area was between 8.52 and 15.56 m^2/g. Higher S_{BET} values of 18.063 m^2/g correlate with a finer median particle size x_{50} is 4.86 µm with a grinding time of 10 min. Boldyrev et al. [189] have highlighted a strong correlation between mechanical activation and specific surface area.

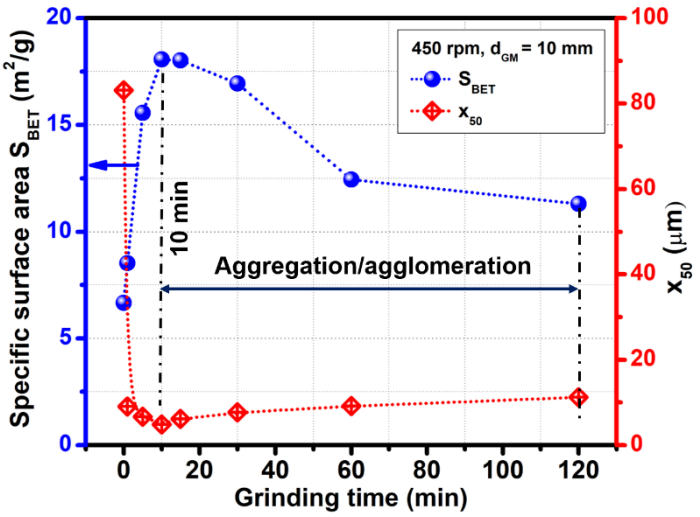

Fig 4.34: Specific surface area with median particle size as a function of grinding time

The specific surface area S_{BET} fell to about 18.023 m^2/g, 16.91 m^2/g, 12.47 m^2/g, and 11.30 m^2/g following increasing median particle size range 6.17 - 11.19 µm with grinding for 15 to 120 min. It is evident that the rate of formation of new surface is limited by time of mechanical activation and it appears that more intensive grinding conditions lead to a decrease in specific surface area S_{BET} values. In accordance with the theoretical grinding process, aggregation and agglomeration, which is driven by a decline of a specific surface area $S_{BET.}$ This is consistent with previously published research [127],[190] which showed that during the initial grinding phase, there was a decrease in median particle size and a rise in specific surface area S_{BET}. Regarding the reactivity of coal gangue as a heterogeneous material, the total surface area available to the alkaline solution reaction can be pointed out. The specific surface area S_{BET}, determined using the Brunauer-Emmett-Teller (BET) method, reflects the total surface area available for adsorption, including contributions from mesopores and macropores and geometric surface area S_m data collected from particle size distribution from laser particle size analyser (LPSA). The two specific surface area S_{BET} measured by the BET method can be compared with the geometric surface area S_m of coal gangue powder as shown in Fig 4.35.

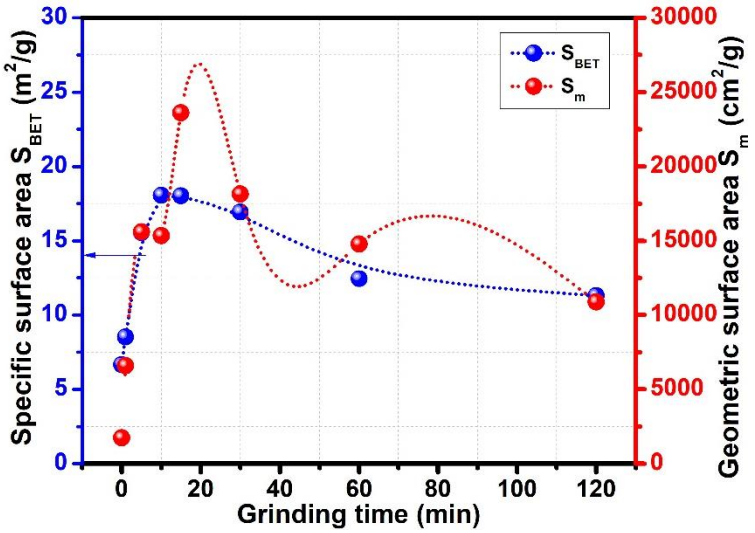

Fig 4.35: Specific surface area with geometric surface area as a function of grinding time

In this research, it can be seen that the two data set mechanically activated coal gangue over activation times of 0 - 1 min and 60 - 120 min is quite close to each other with values of 6.65 - 8.52 m^2/g and 12.447-11.30 m^2/g respectively, whereby the S_{BET} values show a slight deviation between 1.14 - 1.87 m^2/g. In contrast, the geometric surface area S_m, which represents the outer surface area of the particle's coal gangue, showed a much more pronounced difference. The values for S_m varied significantly from 1738 cm^2/g (raw) with mechanically activated coal

gangue 1 min of grinding (6585.10 cm^2/g) with a considerable difference of 4847.05 cm^2/g. In addition, the grinding of mechanically activated coal gangue with a grinding time of 60 - 120 min resulted in a range of 14,792.31-10,882.69 cm^2/g with a significant difference of 3909.62 cm^2/g. Nevertheless, the experimental observations regarding the geometric surface area S_m of coal gangue powder particles support fundamental to rationalize experiment observations even though the fact that the surface area measurements exploiting the physisorption of gases are much more accurate than simple geometric estimates [191]. Fig 4.36 displayed the cumulative pore size produced by the Barrett-Joyner-Halenda (BJH) technique model based on N_2 adsorption. Mesopores and macropores were found raw and mechanically activated coal gangue. Pores with a width of > 50 nm are defined as macropores, pores with a width of 2-50 nm are defined as mesopores and pores with a width of < 2 nm are defined as micropore [192]. In comparison to raw, continuous grinding increased the amount of cumulative pore volume.

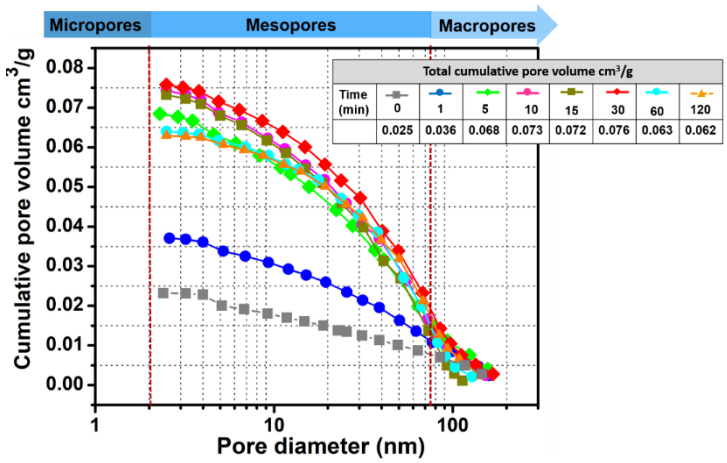

Fig 4.36: Cumulative pore volume of coal gangue with pore diameter (nm)

While the cumulative pore volume of raw coal gangue was 0.025 cm^3/g. Consequently, the cumulative pore volume decreased after 10 min of mechanically activated coal gangue due to aggregation as shown in Fig 4.37. It was likely that changes in the cumulative pore volume and specific surface area S_{BET} could be controlled by grinding time. Significant differences between various cumulative pore volumes can be explained by the porous structure of coal gangue. After 30 mi of grinding, there was an increase in cumulative pore volume to 0.076 cm^3/g. However, the specific surface area S_{BET} did not remain constant, as evidenced by a decrease in its value. Fig 4.29 shows a relative span (RS = 1.91) at 30 min of grinding, which reflects a distribution containing finer particles that likely contribute to the increase in cumulative pore volume. Between 60 to 120 min of grinding, strong aggregation and agglomeration reduced nitrogen penetration into the interior of the mechanically activated coal gangue. As a result, the

cumulative pore volume showed a slight decrease, ranging from 0.063 to 0.062 cm^3/g, while the specific surface area S_{BET} decreased from 12.47 m^2/g to 11.30 m^2/g. These findings align with similar studies conducted by Arbain et al. [193] and further indicate the influence of particle aggregation on the reactivity of coal gangue. This behaviour provides additional insight into the material's reactivity and its potential for use in geopolymer production.

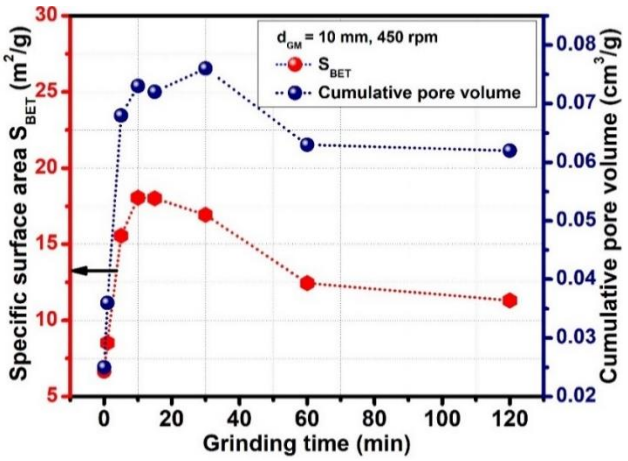

Fig 4.37: Specific surface area as cumulative pore volume with grinding time

4.5.4 Correlation specific surface area and specific grinding energy

The interpretation of the mechanical activation process relies on understanding the relationship between structural changes, such as specific surface area and the formation of fine particles in mechanically activated coal gangue, and the mechanical energy consumed during grinding. Based on the experimental results, the relationships between specific surface area S_{BET}, grinding time (min), and specific grinding energy were established, as shown in Fig 4.38.

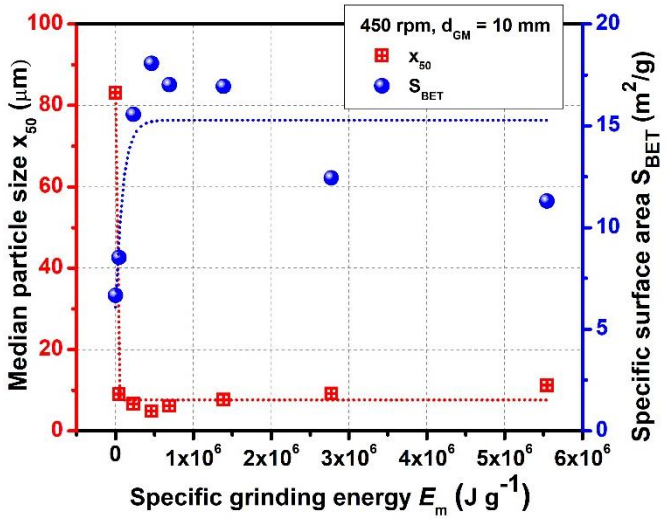

Fig 4.38: Grinding kinetics of mechanically activated coal gangue

The decrease in specific surface area S_{BET} is closely correlated with both the grinding time and the specific grinding energy. The specific grinding energy was calculated using the power consumed by the planetary ball mill with grinding media (P) and non-load power (P_0), along with the grinding time and the mass (m) of the coal gangue powder, as described in eq. (2).

$$E_m \left[\frac{\mathrm{J}}{\mathrm{g}}\right] = \int_0^t \frac{(P - P_o)}{m} dt \quad (2)$$

Fig 4.38 shows the specific grinding energy E_m consumed for each grinding time. The specific grinding energy E_m consumption data recorded range between 4.620E+04 - 2.310E+05 J g^{-1} for the grinding time 1-5 min with specific surface area S_{BET} of 8.52-15.56 m^2/g. The specific grinding energy for a grinding time of 10 min is 4.620E+05 J g^{-1}, whereby the specific surface area S_{BET} is highest at 18.063 m^2/g and decreases thereafter. At this stage, the specific grinding energy is proportional to the generated increase in specific surface area (SSA) related to Rittinger's stage [184]. It has been observed that the specific grinding energy leads to a decrease in the specific surface area S_{BET} after reaching the inflection point of the curve. In this case, the specific grinding energy is 6.930E+05 J g^{-1} for a specific surface area S_{BET} of 18.023 m^2/g and a grinding time of 15 min. These results are in agreement with previous studies by Mucsi et al. [194]. It should be noted that the specific grinding energy varies between 6.930E+05 and 2.7720E+06 J g^{-1}, which is due to the aggregation of the coal gangue with decreasing specific surface area S_{BET}. The total specific grinding energy for a grinding time of 120 min was 5.55E+06 J g^{-1}, with a specific surface area S_{BET} of 11.301 m^2/g. The results suggest that this effectively prevents any comminution as the addition of an order of magnitude of specific grinding energy has minimal effect on reducing particle size as the particle size approaches the grinding limit.

Next, the specific grinding energy is influenced by three operating parameters: rotational speed, grinding media size, and grinding time. The median particle size x_{50} is based on the fact that the stress energy *SE* and the number of collision frequencies *CF* influence the specific grinding energy. When analysing the relationship between the median particle size x_{50} of coal gangue and specific grinding energy, a notable trend emerges. The use of grinding media with a size of 5 - 10 mm leads to achieving an energy input of about 5.99E+05 - 7.07E+06 kJ g^{-1}, and the median particle size drops instantaneously. For grinding media size 5 mm, the results of the three different rotational speed 600 - 700 rpm are very close each other in term of the median particle size x_{50}. Both graphs in Fig 4.39(a-b) and Fig 4.40(a-b) clearly show that in design of

experiment, agglomeration that occurs at median particle sizes x_{50} rise causes the specific grinding energy to 1.20E+06 kJ g^{-1} at 30 and 60 min. In addition, it is noticeable, no agglomeration phenomena of mechanically activated coal gangue with grinding media size 5 and 10 mm after 120 min at specific grinding energy over 4.79E+06 kJ g^{-1}.

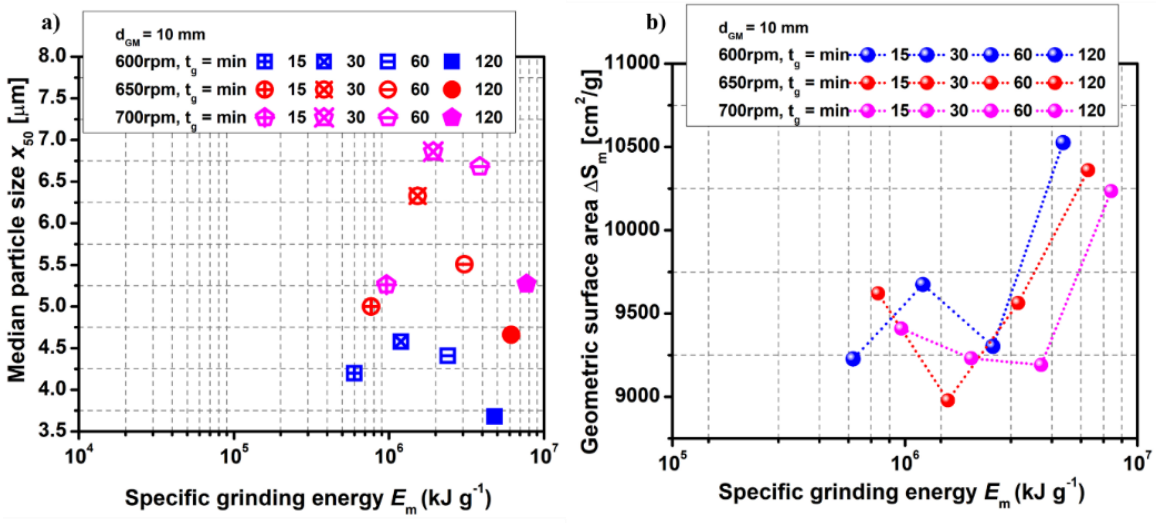

Fig 4.39: (a) Median particle size x_{50} and (b) geometric surface area S_m as function of specific grinding energy: 10 mm d_{GM}

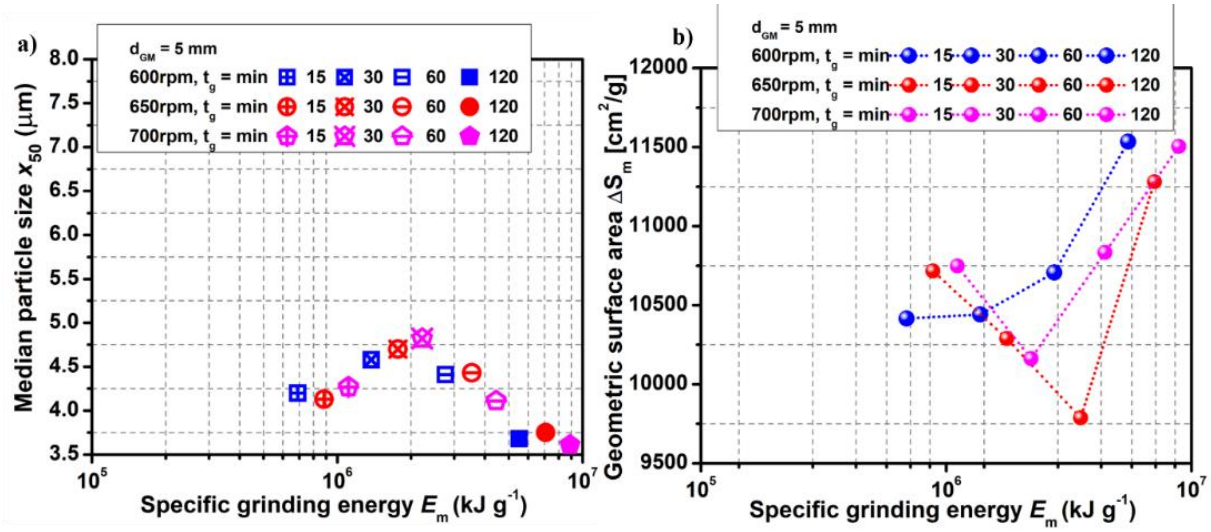

Fig 4.40: (a) Median particle size x_{50} and (b) geometric surface area S_m as function of specific grinding energy: 5 mm d_{GM}

Under optimal specific grinding energy conditions, the median particle size decreased while geometric surface area S_m increased within the ranges of 11,536 – 11505 cm^2/g for grinding media size 5 mm and 10,235 – 10, 525 cm^2/g for 10 mm, with no statistically significant difference between these ranges. Next, Juhász and Opoczky [117] propose that changes in

grinding material, specific surface area SSA, and x_{50} values can help identify different phases of the grinding process, such as the Rittinger, aggregation, or agglomeration sections in Fig 4.39 (a-b) and Fig 4.40 (a-b). Initially, as median particle size decreases, new specific surface area is generated proportionally. Austin and Bagga [195] in their research on cement clinker, demonstrated that the accumulation of fines inside ball mills leads to a decrease in specific surface area as the material becomes finer, eventually resulting in virtually no further increase in specific surface area. The experimental findings presented in Fig 4.39(a-b) and Fig 4.40 (a-b) can be effectively interpreted through the stress model proposed by Kwade and Schwedes [196], which suggests an optimal stress intensity SI for efficient grinding operations. This model defines an optimal stress energy SE level at which particle breakage and agglomerate disintegration occur most effectively. When the agglomerates come to pieces or the crystalline material breaks into pieces, this is called the optimum of the degree of stress energy SE. If the stress energy SE is below than the optimum, the behaviour of aggregates and crystalline materials is the same as the stress energy increases the fineness and specific surface area of the product both increases. If the stress energy SE is higher than the optimum, the situation is different. Conversely, when stress energy SE exceeds the optimum threshold, the dynamics change significantly. At this stage, no further increase in fineness is observed, as the agglomerates are already sufficiently disintegrated. For validation, the stressing intensity SI, defined as the ratio of stressing energy SE to the active mass m_A was calculated and plotted. Specifically, for a grinding media size d_{GM} of 10 mm, the active mass was found to range from 0.91 to 1.27 g when the rotational speed varied between 600 and 700 rpm over a grinding time of 120 min (Fig 4.41).

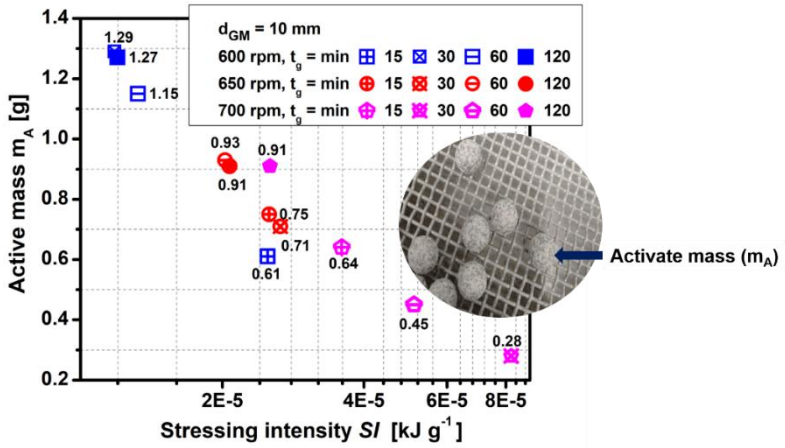

Fig 4.41: Active mass m_A as function of stressing intensity *SI*

The effects of the different relative span (RS) were also investigated with regard to the specific grinding energy in the mill, as shown in Fig 4.42(a-b). To discuss the effects of grinding media size and grinding time, the relative span (RS) was used to evaluate the width of the particle size distribution. As can be seen in Fig 4.42(a-b) the distribution becomes narrower as the particle size decreases. The relative span shows much higher values at a grinding media size of 10 mm (RS = 2.85), which means that the mechanically activated coal gangue material simultaneously represents coarse particles and has a broader particle size distribution curve. Therefore, relative span seems to function of morphology in Fig 4.42b. Whereas grinding media size 5 mm (RS = 2.58). This finding is consistent with the results of mean particle size previously studied by Altun et al. [197]. Their results clearly show that the process and design conditions influence the particle size. The wider the distribution, the larger the standard deviation and the span. On the other hand, Mucsi et al. [114] reported that (RS =18) represents a particularly fine size fraction.

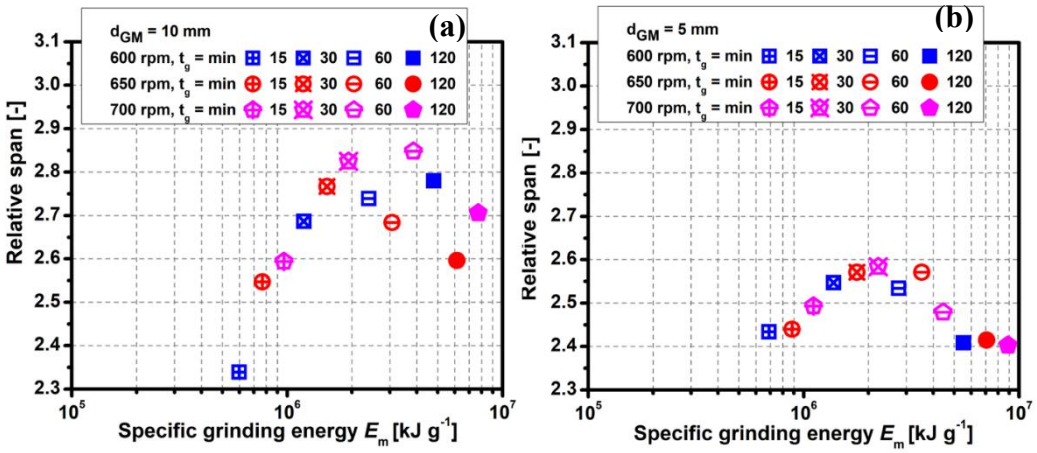

Fig 4.42: Relative span as a function of specific griding energy; (a) 10 mm and (b) 5 mm

4.5.5 The FT-IR of raw and mechanically activated coal gangue

The reactivity of mechanically y activated coal gangue at different grinding times involves a species on the surface of the particles that break its bond with the bulk lattice and form ions to react with an alkaline solution. To investigate the reactivity of coal gangue with varying grinding times, Fig 4.43(a-b) shows photograph images of raw and mechanically activated coal gangue with effects on functional groups with wavenumbers ranging from 4000 to 400 cm^{-1}. The photograph images, therefore, can potentially be applied to the observed physical properties changed of mechanically activated coal gangue as the colour of the raw coal gangue changes slightly toward light grey at different grinding time.

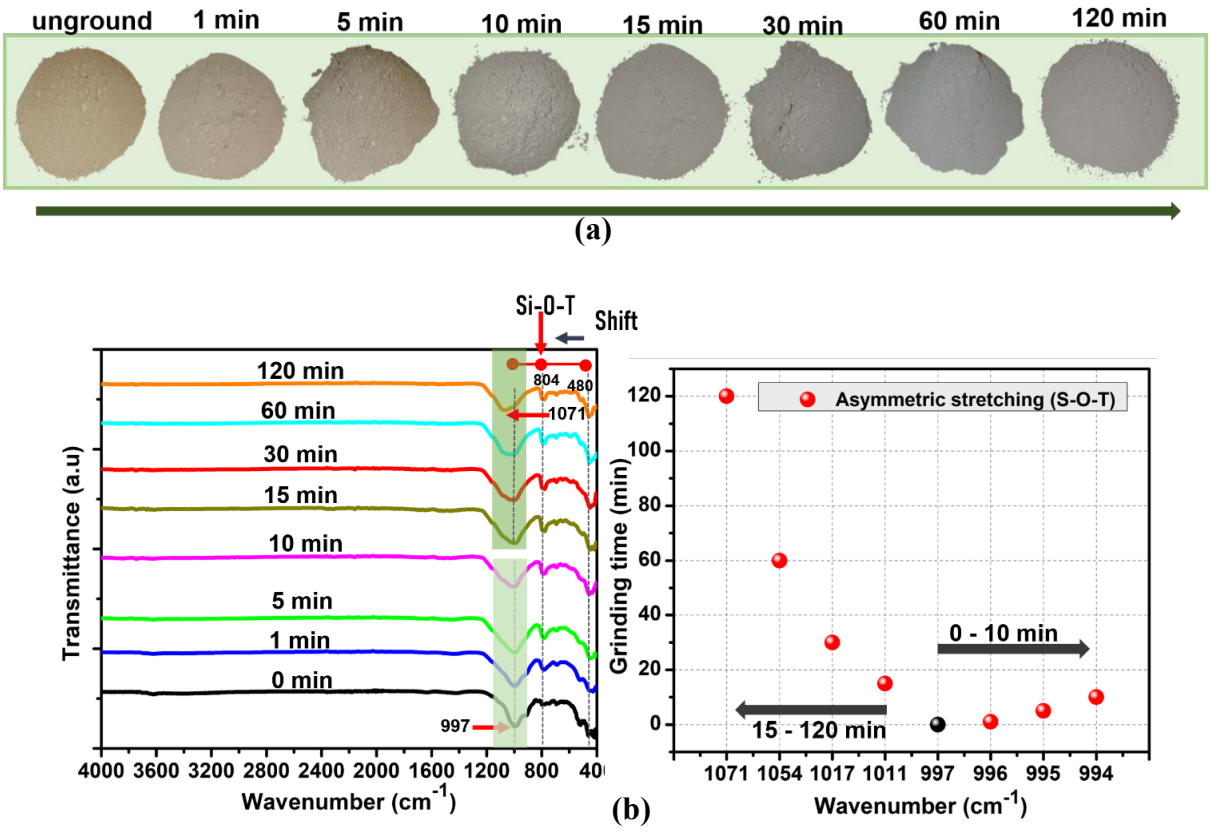

Fig 4.43: Raw and mechanically activated coal gangue (a) Photograph image (b) FT-IR

Consistent with the findings, Cristelo et al. [121] also observed changes in fly ash during mechanical activation. Their study, utilizing a ceramic bowl at 300 rpm for 15 - 240 min, highlighted a darkening of the fly ash after 240 min. This colour change was ascribed to the physical alteration of unburned carbon (coal) content, which became more prominent after prolonged mechanical activation. The potential of Fourier transform-infrared spectroscopy (FT-IR) for the quantification of minerals is therefore based on the fact that the particle size and surface defects are also affected by varying wavenumber depending on the mechanical stress [198]. Coal gangue is a type of silicate mineral characterized by strong atomic polarization due to silicon, resulting in high stability of the Si-O bonds. This study focuses on the positional shifts of key functional groups in response to varying grinding times, particularly the asymmetric stretching vibration of Si-O-T (T = Si or Al). The absence of significant absorption in the 3000 -3700 cm^{-1} indicates minimal hydroxyl stretching [147]. The asymmetric stretching vibration of Si-O-T initially appeared at 997 cm^{-1} in the raw sample. With prolonged grinding, this peak shifted to a higher wavenumber of 1071 cm^{-1} after 120 min, yielding a wavenumber ratio of 997/1071 cm^{-1} = 0.931. Additional shifts were observed at intermediate grinding times, from 1017 cm^{-1} to 1054 cm^{-1} (30 - 60 min) with a ratio of

1017/1054 cm^{-1} = 0.964, and from 1054 cm^{-1} to 1071 cm^{-1} (60 - 120 min) with a ratio of 1054/1071 cm^{-1} = 0.984. Two distinct grinding stages were identified, 1 - 10 min and 15 - 120 min. In the initial 1-10 min of mechanical activation, the asymmetric stretching vibration of Si-O-T shifted to lowest wavenumbers due to changes in interatomic distances and lattice vibrations [199]. In contrast to the mechanically activated coal gangue exhibited a shift toward higher wavenumbers and becoming broader after 15 min of grinding. Nevertheless, the loosening of interatomic bonding is a key consequence of the plastic deformation of solids, leading to the broadening of the wavenumber and increased amorphization due to a reduced degree of crystallinity [200]. While prior studies often explore grinding times ranging from 1 to 10 hours, typically 4 to 20 hours for crystalline materials and up to 120 min for amorphous phase, the study focuses on shorter grinding times (1-120 min). Within this time frame, it observed a reduction in the Si-O-T shift, which correlates with the degree of structural disorder introduced. This interpretation is further supported by a complementary phase analysis, which confirms a progressive decrease in crystallinity with increasing grinding time. Within this reduced time frame, the induced structural disorder was primarily influenced by the temperature generated during the grinding process. This thermal effect is an unavoidable consequence of the high-energy impacts and shear forces during grinding processing. A critical limitation of planetary ball mill is its inefficient heat dissipation, which leads to a rapid and uncontrolled rise in temperature. Under typical operating conditions, considerable frictional heat is generated during grinding in planetary ball mills, often raising temperatures to 90 - 120 °C [201]. However, it was a challenge to isolate the exact influence of temperature in this study, as it is inherently coupled to the mechanical energy input. This observation, combined with the presence of lattice defects in the Si-O-T network Fig 4.43b, suggests that the grinding process also contributed to a visible physical change in the coal gangue Fig 4.43a. In addition, the colour of the mechanically activated coal gangue could be a good indicator of the reactivity of the powder. Next for Design of Experiment (DoE), the typical broad absorption band in the range of 3600 - 3200 cm^{-1} was observed in raw coal gangue appearing as a relatively small peak Fig 4.44. This band is commonly attributed to the (-OH) stretching vibrations of hydrogen bonded water molecules or assigned to OH stretching vibrations more significantly, the structural hydroxyl groups within the clay minerals present such as kaolinite, muscovite and illite as from phase analysis in contain hydroxyl groups (-OH) as part of the crystal lattice [202]. However, a remarkable and significant change was observed in the wavenumber after mechanical activation of coal gangue. The observed (-OH) absorption band at 3600 - 3200 cm^{-1} became distinctly broader and more diffuse.

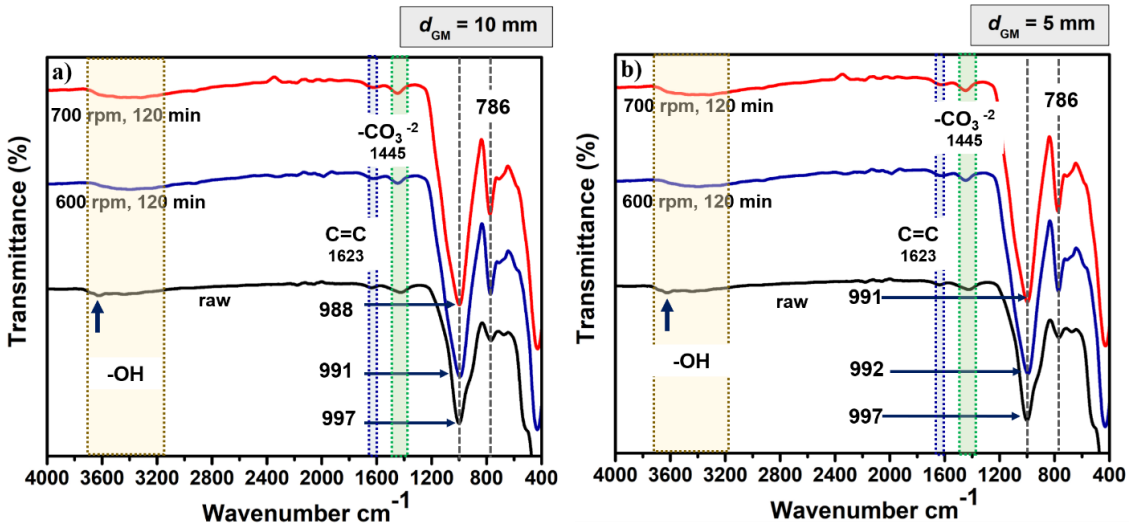

Fig 4.44: FT-IR analysis of raw and selected mechanically activated coal gangue (a) d_{GM} = 10 mm and (b) d_{GM} = 5 mm

A moderate peak observed at 1632 cm^{-1} in the spectra is attributed to the aromatic C=C stretching vibrations. This peak indicates the presence of carbon residues within the coal gangue, consistent with findings in previous studies [203],[204],[205]. The vibration band at wave number 1445 cm^{-1} also moderate intensity. This is due to the stretching vibration of CO_3^{-2} in carbonate ions, indicating that the gangue may contain carbonate [206],[207]. It is generally believed that the most intense peak of all tested samples occurs in the spectra around 1000 cm^{-1}, which corresponds to the asymmetric stretching vibrations of Si-O-T (T = Si or Al), which mainly correspond to silicon oxide and aluminium oxide. Comparing the asymmetric stretching region of Si-O-T at 997 cm^{-1} of raw coal gangue powder, it is found that the asymmetric intensity of mechanically activated coal gangue appears as a sharp band and shifts to lower frequencies. Mechanically activated coal gangue with grinding media 10 mm, 600 - 700 rpm and grinding time 120 min, the Si-O-T shift toward 991 - 988 cm^{-1} than mechanically activated coal gangue with grinding media 5 mm, 600 - 700 rpm and grinding time 120 min Si-O-T shift toward 992-991 cm^{-1}. Similar report according Leonal et al. [208] the alteration of Si-O-T at 1000 cm^{-1} asymmetric stretching. The position and intensity of the bands at 786 cm^{-1} are related to the symmetric stretching vibrations of the Si-O-Si bonds of quartz [209].

4.5.6 Phase analysis of raw and mechanically activated coal gangue

Fig 4.45 presents the X-ray diffraction (XRD) patterns of coal gangue before and after mechanical activation. Prior to mechanical activation, the raw coal gangue exhibits well-defined diffraction peaks characteristic of several crystalline phases, primarily kaolinite type

1:1 clay ($Al_2Si_2O_5(OH)_4$), illite type 2:1 clay ($(K,H_3O)Al_2Si_3AlO_{10}(OH)_2$), albite a mineral from feldspar group ($NaAlSiO_8$), muscovite ($H_2KAl_3(SiO_3)$ and quartz (SiO_2). These findings align with the mineralogical composition previously reported by Gao et al. [210] for similar coal gangue materials.

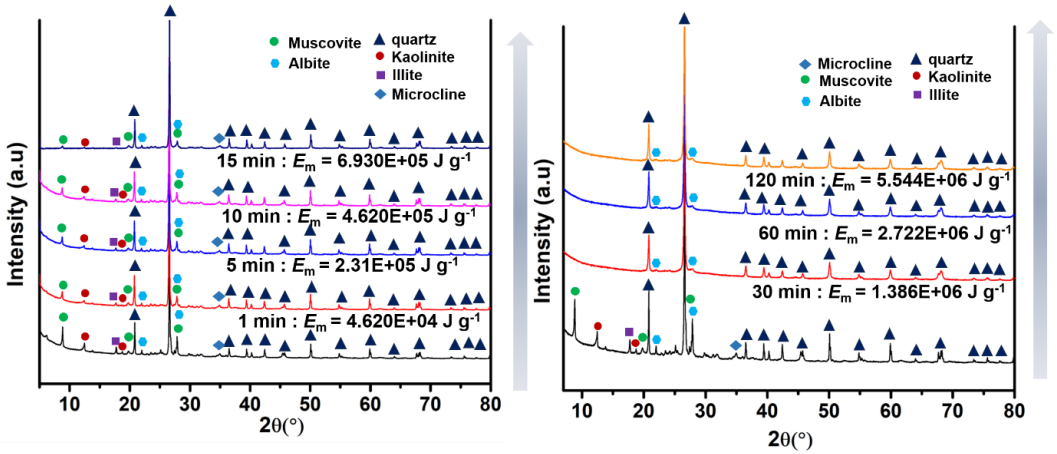

Fig 4.45: XRD pattern of raw and in planetary ball mill mechanically activated coal gangue

Furthermore, the mineralogical of coal gangue resemble that typically observed in mine tailings predominantly consisting of quartz, feldspar, albite, and muscovite [39,40]. The first 10 min of mechanically activated coal gangue resulted limited reduction in the intensity of these mineral peaks, particularly kaolinite, microcline, illite and albite suggesting that the short grinding time was not sufficient to cause significant amorphization of the crystal structures. However, after 15 min of grinding, a slightly decrease in the peaks associated with kaolinite, microcline, illite and albite was observed, indicating the onset of structural disruption and amorphization. Mitrović and Zdujić [211], reported that, after 15 min of grinding kaolin, the characteristic XRD peaks of kaolinite nearly disappeared, indicating a significant loss of crystallinity and the amorphization. Tole et al. [212] have demonstrated the peak of kaolinite as minor mineral with grinding time 20 min disappear by removing the structure of internal hydroxyl and become amorphous. After 30 min of grinding, the XRD signatures of these phases disappeared completely, with the exception of albite and quartz, which remained visible. This pattern is consistent with previous findings. For example, Baki et al. [213] reported a persistence of the muscovite peak after 20 min of grinding, while other researchers observed a complete disappearance of the kaolinite peak within 15 - 20 min of mechanical activation [214]. At longer grinding times (30 - 120 min), corresponding to specific grinding energy 1.386E+06-5.55E+06 J g^{-1}, the albite a type of feldspar mineral reflections where significantly reduced and still visible suggesting partial amorphization. This indicates partial amorphization, as also

shown by the progressive decrease in the line broadening with grinding time due to reduction in crystallite size and increase in the lattice strain. In fact, the observed broadening is the convolution of three types of broadening the instrument broadening, the crystallite size broadening and strain broadening [215] [216]. A related study by Yao et al. [217] showed that feldspar undergoes an increasing degree of amorphization under conditions (planetary ball mill, 500 rpm with 5,8,15 mm grinding media diameter) between 20 and 200 min of grinding. Other researcher who study mechanical activation of vanadium tailing for geopolymer, feldspar peak decreasing with grinding time and significant of a significant decrease in peak intensities was detected in the sample milled for 5 h [218]. In contrast, the quartz peak remained sharp and did not show significant change throughout all grinding times, reflecting its high crystallinity and resistance to mechanical activation breakdown. Quartz is probably not altered due to its higher hardness (its Mohs hardness is 7) [219]. This observation aligns with findings by Chen et al. [220] who reported similar structural persistence in quartz during milling. Kohobhange et al. [221] demonstrated that even after prolonged milling (360 hours), quartz undergoes negligible polymorphic transformation. The experimental design, particularly the parameters of mechanical activation, plays a crucial role in dictating the phase transformations within coal gangue. Building upon previous investigations, by Tole et al. [222], which demonstrated the complete amorphization of kaolinite after 20 min of grinding. For comprehensive phase analysis, a grinding media size 5 - 10 mm, a grinding time of 120 min, and a rotation speed of 600 - 700 rpm selected. These parameters were chosen to investigate the extent of structural changes and amorphization achievable. Furthermore, these specific conditions were also utilized to explore whether adopting minimum and maximum values within the design of experiment would significantly alter the phase composition of the mechanically activated coal gangue. The bonded complex of coal gangue is held together with other minerals such as carbonate, quartz, muscovite and feldspar not by chemical bonding but by intermolecular attraction (Van de Waals) between the weak bonds. The phase transformation of a solid coal gangue is highly dependent on the grinding process and the most important specific grinding energy. Mechanical activation of coal gangue induces significant structural transformations characterized by progressive crystal lattice distortions and enhanced defect formation. The transition from crystalline to amorphous phases at the particle surface represents a critical structural reorganization that fundamentally alters the mechanically activated coal gangue reactivity. It was observed and shown in Fig 4.46(a-b) that the peak of albite reflections was still visible even at the highest specific grinding energy range 7.71+06 kJ g^{-1} - 8.89E+06 kJ g^{-1}, while be attributed to the strong layered structures that remained stable.

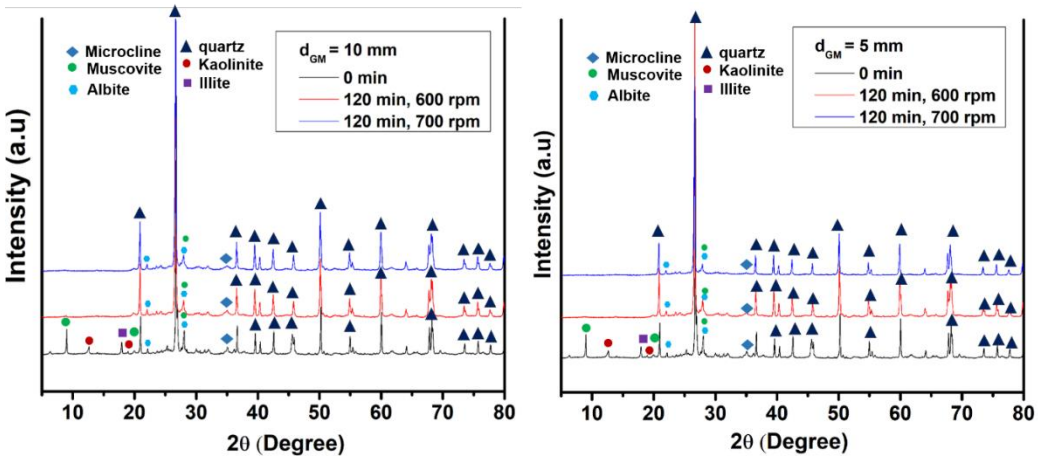

Fig 4.46: XRD analysis of mechanically activated coal gangue; (a) d_{GM} = 10 mm and (b) d_{GM} = 5 mm

On the other hand, based on XRD results albite phase remained almost unchanged, although a slight broadening of the characteristic peak was observed, suggesting plausible crystallite size reduction and accumulation of lattice strain. Quartz still retained some crystallinity even under the most intense conditions. Quartz is probably not altered due to its higher hardness (Mohs hardness = 7) [223]. Moreover, according to a few researchers [25],[26] the due to higher hardness is 7, quartz also acts as a grinding media for the kaolinite particles, thus accelerating the grinding process. It is noteworthy that in all samples during the mechanical activation process of the coal gangue, the intensity of grinding media size 5 - 10 mm, 600 - 700 rpm and 120 min the characteristic peak in albite did not disappear. This indicates that the specific grinding energy transferred to the coal gangue powder by the different grinding media of size 5 - 10 mm causes the formation of point defects in the crystal lattice or dislocations on the surface of the gangue powder and maintains their inert particle that are not reactive.

4.5.7 Leaching of raw and mechanically activated coal gangue

To investigate the effects of mechanical activation at different grinding times (1 - 120 min) and the corresponding changes in specific surface area S_{BET}, the leaching rates of silica (Si) and alumina (Al) from both raw and mechanically activated coal gangue in an 8 M NaOH solution presented in Fig 4.47. The results are essential for the estimation of alumina (Al) and silica (Si) and how the decrease in specific surface area S_{BET} leads to aggregation and agglomerates of the mechanically activated coal gangue, which may affect the properties of the geopolymer.

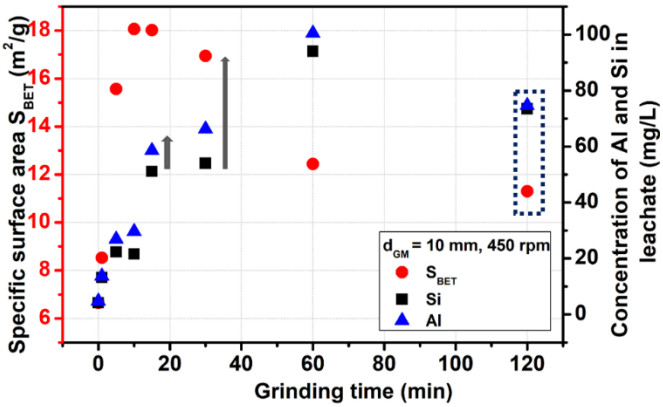

Fig 4.47: Concentration of Al and Si with specific surface area as function of grinding time

The geopolymerization process involves the alkaline activator breaking the $[AlO_4]^-$ and $[SiO_4]^-$ bonds in silicate mineral based raw materials, thereby facilitating the reaction of the $[AlO_4]^-$ and $[SiO_4]^-$ structural monomers in a strong alkali solution. In this study, sodium silicate was also introduced to reinforce the core structural framework of the geopolymer [224]. Consequently, the availability of reactive silica (Si) and alumina (Al) was investigated, as these elements play a crucial role in the gelation process and the overall formation of the geopolymer matrix. The reactive silica (Si) and alumina (Al) content increased after mechanical activation using a planetary ball mill compared to raw coal gangue. As shown in Fig 4.47, the leaching rate of alumina (Al) increased from 5.68mg/L (raw coal gangue) to 101.48 mg/L, while the leaching rate of silica (Si) increased from 4.16 mg/L to a maximum of 93.96 mg/L after 60 min of grinding. Even at shorter grinding times, the impact was evident. For instance, after 10 and 15 min of grinding, the leaching rates for silica (Si) ranged from 21.6 - 51.04 mg/L, and for alumina (Al), they were between 30.6 - 59.6 mg/L. These values continued to climb as grinding progressed, reaching their peak at 60 min. However, a slight reduction in dissolution was observed after 120 min of grinding, with silica (Si) at 73.52 mg/L and alumina (Al) at 75.6. mg/L. Mechanical activation enhances the reactivity of coal gangue by increasing its specific surface area S_{BET} and inducing structural deformations at the particle surfaces, which generally accelerate the leaching process. However, as seen in Fig 4.47, prolonged grinding (120 min) leads to particle agglomeration, significantly affecting the release of silica (Si) and alumina (Al) due to the reduction in specific surface area S_{BET}. The key finding here is that while excess energy stored in the lattice enhances the dissolution of silica (Si) and alumina (Al), agglomeration counteracts this effect, slowing down their release. A similar trend was reported by Rescic et al. [126], who found that the concentration of silica (Si) extracted from kaolin for geopolymer applications decreased after 40 min of grinding in a planetary ball mill at 720 rpm.

However, the study did not explicitly attribute this decline to aggregation or agglomeration. Additionally, previous studies [127],[128] have consistently reported that silica (Si) and alumina (Al) leaching generally increases with grinding time.

4.5.8 Saturated lime solution test of raw and mechanically activated coal gangue

Mechanical activation is a highly effective method for enhancing the pozzolanic reactivity of as the layered coal gangue (phyllosilicates) can undergo structural rearrangements, yielding partially disordered alumina and silica rich phases [225]. This surface structural transformation, occurring at rotational speed within the range of 450 - 700 rpm, is a key factor in improving its reactivity. The increased reactivity is attributed to the disruption of the crystalline lattice, which provides more sites for reaction with calcium hydroxide $Ca(OH)_2$. In this test, the amount of CaO uptake by the mechanically activated coal gangue over a specific period serves as a quantitative indicator of its reactivity, reflecting both its maximum lime binding capacity and the kinetic rate of the binding reaction. Higher CaO uptake signifies greater pozzolanic reactivity. This method, along with a particle size reduction below 5 µm, can lead to materials with excellent reactivity, sometimes referred to as high-reactivity by some authors [226]. While chemical composition and structural disorder are critical, specific surface area is another influential factor in pozzolanic reactivity. Thus, mechanically activated coal gangue for 15, 60, and 120 min were selected for further analysis to investigate this phenomenon. As visually demonstrated in Fig 4.48, the 120 min mechanically activated coal gangue exhibited the highest pozzolanic reactivity, with a CaO uptake of 276.6 mg/g.

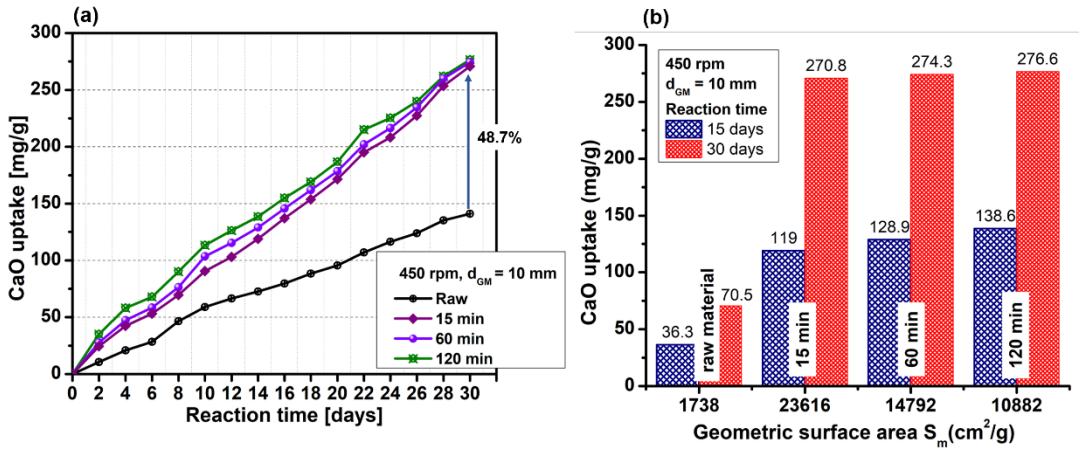

Fig 4.48: The CaO uptake value (a) reactions time (b) geometric surface area

This mechanically activated coal gangue also showed significant swelling after 30 days in the saturated lime solution, evidenced by a substantial 47.8% change in CaO uptake compared to the raw coal gangue. While a higher specific surface area is generally considered beneficial for pozzolanic reactivity, the results of this study reveal a more complex relationship. A direct relationship was not observed between the geometric surface area and the pozzolanic reactivity of the mechanically activated coal gangue. For example, the 120 min mechanically activated coal gangue had a lower geometric surface area of 10,882 cm^2/g compared to the 15 min mechanically activated coal gangue 23,616 cm^2/g. This behaviour suggests that structural disorder plays a more dominant role in enhancing pozzolanic reactivity than specific surface area alone. The extended grinding time for the 120 min mechanically activated coal gangue, despite leading to particle agglomeration and a lower overall surface area, was more effective in breaking down the crystalline structure of the coal gangue. This created a greater proportion of highly reactive of surface particle, amorphous phases. Therefore, the presence of more reactive material outweighed the disadvantage of a smaller surface area, resulting in superior pozzolanic activity. Design of Experiment (DoE) of coal gangue mechanically activated at 600 - 700 rpm (Fig 4.49 and Fig 4.50), an unexpected trend was observed. The 60 min mechanically activated coal gangue exhibited the highest CaO uptake. While the mechanically activated coal gangue 120 min showed a slower decrease, this behaviour is surprising given its higher specific surface area. The lower CaO uptake of the 120 min of mechanically activated coal gangue, despite its larger geometric surface area, points to potential issues such as particle agglomeration. This finding underscores the importance of process control to ensure a uniform and consistent product, maximizing the benefits of mechanical activation.

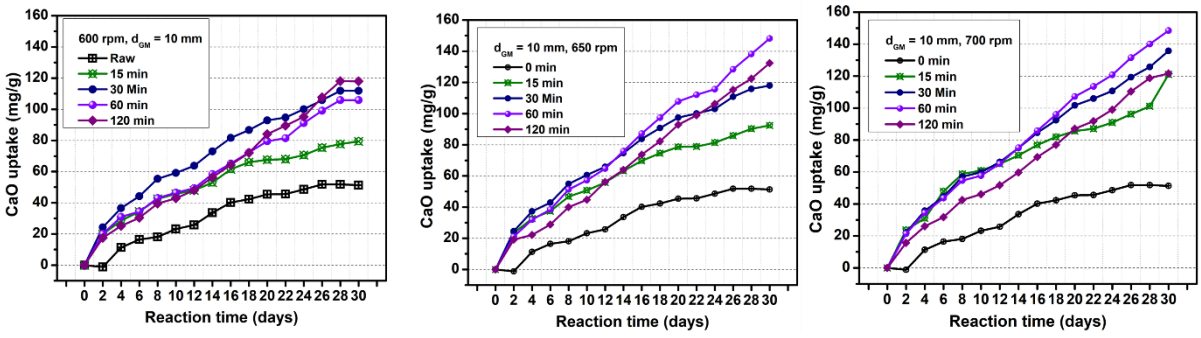

Fig 4.49: The relationship between CaO uptake and reactions time for raw and mechanically activated coal gangue

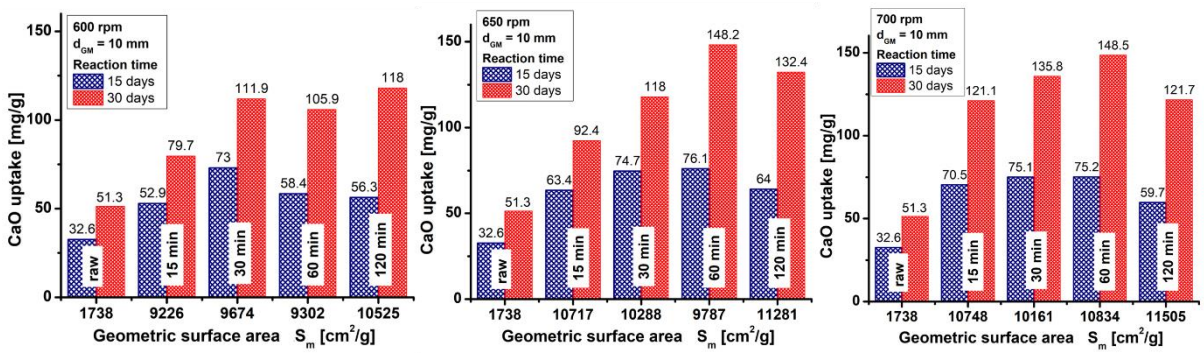

Fig 4.50: Relationship between CaO uptake and geometric surface area for raw and mechanically activated coal gangue

4.6. Performance of geopolymer produced using mechanically activated coal gangue by a planetary ball mill

4.6.1 Effect of NaOH concentration on geopolymerization

Before utilizing a mechanically activated coal gangue for geopolymer production, it's crucial to experimentally determine the optimum alkali activator concentration. An excessive amount of alkali can negatively impact the geopolymer strength. Therefore, the influence of NaOH concentration on the 7 days compressive strength was investigated, using a mechanically activated coal gangue with a median particle size x_{50} of 6.17 µm. In this optimization, the curing was 24 hours. A range of NaOH molarities (8 M, 10 M, and 12 M) were investigated, as shown in Fig 4.51(a).

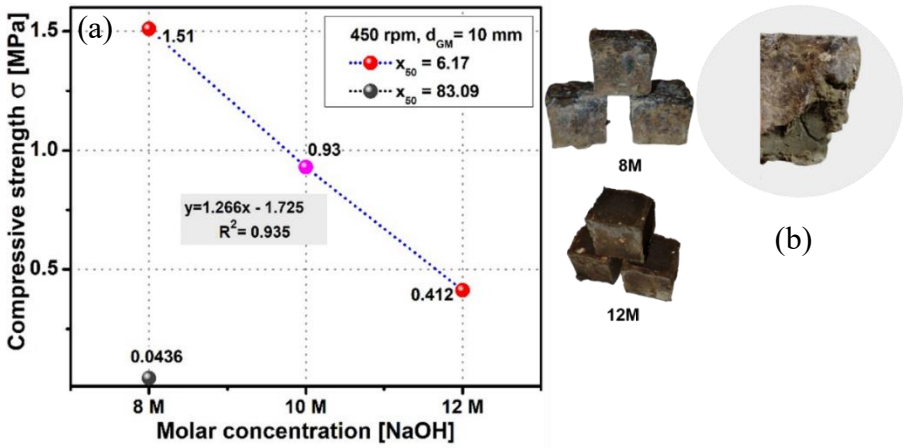

Fig 4.51: Effects of NaOH concentration on the 7-day compressive strength of geopolymer.

The geopolymer sample this molarities consistently exhibited relatively low 7 days compressive strengths, specifically 1.51 MPa, 0.93 MPa, and 0.412 MPa, respectively. This trend indicates a decline in strength beyond certain NaOH concentrations, with the optimal compressive strength observed at 8 M. The observed low compressive strengths suggest that, for geopolymer produce with median particle x_{50} of 6.17µm, an alkaline activator consisting solely of NaOH within the ratio NaO_2/SiO_2 range of 1.99 to 2.74 is insufficient to trigger geopolymerization processes. While this molarities OH^- contributed increasing amounts of intended to form a homogeneous matrix, leading to polycondensation and the formation of a 3D network (typically zeolite-like), was therefore hindered. The inherent rigidity of the geopolymer network is provided by covalent and ionic inorganic bonds, forming polysialate represented by the empirical formula eq. (3):

$$M_n\ (-(SiO_2)_z - AlO_2)_n\ \ wH_2\ O \qquad (3)$$

Consequently, it is necessary to apply this theory to explain the result, since the negatively charged and tetrahedrally coordinated Al^{3+} atoms inside the network are charge-balanced by alkali metal cations from the activating solution. This phenomenon can also be explained by the brown colour and increased viscosity/ductility observed in geopolymer samples treated only with 8 - 12 M NaOH solutions. For example, the image of a specimen during compressive tests is shown in Fig 4.51(b). This aligns with the mechanism proposed by Kumar et al. [104], who suggest that the particles are only coated by the alkaline solution, forming a dense gel. A similar finding was also noted by Essaidi et al. [227].

4.6.2 Effect of NaOH: Na_2SiO_3 concentration on geopolymerization

On the other hand, the trend observed in the mechanical strength of geopolymers with 8 M can only be explained by the addition of extra Na_2SiO_3 as shown in Fig 4.52. The compressive strength of all geopolymer increased with increasing age. The SiO_2/Al_2O_3 ratios considered in this study ranged from 5.83 to 7.94, as the Al component of the coal gangue tends to dissolve more easily than the silicon component. Previous studies have shown that blends with SiO_2/Al_2O_3 ratios of 3.0 - 3.8 have better strength properties. In addition, the ion dissolution rate of mechanically activated coal gangue increased significantly with increasing grinding time, indicating that the mineral structure of the coal gangue powder changed after mechanical activation. This exposed more active surfaces, which added more active substances to the whole system, leading to a significant increase in the geopolymer system. The reason for this

was that after different grinding times, the mineral structure of the coal gangue was destroyed and the active minerals, such as silicate and aluminate, which were trapped inside were exposed. In addition, as the particle size decreased, there was greater contact with the alkaline solution, resulting in more hydration products, which in turn increased the strength of the samples.

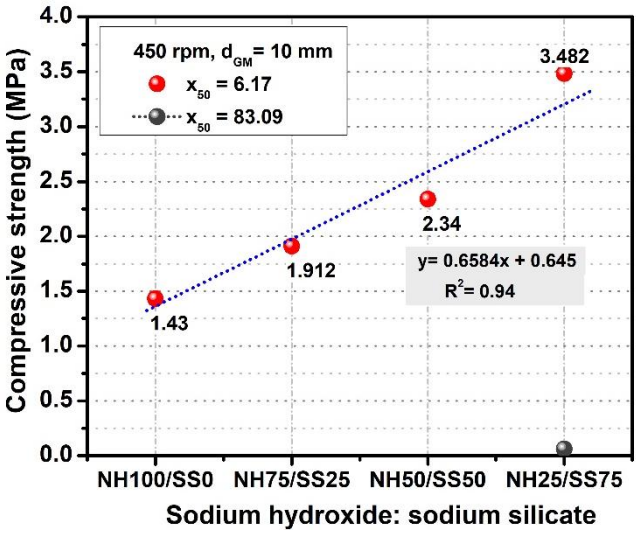

Fig 4.52: Effects of the NaOH: Na_2SiO_3 concentration ratio on the 7-day compressive strength of geopolymer.

4.6.3 Effects of temperature

The results of testing the compressive strength of coal gangue geopolymer and different curing temperature are shown in Fig 4.53. As predicted and observed, the median particle size x_{50} 6.17 µm have effect on the compressive strength of the geopolymer specimens. As the result, the geopolymer can curing with 70 °C at 24 hours. Based on studies, using median particle x_{50} of 6.71 µm and optimization, all mechanically activated coal gangue were tested.

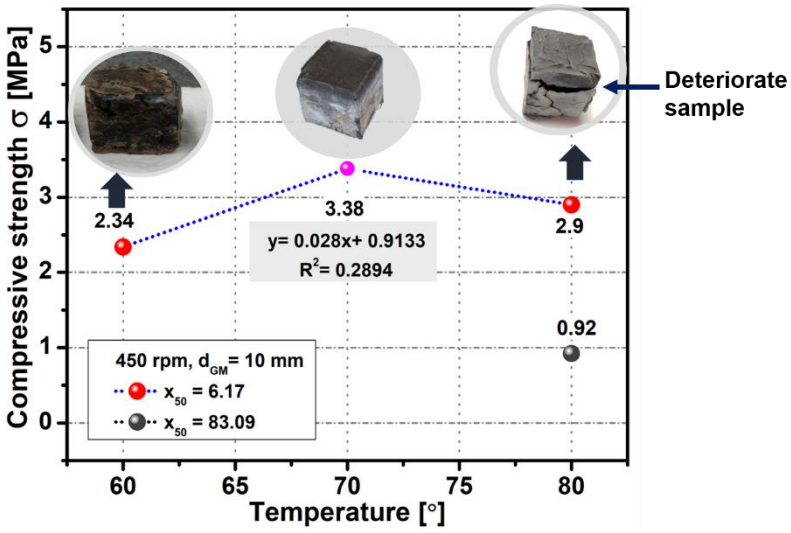

Fig 4.53: Effect of curing temperature on the 7-day compressive strength of geopolymer

4.6.4 Visual observation of geopolymer samples

The effect of different grinding times of coal gangue on the geopolymer sample is shown in Fig 4.54. One factor that also be considered when using coal gangue as a mechanically activated precursor is the colour of the resulting mechanism of complex geopolymerization [228]. The geopolymer sample exhibits a dark grey coloration (raw) accompanied by noticeable large cracks on the outer surface and visible traces of evaporated water within the geopolymer sample.

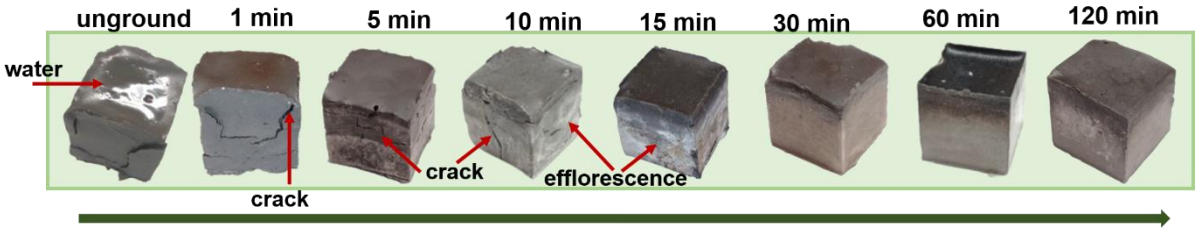

Fig 4.54: Visual observation of coal gangue geopolymer

Even with a relatively short grinding time of just 1 min of mechanically activated coal gangue, a noticeable widening of cracks was observed in the geopolymer sample. It is evident that all samples undergo a transition from the typical dark grey colour to a lighter shade of grey, with the extent of colour change varying depending on the grinding time. This change in coloration can be attributed to the loss of water and the reaction of geopolymerization [229]. Additionally, smaller and finer cracks become noticeable in the sample ground for 5 - 10 min. The removal of water and hydroxyl ions disrupted the polymeric network, leading to the formation of vapor and a gradual increase in pore pressure within the geopolymer gel phase. When this pressure

exceeded the capillary limit of the gel phase, micro-cracking occurred [230]. Moreover, the formation of the gel $[M_z(AlO_2)_x(SiO_2)_y \cdot MOH \cdot H_2O]$ which essentially depends on the degree of dissolution of alumino-silicate materials, is a dominant step in geopolymerization. Alumino-silicate solids react with alkaline solution and form a gel layer [231]. Although coal gangue exhibits a much finer particle size and an increase in specific surface area S_{BET} from 6.6 m^2/g (raw) to 18.06 m^2/g, the contribution of silica (Si) and alumina (Al) minerals to the gel phase is insufficient in the alkaline solution to initiate effective geopolymerization. As a result, this geopolymer forms fewer gelling substances, leading to weak adhesion between the gels and coal gangue particles, a loose structure, and the formation of noticeable cracks [232]. Therefore, the occurrence of cracks is dependent on the reactivity of the coal gangue. In addition, with increasing grinding times of 10 - 15 min, white spots were observed on the geopolymer surface. According to previous studies [233], these efflorescence, characterized by white patches, are caused by excess unreacted Na^+ ions during polymerization. These ions diffuse to the surface and interact with CO_2 in the atmosphere, forming white sodium carbonate deposits on the surface, as described by equation (4) and (5) [234]. Although the cumulative pore volume mechanically activated ranges from 0.072 to 0.073 cm^3/g for coal gangue ground for 10 - 15 min (as shown in Fig 4.36), which significantly increases the migration of the alkaline solution inside the coal gangue particles, efflorescence still occurs due to the incomplete geopolymerization reaction. This is because the alkaline activator, sodium silicate, is a product of silica sand and sodium carbonate [90]. Similar sodium carbonate efflorescence, containing varying amounts of structural Na^+, has been reported by other researchers [235].

$$CO_2(g) + 2OH^-(aq) \rightarrow CO_3^{2-}(aq) + H_2\,O \quad (4)$$

$$2\,Na^+(aq) + CO_3^{2-}(aq) + nH_2O \rightarrow= Na_2\,CO_3\,.nH_2O(s) \quad (5)$$

Moving forward, continue with the investigation of the physical properties of geopolymers produced from mechanically activated coal gangue with 600-700 rpm and grinding media 5 - 10 mm. The photograph of visual observation of geopolymers made from coal gangue with grinding media of size 5 - 10 mm and 600 - 700 rpm is shown in Fig 4.55. As shown in this study, the design of experiment demonstrates a strong influence of mechanically activated coal gangue on the geopolymer.

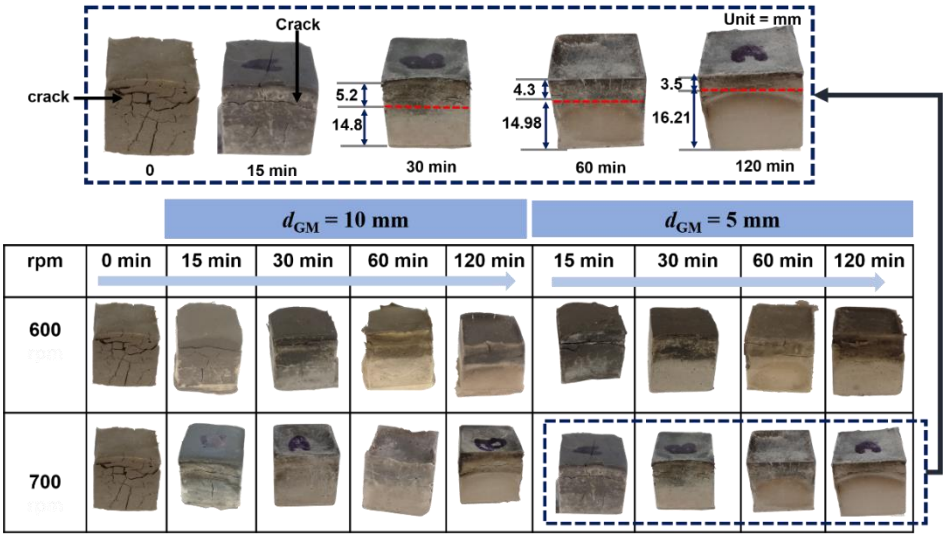

Fig 4.55: Visual observation of coal gangue geopolymer with d_{GM} = 5 - 10 mm, 600 - 700 rpm

The colours of the geopolymer samples became brighter due to improve of reactivity of the coal gangue after 15 min of grinding. Furthermore, in geopolymer samples with a grinding time 15 min it can be seen that crack distribution appearing on the specimen's surfaces. The different water transport rates in large and small pores can lead to different behaviour. However, when more water accumulates in the large pores, it evaporates quickly into the environment due to the high transport coefficients of the large pores. When the water vapor pressure reaches the maximum limit, the dense matrix with lower permeability can no longer absorb the high thermal stresses, which leads to intense thermal cracking on the sample surfaces due to thermal shrinkage. Turning to next investigation of different grinding speed, it can also observe the appearance of the geopolymer from raw to a different design of experiment, not only the change in colour from dark colour of grey (raw) to black (15 min grinding) but can seem clearly two different tones of colour of geopolymer samples with grinding time 30 - 120 min. This finding is probably due to the unhardened sample between 3.5 - 5.2 mm, as shown in Fig 4.55 due to the shorter curing time. The time required for the aluminium-silicate solution to form a fully cured gel depends on the reactivity of the coal gangue. Therefore, a stronger formation of ion pairs is expected, leading to more long-chain silicate oligomers as well as Al-O-Si complexes. Mechanical activation process of the coal gangue appears to promote geopolymerization, however, the reaction in this study requires a longer curing time of more than 24 hours. This indicates that the curing temperature plays an important role in the densification and curing of the geopolymer sample.

4.6.5 Morphology analysis of geopolymer samples

In raw coal gangue, the coordination number of Al-O and Si-O bonds may not have been fully broken, limiting the effectiveness of the bond with the alkaline activator. This lack of complete dissolution results in loose, coarse or unreactive particles that do not bond effectively with the alkaline activator, leading to cracks propagation and voids in the surface of the geopolymer sample. This phenomenon is further supported by the morphology observed in the optical microscopy images shown in Fig 4.56 and scanning electron microscope in Fig 4.57. The geopolymer derived from 30 min of mechanically activated coal gangue exhibited a less dense microstructure due to insufficient activation time. This inadequacy resulted in the persistence of coarse unreacted particles in the matrix. As the result, irregularly shaped particles, not covered by the reaction gel, can be observed in Fig 4.56(b) and Fig 4.57(b).

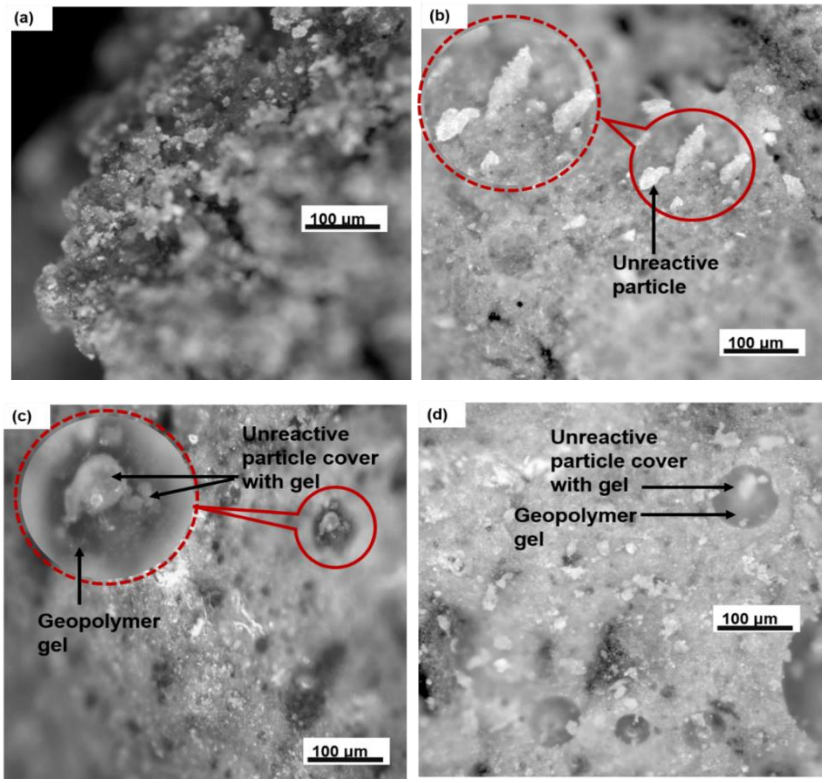

Fig 4.56: Morphology of geopolymer via optical microscope a) raw material, mechanically activated coal gangue (b) 30 min (c) 60 min (d) 120 min

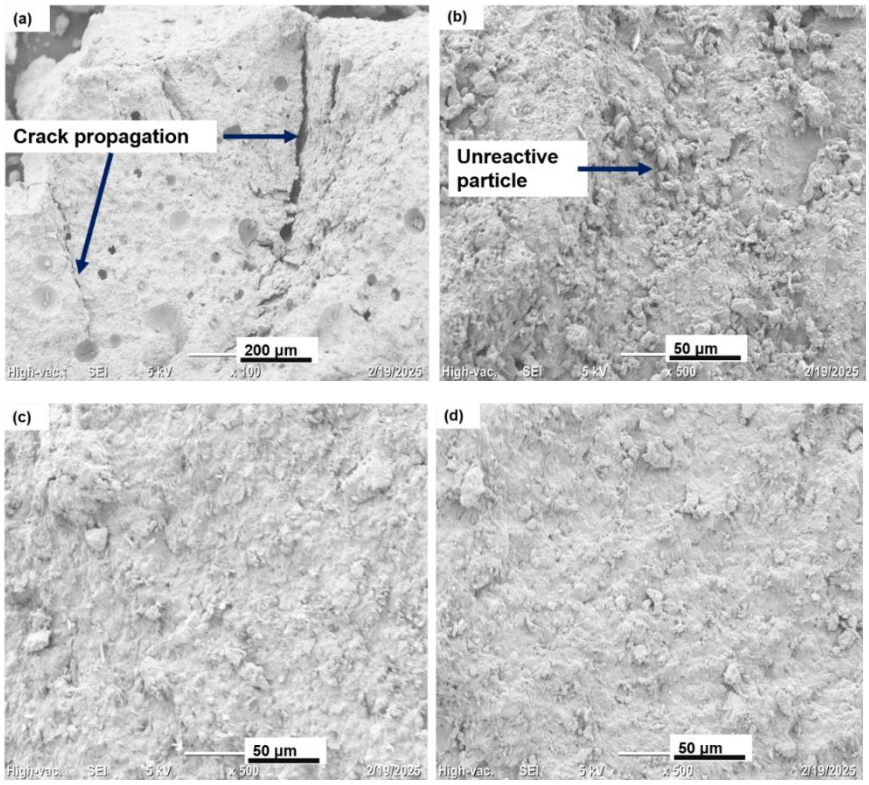

Fig 4.57: Morphology of geopolymer via SEM (a) raw material, mechanically activated coal gangue (b) 30 min (c) 60 min, (d) 120 min

This phenomenon can be attributed to insufficient mechanical activation at this grinding time even though the peak of kaolinite, illite, muscovite and microcline disappear leaving less unreactive albite and quartz domains. The results revealed that the amorphization degree of albite was different with grinding time and specific grinding energy, thus the contribution to the improvement of the reactivity of coal gangue. This was attributed to the greater availability of reactive $[AlO_4]^-$ and $[SiO_4]^-$ from the partial amorphization of albite. As a result of mechanical activation, coal gangue subjected to prolonged grinding times of 60 - 120 min demonstrated significantly improved geopolymerization activity. This enhancement is attributed to the increased formation of gel, which contributed to the development of a denser and more cohesive microstructure. Consequently, it can be reasoned that through mechanical activation, mechanically activated coal gangue is likely more reactive after 60 - 120 min, as the result geopolymer matrix displayed improved structural cohesion, with particle connections becoming more compact, uniform, and homogeneously distributed except in quartz rich regions, as illustrated in Fig 4.56(c-d) and Fig 4.57(c-d). The presence of the geopolymer gel played a crucial role in the development of compressive strength. These findings are consistent with the studies of Zhang et al. [236] and Elfwal et al. [237]. Next, Fig 4.58 show the

morphology selected resulting geopolymers. The Fig 4.58(a-b) with design of experiment d_{GM} = 5 mm, 120 min, 600 -700 rpm appear to be porous and contained a notably more significant number of unreacted coal gangue particles.

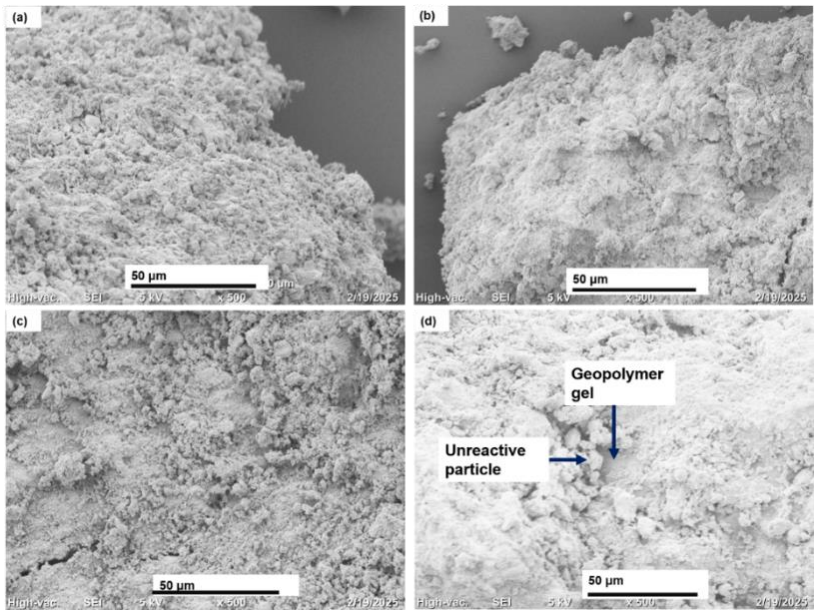

Fig 4.58: Morphology of geopolymer via SEM of d_{GM}=5 mm, 120 min (a) 600 rpm (b) 700 rpm, d_{GM}= 10 mm,120 min (c) 600 rpm (d) 700 rpm

According to Abbas et al. [238], the mechanochemical synthesis of the source material enhanced the surface area, thereby making the geopolymer binder more reactive; this led to an increased creation of geopolymerization gel as the reaction outcome. The presence of this mentioned gel is responsible for creating a geopolymer binder with a more uniform microstructure. The design of experiment in Fig 4.58(c-d) d_{GM} = 10 mm, 120 min, 600 - 700 rpm shows compacted structure with homogeneous gels and fewer unreacted particles resulting in the improvement of mechanical strength. Moreover, the creation of polymerization leads to the densification of the microstructure and a reduction in the pore size of the geopolymer binder. These findings align with previous research on the mechanical activation on geopolymer properties. Luzu et al.[239] demonstrated that mechanical activation fosters a denser and more cohesive microstructure in geopolymer materials, leading to improved mechanical properties. Similarly Temuujin et al.[89], investigated fly ash continuously milled for 20 min at 700 rpm with grinding media d_{GM} 10 mm (attrition milled).

4.6.6 Relationship specific surface area and compressive strength

Next, to evaluate the behaviour of geopolymer specimens made with mechanically activated coal gangue, the compressive strength was investigated (Fig 4.59). At all curing ages, the compressive strength showed a noticeable increase, with the difference becoming more pronounced at later ages. Geopolymers made with mechanically activated coal gangue subjected to grinding time 1 - 5 min exhibited the minimal compressive strength, ranging from 0.43 - 0.81 MPa at 14 days and 0.92 - 1.93 MPa at 28 days.

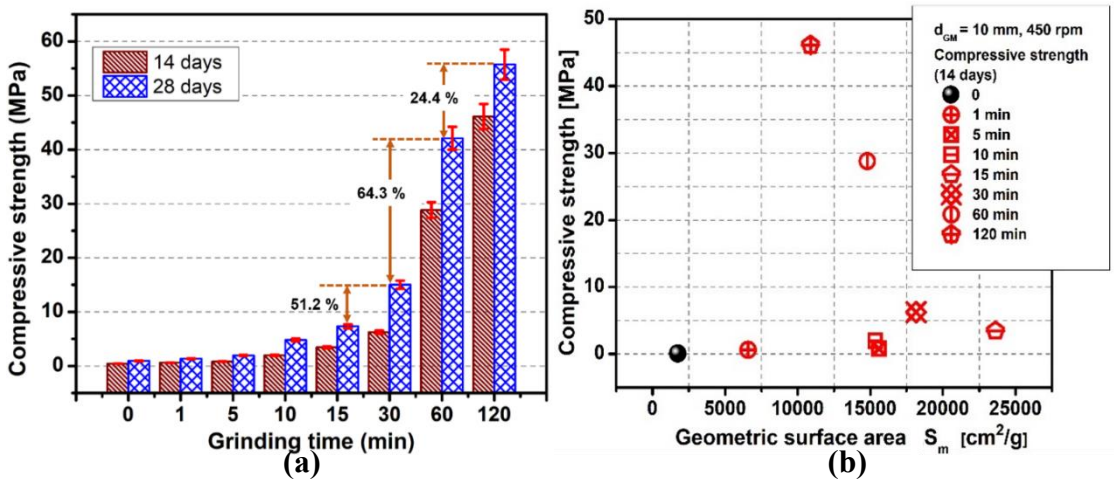

Fig 4.59: Compressive strength of coal gangue geopolymer as function (a) grinding time (b) geometric surface area

This minimal strength, observed within a specific grinding energy range of 4.620E+04 and 2.310E+05 J g^{-1}, indicates insufficient stored energy to facilitate the migration (relaxation) of lattice defects in large numbers. This is reflected in a slower geopolymerization process, resulting in minimal compressive strength due to plastic failure. In contrast, geopolymer samples with mechanically activated coal gangue of 10 - 120 min displayed brittle failure characteristics, as also reported by Luo et al. [240]. However, for mechanically activated coal gangue with a grinding time of 30 min, the compressive strength at 28 days increased from 15.01 MPa to 42.1 MPa (60 min), a rise of 64.3 %. Nevertheless, grinding time between 60 - 120 mins, the compressive strength increased from 42.1 MPa to 55.7 MPa, corresponding to a 24.4 % improvement. The correlation between the grinding time and the geometric surface area of raw and mechanically activated coal gangue was examined in relation to the resulting geopolymer properties, specifically compressive strength. The compressive strength exhibited a nonlinear increase with grinding time, indicating that the geometric surface area of reactive coal gangue does not remain constant throughout the grinding process. The compressive strength at 14 days reached its highest value with a grinding time of 120 min, even though the

geometric surface area decreased to 10882.6 cm^2/g, as shown in Fig 4.59b. This suggests that, while the specific surface area may play a significant role, other factors, such as the specific grinding energy, also contribute to the geopolymer strength. Additionally, the compressive strength as a function of specific grinding energy, it was found that a linear function can describe the correlation, as observed in Fig 4.60.

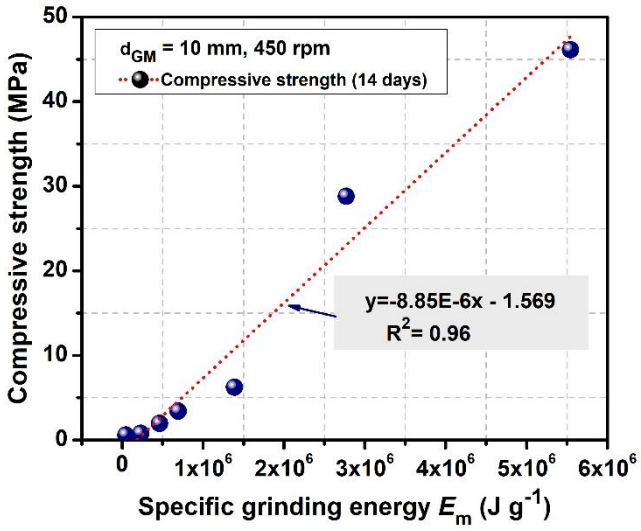

Fig 4.60: Compressive strength as a function of specific grinding energy

This high energy input results in substantial energy being stored within the lattice framework of the coal gangue due to the compression and shear forces induced by grinding. Most of this energy is retained in the particles, causing deformation of the atomic framework, which ultimately influences the geopolymerization process and improves the compressive strength [138]. This behaviour can be explained by the interplay between geometric surface area and specific grinding energy which affect the breaking of the S-O-T chemical bonds. This bond breaking increases the dissolution of silicate (Si) and alumina (Al), which in turn promotes the formation of gels during the geopolymerization process [114],[241]. In a previous study by Balczár et al. [112], using pure kaolin with a grinding time of 120 min at 600 rpm in a Pulverisette 6 planetary ball mill, it was reported that the compressive strength of the geopolymer decreased due to agglomeration. Despite the fact that physical properties like particle size and specific surface area of mechanically activated coal gangue are linearly enhanced by mechanical activation, the strengthening of their geopolymer binders is not proportionate. This is due to the change in the chemical properties (crystallinity and surface reactivity) of the precursors which are the most important parameters responsible for strength development of geopolymer. To evaluate the effect of the reactivity of the mechanically

activated coal gangue with design of experiment grinding media 5 - 10 mm, 600 - 700 rpm, the compressive strength of all geopolymer samples after 14 days is shown in Fig 4.61(a-c). To enable a better comparison of the properties of the geopolymers from mechanically activated coal gangue, a relationship between the compressive strength and the geometric surface area was established. On the other hand, a certain influence on agglomeration due to the grinding of coal gangue leads to a reduction of its surface free energy. Therefore, it is important to understand how the physical properties of mechanically activated coal gangue influence the properties of geopolymers. In general, the results indicate that the reactivity of coal gangue can be modified by fine particles, specific surface area and specific grinding energy in the planetary ball mill. As geometric surface area increases, reactivity increases and led to improve compressive strength. It is shown that the compressive strength during early grinding of coal gangue at 15 min has values between 1.81 - 2.45 MPa in all design of experiment. The design of experiment increased the compressive strength of the geopolymer compared to the raw coal gangue. Geometric surface area contributes reactivity of coal gangue by increased contact area between surface of coal gangue and sodium hydroxide and sodium silicate ratio leading to improve compression strength by bound a lot of sodium hydroxide and sodium silicate ratio. Moreover, an increase in the geometric specific surface area of the mechanically activated coal gangue, as shown in Fig 4.61(a-c) allows better interaction with the alkaline activators, facilitating the dissolution, reorganization and polymerization.

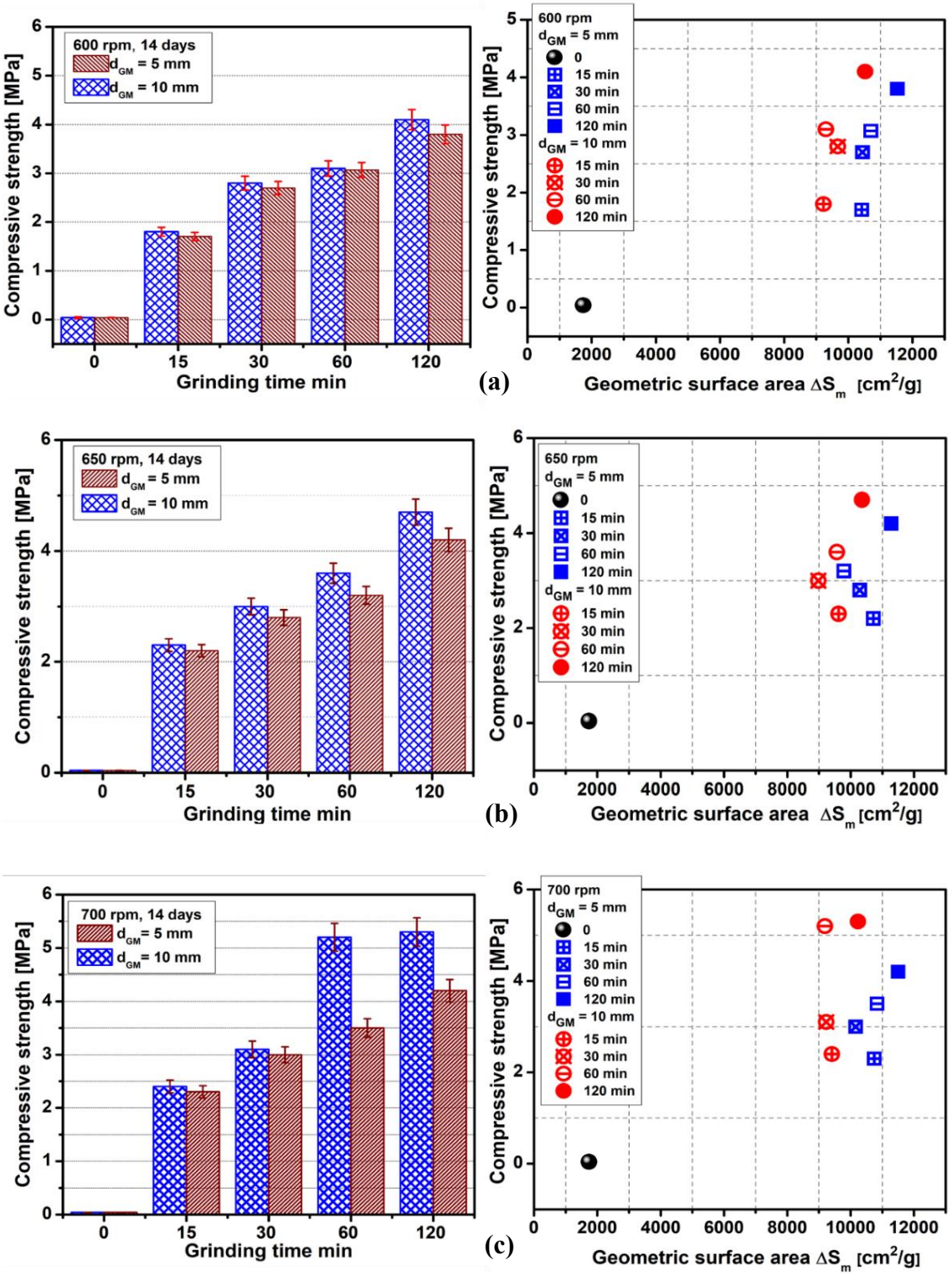

Fig 4.61: Correlation compressive strength of coal gangue geopolymer (a) 600 rpm (b) 650 rpm and (c) 700 rpm with grinding and geometric surface area

Despite the results shown in Fig 4.61 (a-c), the lowest compressive strength of the geopolymer at a grinding time of 15 min could be related to the lower connectivity between the mechanically activated coal gangue and the alkaline activator, suggesting the less cross-linking

geopolymers framework. As a result, we can see cracks in the sample grinding time of 15 min as shown in Fig 4.55. The result obtained in Fig 4.61(a-c) shows that the compressive strength of the geopolymer increases continuously and that there is a clear dependence on the grinding time and the rotational speed. In this case, the strength of 5.53 MPa was achieved with 700 rpm at 120 min, which is due to the higher stress energy caused by the grinding media size 10 mm. On the other hand, it is possible to state that 700 rpm influences heat generated during milling. As a result, compressive strength improved after 15 min of grinding media size 5 - 10 mm, 700 rpm range 2.37- 5.53 MPa. Evidence from a number of experimental studies has established that by decreasing the particle size and increasing the specific surface area, the reactivity properties of raw material can be significantly improved. This relationship emphasizes the compressive strength, which reflects the geometric specific surface and seems to be quite independent.

4.6.7 Reaction of coal gangue geopolymer samples

FT-IR measurements were conducted to examine the potential interactions between raw and mechanically activated coal gangue with the alkaline activator, as shown in Fig 4.62 for 450 rpm and grinding media 10 mm. The frequency at 1640 cm^{-1} corresponds to the presence of H_2O within the geopolymer network structure, as observed in previous studies [109],[110].

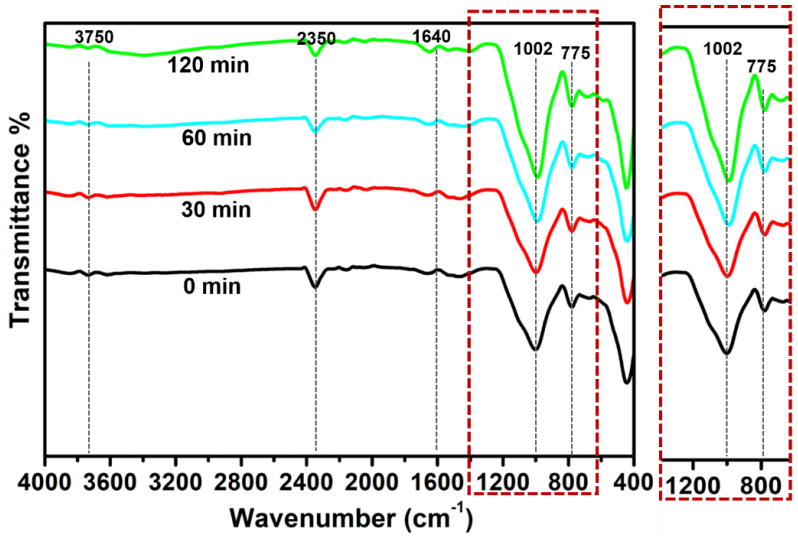

Fig 4.62: Reaction of coal gangue geopolymer

The Si-O-Si and Si-O-Al bands in the geopolymer spectra are attributed to the asymmetric stretching vibration of the Si-O-T (where T = Si or Al) bond, typically observed around 950-1250 cm^{-1} [244],[245]. Based on the data in Fig 4.62, the frequency values for different mechanically activated geopolymer are as follows, 0 min, 1002.51 cm^{-1}; 30 min, 997.65 cm^{-1};

60 min, 990.03 cm^{-1}; and 120 min, 986.65 cm^{-1}. A decline in the frequency number is indicated by a shift of the Si-O-T stretching bands to smaller numbers. The shift of frequency toward the lowest frequency suggests it is an indication of a reaction product related to the alkaline activator in other words, increases in the polymerization reaction between the Si-O-Al bonds, resulting in the formation of aluminosilicate gel. These results are in agreement with previous research [163], [246]. From this data, it can be observed that the coal gangue geopolymer with a grinding time of 30 min shows a frequency that significantly different from the 60 min of geopolymer sample (7.62 cm^{-1}). The frequency of the Si-O-T band shifts to 990.03 cm^{-1} with a grinding time of 60 minutes and further moves to 986.65 cm^{-1} with a grinding time of 120 min. A comparison of these two results reveals a significant difference of 3.38 cm^{-1}. The functional group at 2350 cm^{-1} is attributed to ethanol, which is used to clean the diamond of the FT-IR, a result that is consistent with the findings reported by Bach Delpeuch et al. [247]. The FT-IR spectra of the mechanically activated coal gangue and the coal gangue geopolymer sample, were analyzed within the frequency range of 4000 - 400 cm^{-1}, as depicted in Fig 4.63(a-b).

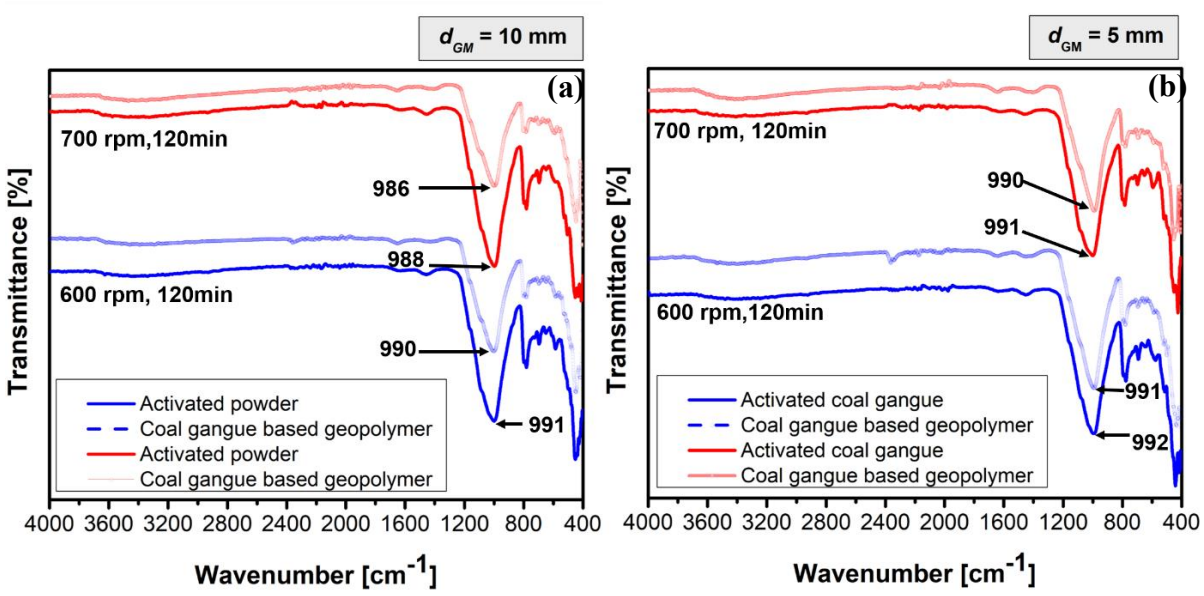

Fig 4.63: FT-IR coal gangue geopolymer gangue (a) d_{GM} = 10 mm and (b) d_{GM} = 5 mm

The peak observed at shifts to a lower wave number after geopolymerisation, indicating structural reorganization. It is associated with dissolution of the coal gangue with strong alkaline activator. Therefore, the reaction of geopolymer increases slowly with the increase in alumina silicate ion and dependent largely on the formation internal polymer network. Upon examination of the spectra, a notable observation was made, the coal gangue geopolymer sample exhibited a significantly more intense band compared to the mechanically mechanically

activated coal gangue sample. These results provide additional supporting evidence for the formation of the aluminosilicate gel structure within the coal gangue geopolymer. The characteristic vibrations around 990 - 986 cm^{-1} for griding media size 10 mm, 600 - 700 rpm and 120 grinding time, in contrast griding media size 5 mm, 600 - 700 rpm and 120 grinding time the fequency is 991 - 990 cm^{-1} have been assigned to asymmetric stretching of linkages between S-O-T. These results are in agreement with Davidovits [163], the shift toward low wavenumber may attributed to the partial replacement SiO_4 specie by AlO_4, resulting in the change in the local Si-O bond.

4.6.8 The mini slump cone flow of fresh geopolymer paste

Regarding the flow behaviour of fresh geopolymer paste at different grinding times with 450 rpm. Grinding times between 0 and 5 min, the slump flow values ranged from 51 to 43 mm, indicating a workable consistency. In contrast, for grinding times between 10 and 120 min, a 100 % flow was observed reaching a flow diameter of 112 mm. The increase in slump cone flow diameter (mm) with extended grinding time highlights the enhanced dispersion ability of the geopolymer paste in the alkaline solution. This phenomenon occurs because prolonged grinding accelerates the dissolution process, leading to the increased release of aluminosilicate precursors, specifically $[AlO_4]^-$ and $[SiO_4]^-$ from the mechanically activated coal gangue surface. Fig 4.64 illustrates the slump cone flow results.

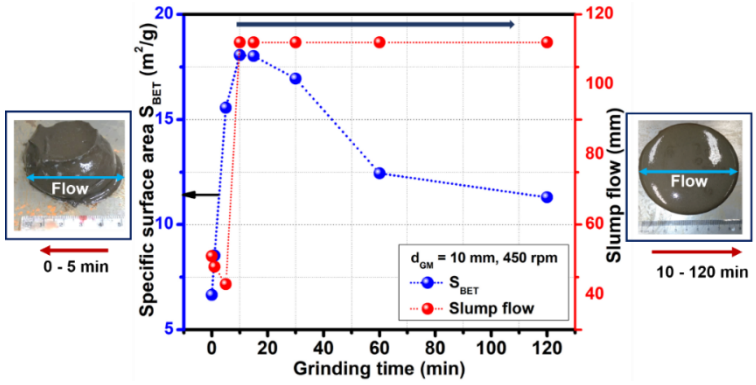

Fig 4.64: Mini slump cone flow geopolymer paste with different grinding times (min)

The mechanical activation of coal gangue breaks off some bonds on its surface which leads to an increase in the energy of crystal lattice and loosening of Si-O-T bond subsequently generating more free active alumina (Al) and silica (Si) to react with alkaline solution [248]. As a result, the viscosity decreased considerably and influenced the demand for alkaline activators, resulting in 100 % flowability of the mixed geopolymer paste after 10 min of

grinding. Recent research has indicated that the hydroxyl free radicals $\bullet OH$ released in the alkaline solutions catalyze the disintegration of the aluminosilicate precursor by breaking the bonds of Si-O-Si, Al-O-Si, and Al-O-Al, besides catalyzing the promotion of isolated aluminate and silicate anion reconstruction via remaking the bonds of Si-O-Si, Al-O-Si, and Al-O-Al [249]. In reaction shown in Fig 4.65, $[Al(OH)_4\ ]^-$ and $[SiO(OH)_3]^-$species are linked to each other by the attraction between one of the OH groups from $[SiO(OH)_3]^-$and Al ion of $[Al(OH)_4\ ]^-$ which results in an intermediate complex. The two OH groups in alkaline activators such as hydroxides and silicates in the intermediate complex then condense to form an aluminosilicate species with the release of an H_2O molecule [52].

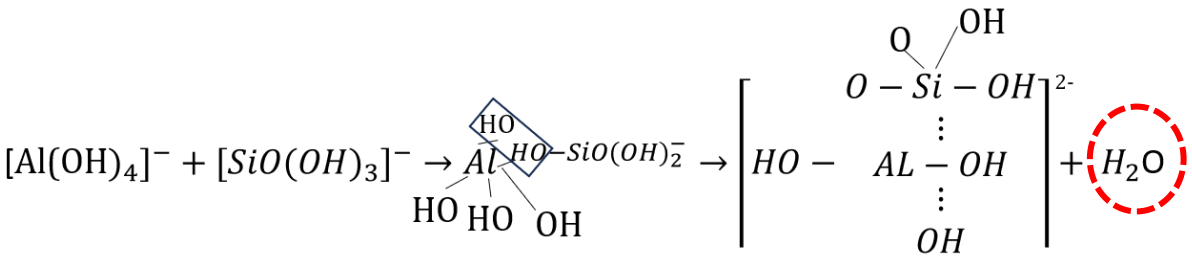

Fig 4.65: Schematically the condensation reaction between $[Al(OH)_4\ ]^-$ and $[SiO(OH)_3]^-$

4.6.9 Setting time of fresh geopolymer paste

The initial and final setting times of geopolymer fresh paste prepared with mechanically activated coal gangue between 10 - 120 min are presented in Fig 4.66a. The final setting time of a geopolymer is defined as the duration from mixing with the alkaline solution until the material begins to develop structural strength and loses its plasticity. According to research by Elyamany et al. [250], the final setting time for geopolymer should not exceed 390 min to avoid delays in construction processes. Therefore, the extended final setting time observed for the coal gangue geopolymer paste at a grinding time of 10 min (600 min) is not necessarily advantageous. The variation in grinding times significantly influenced both the initial and final setting times. The initial setting times of all samples ranged from 106 to 450 min, while the final setting times varied between 165 and 600 min, as shown in Fig 4.66a.

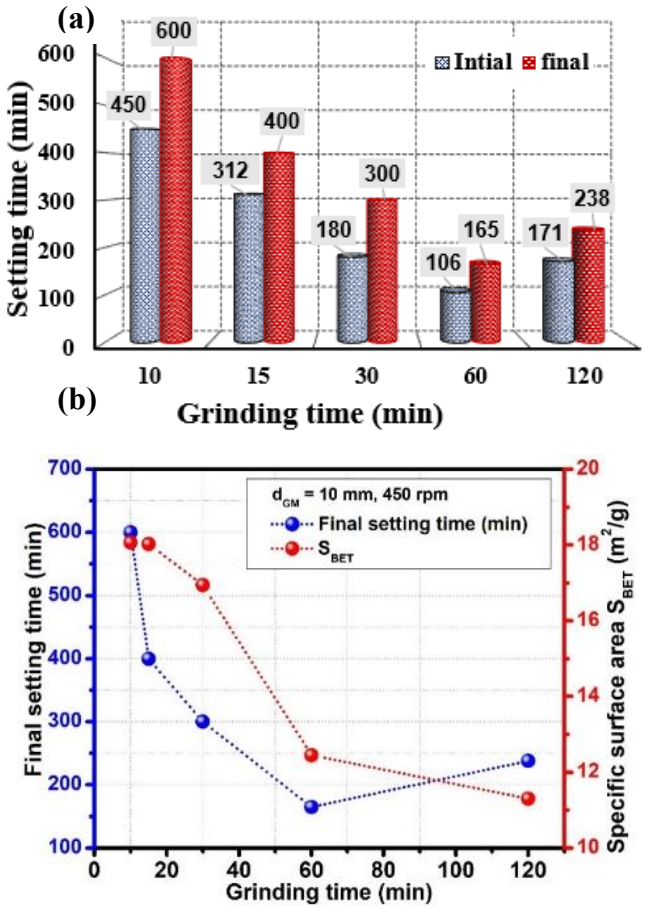

Fig 4.66: (a) Setting time of coal gangue geopolymer paste with different grinding time (min), (b) final setting time and specific surface area S_{BET} as function grinding time (min)

As the grinding time increased, the setting times initially increased and then decreased. The geopolymer prepared with mechanically activated coal gangue at a grinding time of 60 min exhibited the fastest setting times, with an initial setting time of 106 min and a final setting time of 165 min. However, when the coal gangue was mechanically activated for 120 min, the geopolymerization process slowed, resulting in an increase in the initial setting time from 106 min to 171 min and the final setting time from 165 min to 238 min. This trend highlights the correlation between the setting time of fresh geopolymer paste and the properties of mechanically activated coal gangue. Specifically, the relationship between the final setting time and the specific surface area S_{BET} is established, as shown in Fig 4.66b. A greater specific surface area S_{BET} exposes a larger proportion of particles to attack by the alkaline solution, facilitating the dissolution of reactive species. Spreading wetting occurs when an alkaline activator, upon contact with a solid, spreads along the solid interface per unit area [251]. As shown in Fig 4.66b, S_{BET} has a significant influence on the setting time of coal gangue based geopolymer paste. The results indicate that particle agglomeration delays the setting process,

counteracting the expected acceleration due to increased surface area. Although S_{BET} decreases after 10 min of grinding, the geopolymerization mechanism remains influenced by the surface reactivity of gangue particles. Mechanical activation enhances this reactivity, leading to the release of $[AlO_4]^-$ and $[SiO_4]^-$, even in the presence of particle aggregation. A higher specific surface area, correlated with cumulative pore volume, may enhance the kinetics of wetting, as more alkaline activator can penetrate the pores of coal gangue and interact with the surface area [252].

4.7. Discussion

Investigating the relationship between grinding parameters and the reactivity of coal gangue is a priority research area for advancing geopolymer applications. The particle size distribution (PSD), specific surface area (SSA), morphology, change of chemical bond these characteristics together determine the mechanically activated of the coal gangue [116], [117]. The reduction in particle size during mechanical activation beyond its original size leads to changes in the relaxation from brittle fracture to ductile fracture. These changes are accompanied by an accumulation of strain and defects. The continuous impacts and grinding deform the crystal lattice of the material. Consequently, it leads to the growth of high density of defects, such as dislocations, grain boundaries, and even amorphous regions. The increased specific surface area (SSA), combined with higher internal energy states from the distorted lattice, enhances this effect by exposing additional reactive sites and determine the reactivity of coal gangue [189]. Hence, in the early stages of grinding 1-10 min, the specific grinding energy between 4.620E+04 J g^{-1} and 4.62E+05 J g^{-1} in Fig 4.38 is stored in the coal gangue particle and is mostly employed to increase the specific surface area and geometric surface area (Fig 4.35) and finer particle of median particle size x_{50}. As the specific grinding energy increases, the particles tend to adhere to each other due to van der Waals forces forming amorphous surface layers during the grinding process. Sánchez-Soto et al. [255] reported a similar finding. The specific grinding energy ranging from 6.930E+05 - 5.55E+06 J g^{-1}, with a grinding time of 15 to 120 min, did not enhance the fineness of coal gangue. Instead, it led to a decrease in the specific surface area and geometric surface area. This suggests that the applied specific grinding energy primarily induces plastic deformation in the coal gangue rather than causing significant particle breakage [256]. During high energy grinding, severe plastic deformation of coal gangue particles occurs due to grinding media to particle to grinding media, grinding media and particle wall interactions [257], undergoes size reduction, deformation, and refinement through impaction, shear, and friction. This process increases surface energy and

introduces lattice imperfections in active species such as silica (Si) and alumina (Al). Mechanical activation disrupts Al-O and Si-O bonds, weakening the connections between tetrahedral and octahedral layers while generating numerous defects and dislocations [258],[259]. None of the new chemical bonds or disappearances are present on the spectra of FT-IR of the mechanically activated coal gangue with grinding time 1 - 120 min indicating that the mechanical action only alters the surface and improves the reactivity of the particles. At a specific grinding energy of 5.55E+06 J g^{-1} and a grinding time of 120 min, the dislocation of mechanically activated coal gangue increased, and the crystals do not break but underwent plastic deformation, which is typical for amorphous material. The specific grinding energy ranged between 2.772E+06 J g^{-1} (60 min grinding) and 5.55E+06 J g^{-1} (120 min grinding) with significant difference in energy 2.66E+06 J g^{-1} caused a corresponding difference of 0.984 cm^{-1} in the wavenumber of the asymmetric stretching S-O-T molecular bond of the coal gangue (Fig 4.43). For an atom or molecule to move from one site in the structure to another, it must move past other units, implying that there must be a significant activation energy, which must be overcome for coal gangue surface may contain any or all of the defects, as well as missing layers, screw and spiral dislocations [260]. The mechanically activated coal gangue due to the different grinding times has an influence on geopolymerization process. The raw coal gangue with median particle size x_{50} of 83.09 μm, specific surface area S_{BET} of 6.65 m^2/g and geometric surface area of 1738 cm^2/g. After grinding for 1 min, the median particle size dropped to 9.06 μm increasing the specific surface area to 8.62 m^2/g and geometric surface area to 6585 cm^2/g. However, from visual observation and compressive strength, the reaction of geopolymerization is too slow. Despite decreasing the median particle size x_{50} and increasing of the specific surface area of both S_{BET} and geometric surface area, the cumulative pore volumes are close to each other with a range of 0.025 - 0.036 cm^3/g (Fig 4.36). As the results, although specific surface area and geometric surface area decrease after 10 min of grinding, the mechanism of geopolymerization is influenced by the surface reactivity of gangue particles, which is increased by mechanical activation and leads to the release of $[AlO_4]^-$ and $[SiO_4]^-$ without effected by aggregation of mechanically activated powder. The amount of silica (Si) and alumina (Al) in the solution increases as the grinding time of the coal gangue increases, accelerating the polymerization process and the formation of inorganic polymer gels and the final properties of the hardened geopolymer binder. This is likely the main reason why the dissolution of silica (Si) and alumina (Al) significantly improved with increased grinding time. The results indicate that at a specific grinding energy of 5.55E+06 J g^{-1}, agglomeration slows down the complex geopolymerization reaction, particularly affecting the setting time, while

having no adverse impact on compressive strength. Additionally, agglomeration of mechanically activated coal gangue delays setting time, resulting in only a 24.4 % improvement in compressive strength, increasing from 42.1 MPa to 55.7 MPa after 28 days. In contrast, for grinding times between 30 and 60 min, where the difference in specific grinding energy is 1.334E+06 J g^{-1}, compressive strength shows a significant improvement of 64.3 %. Overall, the compressive strength increased from 1.32 MPa to 55.7 MPa across the grinding time range of 1 - 120 min. This made it possible to objectively depict the link between coal gangue reactivity and compressive strength of geopolymer, which was more helpful for understanding how it affected the geopolymerization process. Mechanical activation has altered the reactivity significantly, and a consequent improvement in geopolymer properties was obtained.

Next, the detail investigation of planetary ball mill led to the determination of optimization of grinding media size, rotational speed and grinding time for mechanically activated coal gangue by Design of Experiment (DoE). The mechanical activation of coal gangue in a planetary ball mill has led to significant changes in its physical properties, particularly in terms of the particle size and geometric specific surface area that can be observed. The particle size distribution (Fig 4.30) and geometric specific surface area (Fig 4.39 and Fig 4.40) of the mechanically activated coal gangue particle has been increased and decreased, and key findings from this process are in agreement with optimum stress energy according to the stress model developed by Kwade and Schwedes. In this study, a significant influence of the experimental design on the properties of the mechanically activated coal gangue such as fineness, agglomeration, relative span and geometric surface area was demonstrated. This result emphasizes that the reactivity of coal gangue for geopolymer application is also influenced by the stress energy (SE), collision frequency (CF) and specific grinding energy. Table 4.3 and Table 4.4 summarize all results from the Design of Experiment (DoE), detailing the relationships between rotational speed, grinding time, median particle size, geometric surface area, relative span, and specific grinding energy in relation to the compressive strength of the geopolymer samples. In the mechanical activation of coal gangue, specific grinding energy is the key factor for achieving the desired particle size and is responsible for generating defects that strongly influence the reactivity of coal gangue and the geopolymer properties.

Table 4.3: Overview of mechanically activated coal gangue on geopolymer 14 days compressive strength with grinding media 5 mm

Rotational speed [rpm]	Grinding time [min]	Median particle size, x_{50} [µm]	Geometric surface area [cm^2/g]	Relative span [-]	Specific grinding energy [kJ g^{-1}]	Compressive strength [MPa]
0	0	83.06	1738.05	2.59	0	0.043
600	15	4.2	10416.09	3.32	6.90E+05	1.70
	30	4.58	10441.63	3.55	1.38E+06	2.71
	60	4.41	10706.63	3.91	2.76E+06	3.07
	120	3.68	11534.96	4.30	5.52E+06	3.80
650	15	4.13	10717.68	3.32	8.84E+05	2.25
	30	4.7	10288.82	3.81	1.77E+06	2.84
	60	4.86	9787.36	5.87	3.53E+06	3.27
	120	3.75	11281.58	4.65	7.07E+06	4.21
700	15	4.27	10748.28	3.52	1.11E+06	2.30
	30	4.82	10161.37	4.46	2.22E+06	3.06
	60	4.11	10834.26	4.85	4.44E+06	3.58
	120	3.61	11505.03	4.97	8.89E+06	4.28

Table 4.4: Overview of mechanically activated coal gangue on geopolymer 14 days compressive strength with grinding media 10 mm

Rotational speed [rpm]	Grinding time [min]	Median particle size, x_{50} [µm]	Geometric surface area [cm^2/g]	Relative span [-]	Specific grinding energy [kJ g^{-1}]	Compressive strength [MPa]
0	0	83.06	1738.05	2.59	0	0.043
600	15	3.93	10525.85	4.46	5.99E+05	1.81
	30	5.73	9302.21	4.66	1.20E+06	2.84
	60	5.87	9674.01	4.84	2.40E+06	3.11
	120	6.29	9226.59	5.74	4.79E+06	2.19
650	15	5.00	9619.44	3.95	7.67E+05	2.01
	30	6.33	8978.52	5.10	1.53E+06	3.08
	60	5.51	9562.51	6.38	3.07E+06	3.65
	120	4.66	10360.3	6.97	6.13E+06	4.71
700	15	5.26	9409.00	4.22	9.64E+05	2.42
	30	6.86	9231.00	5.60	1.93E+06	3.15
	60	6.68	9190.44	5.76	3.86E+06	5.20
	120	5.27	10235.26	7.43	7.71E+06	5.51

Although the grinding time of mechanically activated coal gangue grinding is 15 min and the median particle size x_{50} is in the range of 4.13 - 5.26 μm, the contribution of Al-Si mechanically activated coal gangue to the gel phase of the geopolymer is important. With a grinding time of 15 min, there is no doubt that the Design of Experiment (DoE) with specific grinding energy between 5.99E+05 - 1.11E+06 kJ g^{-1} cannot supply sufficient Si and Al element to react with alkaline solution, as the result slow to start the geopolymerization. The virtual observation of the geopolymer samples in Fig 4.55 show, deterioration and the formation of microcracks in the geopolymer sample, as the grinding time increases, the number of these cracks decreases significantly. Comparison of the findings with those of other studies confirms geopolymer with temperature 70 °C at 24 hour is insufficient to increase the level of long-range ordering in geopolymer binder with considerable hardened sample and compressive strength of geopolymer depending on the curing conditions. To overcome this issue, additional curing time could be further considered [231].

5. CONCLUSION

5.1. Conclusion for vibratory ball mill:

This study investigated the influence of mechanical activation (1-120 min) on the properties of coal gangue and its subsequent impact on geopolymerization. The characterization of the mechanically activated coal gangue was examined in detail using a vibratory ball mill under dry conditions. This characterization included, cumulative undersize (particle size distribution), specific surface area and geometric surface area and specific grinding energy. The research specifically related these parameters to the resulting geopolymer properties. The key findings are as follows:

- The optimal fineness of mechanically activated coal gangue was precisely identified at 30 min of grinding x_{50} = 4.20 μm, achieved at a specific grinding energy of 2.97E+02 J g^{-1}.
- The mechanism of mechanical activation in this type of grinding device, when it operated at the maximum specific grinding energy, was primarily the mechanical dispersion (size reduction) of the coal gangue, which resulted in a greater specific surface area (SSA).
- The maximum specific grinding energy of 2.754E +03 J g^{-1} caused limited asymmetric stretching of Si-O-T (T= Al or Si), while preserving the material inert structure. This finding was consistent with both the FT-IR analysis (Fig 4.14) and the XRD analysis (Fig 4.15).
- Mechanical activation significantly enhanced the reactivity of coal gangue, as evidenced by the increase in compressive strength. Compressive strength rose from 0.072 MPa (raw) to 1.25 MPa after 14 days and 1.32 MPa after 28 days with the optimal grinding time of 30 min. Nevertheless, aggregation of the mechanically activated coal gangue negatively affects the final compressive strength (Fig 4.24).

5.2. Conclusion for planetary ball mill:

This study investigated the influence of mechanical activation (1-120 min) on the properties of coal gangue and its subsequent impact on geopolymerization. The characterization of the mechanically activated coal gangue was examined in detail using a planetary ball mill under dry conditions. This characterization included, cumulative undersize (particle size distribution), specific surface area, geometric surface area and specific grinding energy. The

research specifically related these parameters to the resulting geopolymer properties. The key findings are as follows:

- The optimal fineness of mechanically activated coal gangue, defined by a median particle size x_{50} of 4.86 μm, was achieved at a specific grinding energy of 4.63E+05 J g^{-1} corresponding to 10 min of grinding. Beyond this inflection point, aggregation and agglomeration became dominant. This transition was evidenced by changes in the characteristic particle sizes x_{10}, x_{50} and x_{90} (Fig 4.28), the relative span (RS) (Fig 4.29), and the particle morphology (Fig 4.31).
- Aggregation was evident as the specific surface area decreased from 18.02 to 11.30 m^2/g. Concurrently, the geometric surface area dropped sharply from 23,616 to 10,882 cm^2/g (Fig 4.35). This agglomeration effect became significantly more pronounced at the highest specific grinding energy corresponding to the 120 min grinding time
- FT-IR analysis of mechanically activated coal gangue confirmed no formation of new chemical bonds or loss of existing structures, indicating that mechanical activation primarily induces surface modification. The specific grinding energy caused the asymmetric stretching of Si-O-T toward 1071 cm^{-1}, highlighting its role in altering surface properties while preserving the material core structure.
- Extended grinding (120 min) prolonged the initial setting time from 106 min to 171 min and the final setting time from 165 min to 238 min. This delay was attributed to particle agglomeration, which slowed geopolymerization (Fig 4.66). This delay correlated with a decrease in specific surface area (11.301 m^2/g) and cumulative pore volume (0.062 cm^3/g)
- Mechanical activation significantly enhanced the reactivity of coal gangue, as evidenced by a remarkable increase in compressive strength to 46.12 - 55.7 MPa after 120 min of grinding, measured at both 14 and 28 days.
- A Design of Experiment (DoE) approach was employed to determine the optimal grinding conditions. Using a rotational speed between 600 - 700 rpm and grinding media diameter of 5 mm and 10 mm, the optimal median particle size x_{50} for the mechanically activated coal gangue was determined to be in the range of 3.61 - 4.66 μm. This size range correlated with a relative span (RS = 3.32 - 7.43) (Fig 4.42).
- This deagglomeration effect of mechanically activated coal gangue became significantly more pronounced at the highest specific grinding energy, corresponding

to the 120 min grinding time, which resulted in the highest geometric surface area (Fig 4.39 and Fig 4.40).

- The Design of Experiment (DoE) approach confirmed that mechanical activation significantly enhanced the reactivity of the coal gangue. This enhancement was evidenced by a remarkable increase in compressive strength, which ranged from 1.70 - 5.51 MPa across the different specific grinding energy 5.99E+05 kJ g^{-1} - 8.89E+06 kJ g^{-1} levels investigated (Fig 4.61).

6. New scientific results (NSR) of the PhD thesis

NSR 1: Influence of grinding parameters for optimization mechanically activated coal gangue, comparison the results obtained by vibratory and planetary ball mill

The optimization of mechanically activated coal gangue was investigated by examining the effects of different high-energy milling devices and their respective grinding parameters. Two distinct milling devices a vibratory ball mill and a planetary ball mill were used to represent batch and laboratory-scale operations, in order to address the selection of a suitable device for activation. My research establish correlation between median particle size x_{50}, specific surface area SSA as function specific grinding energy. In addition, the relationship among particle characteristics x_{10}, x_{50}, x_{90} and the relative span (RS) was examined. For the planetary ball mill with design of experiment (DoE) was conducted at rotational speeds ranging from 600 to 700 rpm and a grinding media size of 10 mm.

I experimentally proved that initial grinding proportionally increases the specific surface area (SSA) and reduces the median particle size x_{50}. However, this trend reverses beyond a distinct inflection point. Extending the specific grinding energy beyond this point leads to a decrease in SSA due to aggregation/agglomeration, followed by subsequent deagglomeration. This finding is based on a comprehensive evaluation of mechanically activated coal gangue, including an assessment of the grinding kinetics limit and a Design of Experiments (DoE) approach. In addition, the effect of grinding time on the specific surface area S_{BET} includes the area contributed by all surface features, such as internal porosity (pores, cracks, and surface roughness) and geometric surface area which is calculated based on an assumed spherical particle size distribution also highlighted

- *Grinding kinetic limit*:

The mechanically activated coal gangue reached its grinding limit after 30 min in the vibratory ball mill, resulting in particle aggregation. At this point, the mechanically activated coal gangue had a geometric surface area of 3690 cm^2/g. Its particle characteristic of x_{10} (3.93 μm), x_{50} (4.20 μm), x_{90} (13.79 μm) with a relative span (RS = 0.9) and a specific grinding energy of 2.97E+02 J g^{-1}. In the planetary ball mill operated at 450 rpm, particle aggregation/agglomeration of the mechanically activated coal gangue was observed after 10 min of grinding. At this point, the geometric surface area was 15341 cm^2/g with particle sizes of x_{10} (0.49 μm), x_{50} (4.28 μm), x_{90} (11.09 μm), relative span (RS = 2.17) and a specific grinding energy that reached 4.63 E+05 J g^{-1}. **It was revealed that based on characteristic median particle size and specific surface area as function of specific grinding energy correlation was determined using exponential**

function (Table 1, Table 2). **I experimentally proved that that for coal gangue grinding, the grinding limit strongly depends on the energy used and the type of mechanical stress. Specifically, the lowest the stress intensity, the higher the grinding limit (higher specific surface area achieved) within a specific grinding interval**.

Table 1: Fitting correlation median particle size as function specific grinding energy

Type of grinding device	Equation	R^2
Vibratory ball mill	$y = 7.62 + 75.46e^{-0.17308x}$	0.99
Planetary ball mill	$y = 7.62 + 75.46e^{-8.5637E-5x}$	0.99

Table 2: Fitting correlation geometric surface area as function specific grinding energy

Type of grinding device	Equation	R^2
Vibratory ball mill	$y = 3640.26 - 1951.09e^{-0.0052x}$	0.83
Planetary ball mill	$y = 16659.21 - 15143.6e^{-9.761E-5x}$	0.61

- *Design of Experiment (DoE)*:

The experimental analysis revealed a relationship between geometric surface area as a function of grinding time, specific grinding energy, stress intensity *SI*, and active mass (estimated by quantifying the mass of powder adhering to the grinding media). This establishes a comprehensive framework for predicting mechanically activated coal gangue above 600 rpm thereby providing a quantitative basis for grinding process optimization. The Design of Experiment (DoE) showed maximum specific grinding energy between 4.79E+06 -7.71E+06 kJ g^{-1} where the mechanically activated coal gangue shifted to deagglomeration (120 min grinding time).

- *Specific surface area (SSA):*

Experimental results showed that the S_{BET} values for the mechanically activated coal gangue ranged from 7.67-12.47 m^2/g when processed by a vibratory ball mill, and from 8.52 to 18.06 m^2/g when processed by a planetary ball mill. The results are relatively close, particularly at the 120 min of grinding, where the specific surface area was 11.50 m^2/g for the vibratory mill and 12.45 m^2/g for the planetary ball mill, respectively. Meanwhile, the geometric surface area was 0.34 m^2/g for the vibratory ball mill and 1.08 m^2/g for the planetary ball mill at 120 of grinding. The dissolution reaction occurs on the external and readily accessible surfaces of the particle when it is mixed in the alkaline activator. For this reason, the geometric surface area values (which focus on the outer particle size) can be more directly relevant affecting the

reactivity of mechanically activated coal gangue. As the result, compressive strength of geopolymer is higher with geometric surface area 1.08 m^2/g.

NSR 2: Influence of aggregation/agglomeration and deagglomeration of mechanically activated coal gangue on geopolymer compressive strength

To study and investigate the influence of particle rearrangement mechanisms (aggregation/ agglomeration, and deagglomeration) on the resulting compressive strength of geopolymer.

I experimentally demonstrated that the aggregation/agglomeration and subsequent deagglomeration of mechanically activated coal gangue significantly affect the geopolymer compressive strength. This finding is based on a correlation of geometric surface area and compressive strength as a function of the specific grinding energy which can be written by exponential function.

- *Vibratory ball mill:*

The highest compressive strength of 1.25 MPa (14 days of curing) was using mechanically activated coal gangue 30 min, which also exhibited the highest geometric surface area of 3690 cm^2/g and specific grinding energy 2.97E+02 J g^{-1}. As expected, the increase in specific surface area contributed positively to the particle reactivity of mechanically activated coal gangue and dissolution kinetics during geopolymerization. However, beyond the optimal specific grinding energy, particularly after 30 min, the compressive strength began to decline to between 0.92 - 0.96 MPa (26.4 %) despite further specific grinding energy 2.754 E +03 J g^{-1}, as aggregation had a negative effect on the compressive strength.

- *Planetary ball mill:*

The coal gangue mechanically activated for 120 min exhibited the performance in highest compressive strength (46.7 MPa) after 14 days, despite possessing a decreasing of geometric surface area of 10,882 cm^2/g. The compressive strength of geopolymer exhibited suggesting that the aggregation/agglomeration of mechanically activated coal gangue particles does not affect the final compressive strength for grinding process 450 rpm, 10 mm grinding size. Design of Experiment (DoE) of 600 - 700 rpm and similar a grinding media size, the analysis revealed that the condition of deagglomeration was indicated by highest geometric surface 8978 to 10,360 cm^2/g and the maximum specific grinding energy between 4.79E+06 - 7.71E+06 kJ g^{-1}. The analysis indicated that compressive strength in this DoE was not negatively affected by aggregation/agglomeration and deagglomeration. This providing a crucial mechanistic link between mechanically activated coal gangue particle characteristics and final geopolymer mechanical performance.

It was found that an exponential function can accurately describe the geometric surface area as a function of specific grinding energy. A very high R^2 value 0.8 proves the goodness-of-fit of this model. For compressive strength as a function of specific grinding energy, the relationship can be modelled using an exponential function for the vibratory ball mill and a linear function for the planetary ball mill (Table 3 and Table 4).

Table 3: Fitting correlation of geometric surface area as function specific grinding energy

Type of grinding device	Equation	R^2
Vibratory ball mill	$y = 3640.26 - 1951.09e^{-0.0052x}$	0.82
Planetary ball mill	$y = 7.62 + 75.46e^{-8.56E-5x}$	0.99
	$y = 9858.92 - 8119e^{-4.20E-6x}$	0.96
	$y = 9634.81 - 7896e^{-1.01E-5x}$	0.97
	$y = 9557.78 - 7819.64e^{-4.01E-6x}$	0.96

Table 4: Fitting correlation of compressive strength as function specific grinding energy

Type of grinding device	Equation	R^2
Vibratory ball mill	$y = 1.04 - 1.051e^{-0.00497x}$	0.69
Planetary ball mill	$y = 8.77E-6 - 1.16x$	0.96
	$y = 6.67E-7 + 1.24x$	0.75
	$y = 7.63E-7 + 1.42x$	0.75
	$y = 5.85E-7 + 1.58x$	0.67

NSR 3: The effect agglomeration of mechanically activated coal gangue on the leaching test, setting time of geopolymer paste, and compressive strength of geopolymer.

To study the effects of agglomeration on mechanically activated coal gangue, samples were selected from the planetary ball mill processed at 450 rpm, using 10 mm grinding media size, with grinding times ranging from 1 to 120 min.

I experimentally demonstrated the relationship by which particle agglomeration of mechanically activated coal gangue influences the geopolymerization process. This finding is based on a comprehensive evaluation of the leaching test results, the setting time of the geopolymer paste, and the final compressive strength of geopolymer samples.

- *Leaching test:*

Mechanical activation enhances the reactivity of coal gangue by increasing its geometric surface area S_m and inducing structural defect and disordered at particle surfaces, which

generally accelerate the leaching process. However, prolonged grinding of 120 min leads to particle agglomeration of the mechanically activated coal gangue. As the result, significantly affects the release of silica (Si) and alumina (Al). The concentrations of Si and Al in the leachate decrease from 93.96 mg/L to 73.52 mg/L (Si) and from 101.48 mg/L to 75.6 mg/L (Al) representing a proportional decrease between 21 % and 26 % after 120 min of grinding time

- *Setting time of geopolymer paste:*

Mechanically activated coal gangue for 120 min was observed to significantly slow the geopolymerization process. This effect was evident in increase in setting times of geopolymer paste, with the initial setting time rising from 106 min to 171 min and the final setting time increasing from 165 min to 238 min.

- *Compressive strength:*

For mechanically activated coal gangue with a grinding time of 30 min, the compressive strength at 28 days was 15.01 MPa. Increasing the grinding time to 60 min led to a substantial increase in compressive strength, reaching 42.1 MPa which represent a 64.3 %. Subsequently, increasing the grinding time between 60 and 120 min resulted in compressive strength further increasing from 42.1 MPa to 55.7 MPa corresponding to a 24.4 % improvement at 28 days. The maximum compressive strength of 46.12 MPa at 14 days and 55.7 MPa at 28 days was achieved at a grinding time 120 min despite the observed agglomeration of mechanically activated coal gangue, which had a geometric surface area of 10,882 cm^2/g.

The key finding is that while excess energy stored in the lattice enhances the dissolution of silica (Si) and alumina (Al), agglomeration counteracts this effect, which ultimately slows the geopolymerization process.

NSR 4: Influence of mechanical stress on structural disorder of mechanically activated coal gangue.

This research establishes a mechanistic framework that links specific grinding energy consumption to the formation of structural disorder mechanisms that govern the transition from mechanical dispersion to surface activation.

I experimentally demonstrate that the mechanical activation of coal gangue is profoundly influenced by mechanical stress and specific grinding energy consumption, leads to structural disorder and defects. The corresponding shifts in vibrational modes fundamentally revealing that the asymmetric stretching vibration of Si-O-T, (T= Si or Al) is the most important factor governing its reaction in geopolymerization.

- *Vibratory ball mill:*

With a maximum specific grinding energy of 2.754E+03 J g^{-1}, the grinding process primarily imparts mechanical stress (compression, impact, friction, shear) leading to mechanical dispersion with only minimal surface activation. This is confirmed by the limited shift in the molecular bond to vibrate, asymmetric stretching vibration Si-O-T, (T= Si or Al) from 997 - 993 cm^{-1} which indicates minimal structural defect formation. This establishes that, below this specific grinding energy, limited increase in activation is governed solely by mechanical dispersion

- *Planetary ball mill:*

By varying the revolution per minute (rpm), grinding media size and grinding time, the coal gangue is agitated at a high speed over a wide specific grinding energy range of 4.6E+04 – 8.89E+09 J g^{-1}. This process significantly increases the activation energy that stored in non-equilibrium and disordered crystal lattice of coal gangue. The resulting surface activation of mechanically activated coal gangue is confirmed by prominent shifts in the vibrational modes of key functional groups, particularly in shifts asymmetric stretching vibrations Si-O-T (T= Si or Al) which shift to range 998 cm^{-1} and 1071 cm^{-1}

NSR 5: Effects of geometric surface area and pozzolanic reactivity

My research establishes the relationship between grinding process parameters and the pozzolanic reactivity of coal gangue.

I experimentally demonstrated the factors governing CaO uptake in mechanically activated coal gangue. Through investigation, the results indicate that CaO uptake measurement is influent not only by geometric surface area (numerous asperities and surface roughness) but also structure defects of mechanically activated coal gangue. Nevertheless, Design of Experiment (DoE) of 600 - 700 rpm demonstrate the overall performance of CaO uptake. While pozzolanic reactivity is typically assessed for cement industry, this study is establishing the direct applicability of mechanically activated coal gangue reactivity to geopolymer system, leveraging a method that is easy and reliable.

- *Vibratory ball mill:*

The CaO uptake of the mechanically activated coal gangue, measured over 30 days (15th titration), varied with the geometric surface area. The highest geometric surface area 3690 cm^2/g of mechanically activated coal gangue was achieved after 30 min of grinding, corresponding to a peak CaO uptake of 75.2 mg/g. Nevertheless, a subsequent decrease in CaO uptake, ranging from 66.2 - 69.2 mg/g was observed at 60 and 120 min. This decline resulted

from a reduction in geometric surface area due to particle aggregation (3493 - 3496 cm^2/g). Furthermore, the surface activation validates by functional group of mechanically activated coal gangue that cause molecular bond to vibrate (stretch and bend) structural particularly the asymmetric stretching vibrations of Si-O-T (T= Si or Al) 993 cm^{-1} did not change significant.

- *Planetary ball mill*:

The coal gangue mechanically activated for 120 min yielded a dramatically lower geometric surface area of 10,882 cm^2/g compared to the 15 min activated coal gangue, which measured 23,616 cm^2/g. This result suggests that the change specific surface over extended grinding time demonstrates that the resulting structural disorder, rather than the specific surface area alone, plays the dominant role in enhancing pozzolanic reactivity. The Design of Experiment (DoE), the maximum geometric surface area of 10,235 - 10,360 cm^2/g for mechanically activated coal gangue (120 min) did not yield the maximum CaO uptake range 121.7 - 132.4 mg/g (30 days reaction time). The maximum geometric surface area resulted in declined CaO uptake compared to grinding times of 30 and 60 min despite the significant structural disorder or defects present in the mechanically activated coal gangue particularly the asymmetric stretching vibrations of Si-O-T (T= Si or Al) towards 990 - 998 cm^{-1} at 650 - 700 rpm with grinding time 120 min. The 600 rpm yielded the highest CaO uptake of 118 mg/g of mechanically activated coal gangue 120 min (30 days reaction time). Thus, the experimental results demonstrated that the CaO uptake from the Design of Experiments (DoE) for mechanically activated coal gangue exhibited a different trend in the planetary ball mill when the rotational speed exceeded 600 rpm.

7. SUMMARY

My PhD thesis directly addresses key mandates of the European Union (EU) and makes a significant contribution to global sustainability objectives. Although the ongoing operation of mines to extract essential metal and energy resources remains crucial for global development, it inevitably generates substantial waste streams, particularly gangue and tailings, which require innovative management to mitigate major environmental impacts. By aligning with the principles of Sustainable Development Goal 12 and adopting circular practices, the mining sector can significantly reduce its environmental footprint. This research specifically supports the Clean Industry Deal, which highlights a planned Circular Economy Act for 2026 to accelerate this transition.

My research is focused on the coal gangue waste, a significant by-product of mining operations at the Bükkábrány opencast lignite mine in Borsod-Abaúj-Zemplén County, Hungary. While the circular economy model requires closed material loops that drastically reduce raw resource extraction, this waste material presents a major technical challenge, its complex and highly heterogeneous mineralogical composition severely restricts its inherent reactivity. To overcome this limitation, my thesis employs controlled mechanical activation. Specifically, I use two distinct grinding devices to systematically and energy-efficiently enhance the reactivity of the coal gangue. This innovative approach ultimately enables the precise tailoring of geopolymer properties for advanced, sustainable construction applications, transforming a problematic waste into a high-performance resource.

The experimental work began with a preliminary characterisation of the raw coal gangue samples, an essential first step to establish a reliable scientific baseline before any mechanical activation. Initial sample preparation included a critical drying stage, the collected material was oven-dried at 105 °C for 24 hours until a constant mass was reached, ensuring precise removal of free water for accurate compositional and physical analyses. The foundational experimental was then established. First, an initial geopolymer optimisation using raw coal gangue x_{50} of 83.09 was conducted to define the control parameters. Second, the investigation grinding parameters for the planetary ball mill were systematically analysed. To maintain methodological integrity throughout the thesis, a clear sample designation was implemented, coal gangue 1 was used exclusively for all preliminary trials testing while coal gangue 2 was selected for all final thesis results.

The mechanical activation of coal gangue, initially carried out using a vibratory ball mill, specifically selected for its ability to apply lower stress intensity (SI). The resulting mechanically activated coal gangue powder was then subjected to a comprehensive characterisation. These analyses included precise determination of particle size distribution (PSD), specific surface area (SSA), and calculation of specific grinding energy. Reactivity was quantified through leaching tests and pozzolanic reactivity. Furthermore, the coal gangue was analysed using Fourier-Transform Infrared Spectroscopy (FT-IR) to determine functional groups and molecular vibrational changes (stretching and bending) indicative of activation, alongside X-ray Diffraction (XRD) for phase analysis. Consequently, these comprehensive analytical results are crucial for precisely defining the grinding kinetics limit. This limit is scientifically identified as the point at which the median particle size x_{50} value to dropped. This detailed characterisation is vital because coal gangue powder particles are inherently susceptible to aggregation or agglomeration due to relatively weak Van der Waals forces, while simultaneously undergoing disaggregation and amorphization under the applied mechanical stresses (compression, impact, shear, and attrition).

The second major experimental phase focused on developing the geopolymer binder using mechanically activated coal gangue. This process began with optimisation of the alkaline activator. Initially, geopolymer binders produced from coal gangue activated using of vibratory ball mill showed limited improvement, compressive strength improved by less than 2 MPa. The geopolymer specimens in the compression tests displayed a viscous/ductile failure, deviating from typical brittle fracture, indicating poor geopolymerization reaction mechanism. To overcome this limitation, I initiated mechanical activation using a second grinding device, the planetary ball mill, which has a significantly higher stress intensity SI and specific grinding energy. Following repeat characterisation of this high SI activated coal gangue mirroring the comprehensive suite of tests performed for the vibratory ball mill material a major breakthrough was achieved. The resulting geopolymer binders exhibited strong correlation between geometric surface area and specific grinding energy, correlation compressive strength and specific grinding energy, culminating in a maximum compressive strength of 55 MPa. This result definitively demonstrates the critical importance of high-energy mechanical activation for realising the full reactive potential of coal gangue.

The scientific findings of this PhD thesis offer advanced utilization of secondary raw materials. Geopolymer technology represents a highly attractive and viable alternative to Portland cement, primarily because it offers the potential to substantially reduce CO_2 emissions associated with traditional cement manufacturing. Geopolymers are synthesized by the

dissolution of aluminosilicate source material (such as the activated coal gangue) in a highly alkaline solution, which acts as the activator. The subsequent polycondensation reaction between the dissolved aluminium (Al) and silicon (Si) complexes leads to the formation of a stable, three-dimensional polymeric network defined by Si-O-Al bonds. While this thesis successfully establishes the necessary foundation for mechanical activation, future investigation focusing on the controlled application of temperature could be included to further optimize reaction kinetics, maximize reactivity, and precisely tailor the final product properties for specific industrial applications.

8. LIST OF PUBLICATIONS

Journal publications:

1. S.N.A. Bakil, Marton Toth, Jamal-Eldin F.M. Ibrahim, Gábor Mucsi. Influence of mechanical activation of coal gangue on the strength and microstructure of geopolymer. Construction and Building Material. 2025 https://authors.elsevier.com/sd/article/S0950-0618(25)02128-2.

2. S.N.A. Bakil, Sofiia Dibrova, Sandra Breitung-Faes, Gábor Mucsi. Optimizing coal gangue reactivity for geopolymer applications: A comprehensive study on high-energy grinding parameters. Powder Technology. 2025 https://doi.org/10.1016/j.powtec.2025.121441.

3. S.N. Abd Bakil, Mucsi Gabor, Investigation mechanical activation coal gangue for geopolymer. No. 66 Proceedings of the 15th *fib* International PhD Symposium in Civil Engineering - 28-30 August 2024.Page 883

4. S.N. Abd Bakil, Mucsi Gabor, Low grade clay as raw material for geopolymer. University of Miskolc. Hungary.16 Nov 2022. https://doi.org/10.33030/geosciences.2023.01.006

5. Siti Natrah Abd Bakil, Ference Kristaly, Gábor Mucsi. Preliminary study of low-grade clay as secondary raw material for geopolymer. https://ojs.uni-miskolc.hu/index.php/geosciences/article/view/2287/1784

List of conferences:

1. S.N. Abd Bakil, Mucsi Gabor, Annual Meeting of the DECHEMA/VDI Specialist Groups 2025, Tu Clausthal, Germany. Poster presentation.

2. S.N. Abd Bakil, Mucsi Gabor, Investigation Mechanical Activation Coal Gangue for Geopolymer. No. 66 Proceedings of the 15th *fib* International PhD Symposium in Civil Engineering - 28-30 August 2024.Page 883

3. S.N. Abd Bakil, Mucsi Gabor, Low grade clay as raw material for geopolymer. MicroCAD, University of Miskolc. Hungary.16 Nov 2022.

9. REFERENCES

[1] H. Niu, L.R. Adrianto, A.G. Escobar, V. Zhukov, P. Perumal, J. Kauppi, P. Kinnunen, M. Illikainen, Potential of Mechanochemically Activated Sulfidic Mining Waste Rock for Alkali Activation, J. Sustain. Metall. 7 (2021) 1575–1588. https://doi.org/10.1007/s40831-021-00466-9.

[2] A. Saedi, A. Jamshidi-Zanjani, A.K. Darban, A review on different methods of activating tailings to improve their cementitious property as cemented paste and reusability, J. Environ. Manage. 270 (2020) 110881. https://doi.org/10.1016/j.jenvman.2020.110881.

[3] G. Huang, Y. Ji, J. Li, Z. Hou, Z. Dong, Improving strength of calcinated coal gangue geopolymer mortars via increasing calcium content, Constr. Build. Mater. 166 (2018) 760–768. https://doi.org/10.1016/j.conbuildmat.2018.02.005.

[4] B. Erdei, M. Dolezych, L. Hably, The buried Miocene forest at Bükkábrány, Hungary, Rev. Palaeobot. Palynol. 155 (2009) 69–79. https://doi.org/10.1016/j.revpalbo.2009.01.003.

[5] 2030 climate targets - European Commission, (n.d.). https://climate.ec.europa.eu/eu-action/climate-strategies-targets/2030-climate-targets_en (accessed April 6, 2025).

[6] D.H. Dang, K.A. Thompson, L. Ma, H.Q. Nguyen, S.T. Luu, M.T.N. Duong, A. Kernaghan, Toward the Circular Economy of Rare Earth Elements: A Review of Abundance, Extraction, Applications, and Environmental Impacts, Arch. Environ. Contam. Toxicol. 81 (2021) 521–530. https://doi.org/10.1007/s00244-021-00867-7.

[7] S. Hosseini, N.A. Brake, M. Nikookar, Ö. Günaydın-Şen, H.A. Snyder, Mechanochemically activated bottom ash-fly ash geopolymer, Cem. Concr. Compos. 118 (2021) 103976. https://doi.org/10.1016/j.cemconcomp.2021.103976.

[8] H. Ma, H. Zhu, C. Yi, J. Fan, H. Chen, X. Xu, T. Wang, Preparation and Reaction Mechanism Characterization of Alkali-activated Coal Gangue–Slag Materials, Materials 12 (2019) 2250. https://doi.org/10.3390/ma12142250.

[9] B.J. Frasson, R.C.A. Pinto, J.C. Rocha, Influence of different sources of coal gangue used as aluminosilicate powder on the mechanical properties and microstructure of alkali-activated cement, Mater. Constr. 69 (2019) 199. https://doi.org/10.3989/mc.2019.12618.

[10] J. Geng, M. Zhou, T. Zhang, W. Wang, T. Wang, X. Zhou, X. Wang, H. Hou, Preparation of blended geopolymer from red mud and coal gangue with mechanical co-grinding preactivation, Mater. Struct. 50 (2016) 109. https://doi.org/10.1617/s11527-016-0967-5.

[11] J. Chen, X. Guan, M. Zhu, J. Gao, Mechanism on Activation of Coal Gangue Admixture, Adv. Civ. Eng. 2021 (2021) 1–17. https://doi.org/10.1155/2021/5436482.

[12] Y. Cheng, M. Hongqiang, C. Hongyu, W. Jiaxin, S. Jing, L. Zonghui, Y. Mingkai, Preparation and characterization of coal gangue geopolymers, Constr. Build. Mater. 187 (2018) 318–326. https://doi.org/10.1016/j.conbuildmat.2018.07.220.

[13] The thermal activation process of coal gangue selected from Zhungeer in China | SpringerLink, (n.d.). https://link.springer.com/article/10.1007/s10973-016-5711-4 (accessed October 15, 2022).

[14] B. Huo, Q. Zhang, M. Li, S. Xing, Using recycled gangue to capture CO2 and prepare alkali-activated backfill paste: Adsorption and microevolution mechanisms, Fuel 358 (2024) 130194. https://doi.org/10.1016/j.fuel.2023.130194.

[15] C. Li, J. Wan, H. Sun, L. Li, Investigation on the activation of coal gangue by a new compound method, J. Hazard. Mater. 179 (2010) 515–520. https://doi.org/10.1016/j.jhazmat.2010.03.033.

[16] Q. Yang, F. Zhang, X. Deng, H. Guo, C. Zhang, C. Shi, M. Zeng, Extraction of alumina from alumina rich coal gangue by a hydro-chemical process, R. Soc. Open Sci. 7 (2020) 192132. https://doi.org/10.1098/rsos.192132.
[17] P. Baláž, M. Achimovičová, M. Baláž, P. Billik, Z. Cherkezova-Zheleva, J.M. Criado, F. Delogu, E. Dutková, E. Gaffet, F.J. Gotor, R. Kumar, I. Mitov, T. Rojac, M. Senna, A. Streletskii, K. Wieczorek-Ciurowa, Hallmarks of mechanochemistry: from nanoparticles to technology, Chem. Soc. Rev. 42 (2013) 7571–7637. https://doi.org/10.1039/C3CS35468G.
[18] S. Wang, Q. Wang, L. Xu, J. Ma, Q. Shi, N. Zhang, J. Sun, Investigating the ball-milled calcined coal gangue on the hydration of limestone blended cement, Constr. Build. Mater. 472 (2025) 140836. https://doi.org/10.1016/j.conbuildmat.2025.140836.
[19] G. Yao, T. Cui, J. Zhang, J. Wang, X. Lyu, Effects of mechanical grinding on pozzolanic activity and hydration properties of quartz, Adv. Powder Technol. 31 (2020) 4500–4509. https://doi.org/10.1016/j.apt.2020.09.028.
[20] (PDF) Molecular Network Polyamorphism in Mechanically Activated Arsenic Selenides Under Deviation from As2Se3 Stoichiometry, ResearchGate (2025). https://doi.org/10.3390/molecules30030642.
[21] L. Zhu, C. Liu, G. Duan, Z. Liu, L. Shen, Y. Zhou, K. Fang, Investigation on the activation mechanisms of coal gangue and the corresponding CO2 mineralization potential, Front. Mater. 12 (2025). https://doi.org/10.3389/fmats.2025.1567799.
[22] W. Xiao, D. Zhou, Z. Wang, T. Qi, Y. Lin, G. Li, Y. Li, D. Wang, Selective extraction of rare earth elements and cobalt from iron residue containing rare earth using mechanical activation and reductive leaching method, Sep. Purif. Technol. 337 (2024) 126447. https://doi.org/10.1016/j.seppur.2024.126447.
[23] Q. Wang, X. Li, S. Ma, H. Yang, W. Shi, Q. Chang, Y. Wang, H. Jin, Mechanical activation of metakaolin through milling: Impact on the geopolymerization process, J. Non-Cryst. Solids 650 (2025) 123373. https://doi.org/10.1016/j.jnoncrysol.2024.123373.
[24] G. Mucsi, S. Kumar, B. Csőke, R. Kumar, Z. Molnár, Á. Rácz, F. Mádai, Á. Debreczeni, Control of geopolymer properties by grinding of land filled fly ash, Int. J. Miner. Process. 143 (2015) 50–58. https://doi.org/10.1016/j.minpro.2015.08.010.
[25] E.F. Aglietti, J.M. Porto Lopez, E. Pereira, Mechanochemical effects in kaolinite grinding. I. Textural and physicochemical aspects, Int. J. Miner. Process. 16 (1986) 125–133. https://doi.org/10.1016/0301-7516(86)90079-7.
[26] S. Ahmed, T. Meng, M. Taha, Utilization of red mud for producing a high strength binder by composition optimization and nano strengthening, Nanotechnol. Rev. 9 (2020) 396–409. https://doi.org/10.1515/ntrev-2020-0029.
[27] Critical Raw Materials Act - European Commission, (n.d.). https://single-market-economy.ec.europa.eu/sectors/raw-materials/areas-specific-interest/critical-raw-materials/critical-raw-materials-act_en (accessed September 9, 2025).
[28] M. Tayebi-Khorami, M. Edraki, G. Corder, A. Golev, Re-Thinking Mining Waste through an Integrative Approach Led by Circular Economy Aspirations, Minerals 9 (2019) 286. https://doi.org/10.3390/min9050286.
[29] M. Amrani, Y. Taha, Y. El Haloui, M. Benzaazoua, R. Hakkou, Sustainable Reuse of Coal Mine Waste: Experimental and Economic Assessments for Embankments and Pavement Layer Applications in Morocco, Minerals 10 (2020) 851. https://doi.org/10.3390/min10100851.
[30] D. Sheng, J. Lan, Z. Du, Y. Ma, M. Zhou, H. Hou, Preparation of Cementitious Materials from Mechanochemically Modified Copper Smelting Slag Compounded with High-Aluminum Fly Ash, Materials 17 (2024) 546. https://doi.org/10.3390/ma17030546.

[31] M. Edraki, T. Baumgartl, E. Manlapig, D. Bradshaw, D.M. Franks, C.J. Moran, Designing mine tailings for better environmental, social and economic outcomes: a review of alternative approaches, Spec. Vol. Sustain. Agenda Miner. Energy Supply Demand Netw. Integr. Anal. Ecol. Ethical Econ. Technol. Dimens. 84 (2014) 411–420. https://doi.org/10.1016/j.jclepro.2014.04.079.
[32] M. Edraki, T. Baumgartl, E. Manlapig, D. Bradshaw, D.M. Franks, C.J. Moran, Designing mine tailings for better environmental, social and economic outcomes: a review of alternative approaches, Spec. Vol. Sustain. Agenda Miner. Energy Supply Demand Netw. Integr. Anal. Ecol. Ethical Econ. Technol. Dimens. 84 (2014) 411–420. https://doi.org/10.1016/j.jclepro.2014.04.079.
[33] S. Kalisz, K. Kibort, J. Mioduska, M. Lieder, A. Małachowska, Waste management in the mining industry of metals ores, coal, oil and natural gas - A review, J. Environ. Manage. 304 (2022) 114239. https://doi.org/10.1016/j.jenvman.2021.114239.
[34] A. Abbadi, G. Mucsi, A review on complex utilization of mine tailings: Recovery of rare earth elements and residue valorization, J. Environ. Chem. Eng. 12 (2024) 113118. https://doi.org/10.1016/j.jece.2024.113118.
[35] Clean Industrial Deal - European Commission, (n.d.). https://commission.europa.eu/topics/eu-competitiveness/clean-industrial-deal_en (accessed September 9, 2025).
[36] A. Wang, Y. Pan, J. Zhao, P. Liu, Y. Wang, Y. Chu, K. Liu, D. Sun, Research progress of resourceful and efficient utilization of coal gangue in the field of building materials, J. Build. Eng. 99 (2025) 111526. https://doi.org/10.1016/j.jobe.2024.111526.
[37] N. Islam, S. Rabha, K.S.V. Subramanyam, B.K. Saikia, Geochemistry and mineralogy of coal mine overburden (waste): A study towards their environmental implications, Chemosphere 274 (2021) 129736. https://doi.org/10.1016/j.chemosphere.2021.129736.
[38] V.A. Baki, X. Ke, A. Heath, J. Calabria-Holley, C. Terzi, Improving the pozzolanic reactivity of clay, marl and obsidian through mechanochemical or thermal activation, Mater. Struct. 57 (2023) 9. https://doi.org/10.1617/s11527-023-02280-z.
[39] Disposal of mine tailings via geopolymerization, J. Clean. Prod. 284 (2021) 124756. https://doi.org/10.1016/j.jclepro.2020.124756.
[40] Mine tailings-based geopolymers: Properties, applications and industrial prospects, Ceram. Int. 47 (2021) 17826–17843. https://doi.org/10.1016/j.ceramint.2021.03.180.
[41] S.M.A. Qaidi, B.A. Tayeh, A.M. Zeyad, A.R.G. de Azevedo, H.U. Ahmed, W. Emad, Recycling of mine tailings for the geopolymers production: A systematic review, Case Stud. Constr. Mater. 16 (2022) e00933. https://doi.org/10.1016/j.cscm.2022.e00933.
[42] W.P. Zakka, N.H. Abdul Shukor Lim, M. Chau Khun, A scientometric review of geopolymer concrete, J. Clean. Prod. 280 (2021) 124353. https://doi.org/10.1016/j.jclepro.2020.124353.
[43] Coal, IEA (n.d.). https://www.iea.org/energy-system/fossil-fuels/coal (accessed January 2, 2025).
[44] A. Gupta, N. Gupta, K.K. Saxena, Experimental study of the mechanical and durability properties of Slag and Calcined Clay based geopolymer composite, Adv. Mater. Process. Technol. (2021) 1–15. https://doi.org/10.1080/2374068X.2021.1948709.
[45] H.E.-D.M. Saleh, R.A. Rahman, Cement Based Materials, BoD – Books on Demand, 2018.
[46] J.L. Provis, Geopolymers and other alkali activated materials: why, how, and what?, Mater. Struct. 47 (2014) 11–25. https://doi.org/10.1617/s11527-013-0211-5.
[47] J. Davidovits, Why Alkali-Activated Materials (AAM) are NOT Geopolymers ?, 2018.
[48] W.M. Kriven, C. Leonelli, J.L. Provis, A.R. Boccaccini, C. Attwell, V.S. Ducman, C. Ferone, S. Rossignol, T. Luukkonen, J.S.J. van Deventer, J.V. Emiliano, J.E. Lombardi,

Why geopolymers and alkali-activated materials are key components of a sustainable world: A perspective contribution, J. Am. Ceram. Soc. 107 (2024) 5159–5177. https://doi.org/10.1111/jace.19828.
[49] F.A. Shilar, S.V. Ganachari, V.B. Patil, T.M.Y. Khan, S. Javed, R.U. Baig, Optimization of Alkaline Activator on the Strength Properties of Geopolymer Concrete, Polymers 14 (2022) 2434. https://doi.org/10.3390/polym14122434.
[50] J. Davidovits, Geopolymers: Inorganic polymeric new materials, J. Therm. Anal. Calorim. 37 (2005) 1633–1656. https://doi.org/10.1007/bf01912193.
[51] J. Davidovits, Geopolymers: inorganic polymeric new materials, J. Therm. Anal. Calorim. 37 (1991) 1633–1656.
[52] L. Weng, K. Sagoe-Crentsil, Dissolution processes, hydrolysis and condensation reactions during geopolymer synthesis: Part I—Low Si/Al ratio systems, J. Mater. Sci. 42 (2007) 2997–3006. https://doi.org/10.1007/s10853-006-0820-2.
[53] Methods to evaluate and quantify the geopolymerization reactivity of waste-derived aluminosilicate precursor in alkali-activated material: A state-of-the-art review, Constr. Build. Mater. 362 (2023) 129784. https://doi.org/10.1016/j.conbuildmat.2022.129784.
[54] B. Singh, G. Ishwarya, M. Gupta, S.K. Bhattacharyya, Geopolymer concrete: A review of some recent developments, Constr. Build. Mater. 85 (2015) 78–90. https://doi.org/10.1016/j.conbuildmat.2015.03.036.
[55] J.L. Provis, R.M. Harrex, S.A. Bernal, P. Duxson, J.S.J. van Deventer, Dilatometry of geopolymers as a means of selecting desirable fly ash sources, J. Non-Cryst. Solids 358 (2012) 1930–1937. https://doi.org/10.1016/j.jnoncrysol.2012.06.001.
[56] M. Yang, J. Sun, C. Dun, Y. Duan, Z. Meng, Cementitious activity optimization studies of iron tailings powder as a concrete admixture, Constr. Build. Mater. 265 (2020) 120760. https://doi.org/10.1016/j.conbuildmat.2020.120760.
[57] Y.-M. Liew, C.-Y. Heah, A.B. Mohd Mustafa, H. Kamarudin, Structure and properties of clay-based geopolymer cements: A review, Prog. Mater. Sci. 83 (2016) 595–629. https://doi.org/10.1016/j.pmatsci.2016.08.002.
[58] P. Baláž, W.S. Choi, M. Fabián, Mechanochemistry in the preparation of advanced materials, (2006).
[59] V. Nikolić, M. Komljenović, Z. Baščarević, N. Marjanović, Z. Miladinović, R. Petrović, The influence of fly ash characteristics and reaction conditions on strength and structure of geopolymers, Constr. Build. Mater. 94 (2015) 361–370. https://doi.org/10.1016/j.conbuildmat.2015.07.014.
[60] F. Puchegger, Zum mechanischen und chemischen Verhalten von Calcitspaltflächen, Naturwissenschaften 39 (1952) 428–429.
[61] P.Y. Butyagin, Structural Disorder and Mechanochemical Reactions in Solids, Russ. Chem. Rev. 53 (1984) 1025. https://doi.org/10.1070/RC1984v053n11ABEH003138.
[62] P. Baláž, Mechanical activation in hydrometallurgy, Int. J. Miner. Process. 72 (2003) 341–354. https://doi.org/10.1016/S0301-7516(03)00109-1.
[63] G. Tarján, Mineral Processing: Fundamentals, comminution, sizing, and classification, Akadémiai Kiadó, 1981.
[64] Z. Bujňáková, P. Baláž, A. Zorkovská, M.J. Sayagués, J. Kováč, M. Timko, Arsenic sorption by nanocrystalline magnetite: An example of environmentally promising interface with geosphere, J. Hazard. Mater. 262 (2013) 1204–1212. https://doi.org/10.1016/j.jhazmat.2013.03.007.
[65] A. Juhasz, Mechanochemical activation of silicate minerals by dry fine grinding, Aufbereitungstechnik 10 (1974) 558–562.

[66] P. Blazy, L.P. Zarogatsky, E.A. Jdid, M. Hamdadou, Vibroinertial comminution — principles and performance, Int. J. Miner. Process. 41 (1994) 33–51. https://doi.org/10.1016/0301-7516(94)90004-3.
[67] M. Senna, How can we make solids more reactive? Basics of mechanochemistry and recent new insights, ChemTexts 3 (2017) 4. https://doi.org/10.1007/s40828-017-0041-0.
[68] A. Kienle, A. Seidel-Morgenstern, K. Sundmacher, Integrated Chemical Processes: Synthesis, Operation, Analysis and Control, John Wiley & Sons, 2006.
[69] B. Pavlović, N. Trinajstić, ON SYMMETRY AND ASYMMETRY IN LITERATURE††This essay is dedicated to Zagreb, the capital of Croatia and a beautiful city with a nice blend of historical core and modern parts, rich with evidence for all aspects of urban symmetry, asymmetry, and anti-symmetry., in: I. Hargittai (Ed.), Symmetry, Pergamon, 1986: pp. 197–227. https://doi.org/10.1016/B978-0-08-033986-3.50022-7.
[70] V.V. Boldyrev, K. Tkáčová, Mechanochemistry of Solids: Past, Present, and Prospects, J. Mater. Synth. Process. 8 (2000) 121–132. https://doi.org/10.1023/A:1011347706721.
[71] P. Baláž, Mechanochemistry in nanoscience and minerals engineering, 2008, (2008).
[72] A. Kwade, A Stressing Model for the Description and Optimization of Grinding Processes, Chem. Eng. Technol. 26 (2003) 199–205. https://doi.org/10.1002/ceat.200390029.
[73] A. Kwade, Mill selection and process optimization using a physical grinding model, Int. J. Miner. Process. 74 (2004) S93–S101. https://doi.org/10.1016/j.minpro.2004.07.027.
[74] Experimental and Computational Investigation of Knoevenagel Condensation in Planetary Ball Mills - Burmeister - 2014 - Chemical Engineering & Technology - Wiley Online Library, (n.d.). https://onlinelibrary.wiley.com/doi/abs/10.1002/ceat.201300738 (accessed October 29, 2024).
[75] G. Mucsia, Z. Molnára, S. Kumarb, Geopolymerisation of Mechanically Activated Lignite and Brown Coal Fly Ash, (n.d.).
[76] R. Szabó, F. Kristály, S. Nagy, R. Singla, G. Mucsi, S. Kumar, Reaction, structure and properties of eco-friendly geopolymer cement derived from mechanically activated pumice, Ceram. Int. (2022). https://doi.org/10.1016/j.ceramint.2022.10.204.
[77] M.T. Yamchelou, D.W. Law, I. Patnaikuni, J. Li, Alkali activation of mechanically activated low-grade clay, J. Sustain. Cem.-Based Mater. 10 (2021) 272–288. https://doi.org/10.1080/21650373.2020.1838355.
[78] S. Pradhan, Z. Li, S. Qian, A thermo-mechano-chemical activation technique to use quartz rich marine clay for one-part geopolymer preparation, Cem. Concr. Compos. 140 (2023) 105057. https://doi.org/10.1016/j.cemconcomp.2023.105057.
[79] G. Yao, Q. Liu, J. Wang, P. Wu, X. Lyu, Effect of mechanical grinding on pozzolanic activity and hydration properties of siliceous gold ore tailings, J. Clean. Prod. 217 (2019) 12–21. https://doi.org/10.1016/j.jclepro.2019.01.175.
[80] R. Szabó, M. Szűcs, M. Ambrus, G. Mucsi, Increasing the Pozzolanic Reactivity of Recovered CDW Cement Stone by Mechanical Activation, Mater. Proc. 13 (2023) 27. https://doi.org/10.3390/materproc2023013027.
[81] A. Longos, A.A. Tigue, R.A. Malenab, I.J. Dollente, M.A. Promentilla, Mechanical and thermal activation of nickel-laterite mine waste as a precursor for geopolymer synthesis, Results Eng. 7 (2020) 100148. https://doi.org/10.1016/j.rineng.2020.100148.
[82] A. Bouaziz, R. Hamzaoui, S. Guessasma, R. Lakhal, D. Achoura, N. Leklou, Efficiency of high energy over conventional milling of granulated blast furnace slag powder to improve mechanical performance of slag cement paste, Powder Technol. 308 (2017) 37–46. https://doi.org/10.1016/j.powtec.2016.12.014.

[83] R. Han, X. Guo, J. Guan, X. Yao, Y. Hao, Activation Mechanism of Coal Gangue and Its Impact on the Properties of Geopolymers: A Review, Polymers 14 (2022) 3861. https://doi.org/10.3390/polym14183861.
[84] B. Figiela, K. Korniejenko, A. Bulut, B. Şahin, G. Azizağaoğlu, K. Pławecka, B. Kozub, Influence of the Size of Milled Coal Gangue Particles on the Mechanical Properties of Geopolymers, Mater. Proc. 13 (2023) 4. https://doi.org/10.3390/materproc2023013004.
[85] Z. Li, Y. Gao, J. Zhang, C. Zhang, J. Chen, C. Liu, Effect of particle size and thermal activation on the coal gangue based geopolymer, Mater. Chem. Phys. 267 (2021) 124657. https://doi.org/10.1016/j.matchemphys.2021.124657.
[86] Y. Zhao, C. Yang, K. Li, F. Qu, C. Yan, Z. Wu, Toward understanding the activation and hydration mechanisms of composite activated coal gangue geopolymer, Constr. Build. Mater. 318 (2022) 125999. https://doi.org/10.1016/j.conbuildmat.2021.125999.
[87] B. Frasson, R. Pinto, J. Rocha, Influence of different sources of coal gangue used as aluminosilicate powder on the mechanical properties and microstructure of alkali-activated cement, Mater. Constr. 69 (2019) e199–e199.
[88] V.A. Baki, X. Ke, A. Heath, J. Calabria-Holley, C. Terzi, M. Sirin, The impact of mechanochemical activation on the physicochemical properties and pozzolanic reactivity of kaolinite, muscovite and montmorillonite, Cem. Concr. Res. 162 (2022) 106962. https://doi.org/10.1016/j.cemconres.2022.106962.
[89] J. Temuujin, B. Davaabal, U. Rentsennorov, E. Odbaatar, D. Enkhbayar, T. Tsend-Ayush, S. Danzandorj, C.H. Ruescher, K.J.D. MacKenzie, Characterization of Alkali Activated Materials Prepared from Continuous Attrition and Ball Milled Fly Ashes, Minerals 13 (2023) 490. https://doi.org/10.3390/min13040490.
[90] S. Pradhan, Z. Li, S. Qian, A thermo-mechano-chemical activation technique to use quartz rich marine clay for one-part geopolymer preparation, Cem. Concr. Compos. 140 (2023) 105057. https://doi.org/10.1016/j.cemconcomp.2023.105057.
[91] Q. Wan, Y. Zhang, R. Zhang, Using mechanical activation of quartz to enhance the compressive strength of metakaolin based geopolymers, Cem. Concr. Compos. 111 (2020) 103635. https://doi.org/10.1016/j.cemconcomp.2020.103635.
[92] Utilization of zinc slag through geopolymerization: Influence of milling atmosphere, Int. J. Miner. Process. 123 (2013) 102–107. https://doi.org/10.1016/j.minpro.2013.06.001.
[93] Y. Song, X. Zhang, J. Xu, S. Jiang, Z. Yanhui, Mechanical properties and water resistance of alkali-activated flood-control stone incorporating ball-milling treated Yellow River silt, Case Stud. Constr. Mater. 22 (2025) e04640. https://doi.org/10.1016/j.cscm.2025.e04640.
[94] M. Baláž, Environmental mechanochemistry, Springer, 2021.
[95] Mechanical activation of cement with addition of fly ash, Mater. Lett. 39 (1999) 115–121. https://doi.org/10.1016/S0167-577X(98)00226-2.
[96] A critical review on mechanochemical processing of fly ash and fly ash-derived materials, Sci. Total Environ. 860 (2023) 160529. https://doi.org/10.1016/j.scitotenv.2022.160529.
[97] I. Krycer, J.A. Hersey, A comparative study of comminution in rotary and vibratory ball mills, Powder Technol. 27 (1980) 137–141. https://doi.org/10.1016/0032-5910(80)85015-7.
[98] S. Kumar, R. Kumar, T.C. Alex, A. BANDOPADHYAY, s. P. Mehrotra, Influence of reactivity of fly ash on geopolymerisation, Adv. Appl. Ceram. 106 (2007) 120–127. https://doi.org/10.1179/174367607X159293.
[99] Y.-S. Chu, B. Davaabal, D.-S. Kim, S.-K. Seo, Y. Kim, C. Ruescher, J. Temuujin, Reactivity of fly ashes milled in different milling devices, 58 (2019) 179–188. https://doi.org/10.1515/rams-2019-0028.

[100] T. Sangu, Y. Xin, T. Hitomi, K. Kato, T. Shirai, Influence of ball materials on the surface activation behavior of coal ash particles during a mechanochemical process, Ceram. Int. 49 (2023) 34327–34332. https://doi.org/10.1016/j.ceramint.2023.06.219.
[101] A. Nana, E.N. Sakue, P. Venyite, S.C.D. Anensong, N. Epey, A.A. Adediran, E. Kamseu, S. Kumar, C. Leonelli, Effect of milled pegmatite quarry wastes powders on structure, microstructure and mechanical properties of pegmatite-based geopolymers, Materialia 33 (2024) 102022. https://doi.org/10.1016/j.mtla.2024.102022.
[102] H. Niu, P. Kinnunen, H. Sreenivasan, E. Adesanya, M. Illikainen, Structural collapse in phlogopite mica-rich mine tailings induced by mechanochemical treatment and implications to alkali activation potential, Miner. Eng. 151 (2020) 106331. https://doi.org/10.1016/j.mineng.2020.106331.
[103] Pozzolanic activity of mechanochemically and thermally activated kaolins in cement, Cem. Concr. Res. 77 (2015) 47–59. https://doi.org/10.1016/j.cemconres.2015.04.017.
[104] S. Kumar, R. Kumar, Mechanical activation of fly ash: Effect on reaction, structure and properties of resulting geopolymer, Ceram. Int. 37 (2011) 533–541. https://doi.org/10.1016/j.ceramint.2010.09.038.
[105] R. Gao, Z. Zhou, J. Yang, J. Zhang, Innovative assessment of reactivity in fly ash: The role of particle size distribution characteristics, Open Ceram. 20 (2024) 100680. https://doi.org/10.1016/j.oceram.2024.100680.
[106] L. Zhu, C. Liu, G. Duan, Z. Liu, L. Jin, Y. Zhou, K. Fang, Research on the Mechanical Activation Mechanism of Coal Gangue and Its CO2 Mineralization Effect, Sustainability 17 (2025) 2364. https://doi.org/10.3390/su17062364.
[107] H. Guo, H. Wang, H. Li, H. Xue, L. Wei, Y. Li, Y. Chen, Q. Li, H. Dong, Comparison of performance, hydration behavior, and environmental benefits of coal gangue cementitious materials prepared by wet and dry grinding methods, Constr. Build. Mater. 471 (2025) 140665. https://doi.org/10.1016/j.conbuildmat.2025.140665.
[108] A. Moussadik, F. Ouzoun, H. Ez-zaki, M. Saadi, A. Diouri, Mineralogical study of a binder based on alkali-activated coal gangue, Mater. Today Proc. (2023). https://doi.org/10.1016/j.matpr.2023.07.091.
[109] Y. Zhao, J. Qiu, Z. Ma, X. Sun, Eco-friendly treatment of coal gangue for its utilization as supplementary cementitious materials, J. Clean. Prod. 285 (2021) 124834. https://doi.org/10.1016/j.jclepro.2020.124834.
[110] W. Zhang, C. Dong, P. Huang, Q. Sun, M. Li, J. Chai, Experimental Study on the Characteristics of Activated Coal Gangue and Coal Gangue-Based Geopolymer, Energies 13 (2020) 2504. https://doi.org/10.3390/en13102504.
[111] J. Geng, M. Zhou, Y. Li, Y. Chen, Y. Han, S. Wan, X. Zhou, H. Hou, Comparison of red mud and coal gangue blended geopolymers synthesized through thermal activation and mechanical grinding preactivation, Constr. Build. Mater. 153 (2017) 185–192. https://doi.org/10.1016/j.conbuildmat.2017.07.045.
[112] I. Balczár, T. Korim, A. Kovács, É. Makó, Mechanochemical and thermal activation of kaolin for manufacturing geopolymer mortars – Comparative study, Ceram. Int. 42 (2016) 15367–15375. https://doi.org/10.1016/j.ceramint.2016.06.182.
[113] I. Tole, K. Habermehl-Cwirzen, M. Rajczakowska, A. Cwirzen, Activation of a Raw Clay by Mechanochemical Process—Effects of Various Parameters on the Process Efficiency and Cementitious Properties, Materials 11 (2018) 1860. https://doi.org/10.3390/ma11101860.
[114] G. Mucsi, S. Kumar, B. Csőke, R. Kumar, Z. Molnár, Á. Rácz, F. Mádai, Á. Debreczeni, Control of geopolymer properties by grinding of land filled fly ash, Int. J. Miner. Process. 143 (2015) 50–58. https://doi.org/10.1016/j.minpro.2015.08.010.

[115] B. Chen, L. Pang, Z. Zhou, Q. Chang, P. Fu, Study on the activation mechanism and hydration properties of gold tailings activated by mechanical-chemical-thermal coupling, J. Build. Eng. 48 (2022) 104014. https://doi.org/10.1016/j.jobe.2022.104014.
[116] E.F. Aglietti, J.M. Porto Lopez, E. Pereira, Mechanochemical effects in kaolinite grinding. I. Textural and physicochemical aspects, Int. J. Miner. Process. 16 (1986) 125–133. https://doi.org/10.1016/0301-7516(86)90079-7.
[117] A.Z. Juhasz, L. Opoczky, Mechanical activation of minerals by grinding pulverizing and morphology of particles, (1990). https://www.osti.gov/biblio/6916604 (accessed February 13, 2023).
[118] K. Kato, Y. Xin, T. Hitomi, T. Shirai, Surface modification of fly ash by mechano-chemical treatment, Ceram. Int. 45 (2019) 849–853. https://doi.org/10.1016/j.ceramint.2018.09.254.
[119] Effect of mechanical activation of fly ash on the properties of geopolymer cured at ambient temperature, J. Mater. Process. Technol. 209 (2009) 5276–5280. https://doi.org/10.1016/j.jmatprotec.2009.03.016.
[120] Effects of alkaline activators on pore structure and mechanical properties of ultrafine metakaolin geopolymers cured at room temperature, Constr. Build. Mater. 361 (2022) 129678. https://doi.org/10.1016/j.conbuildmat.2022.129678.
[121] N. Cristelo, P. Tavares, E. Lucas, T. Miranda, D. Oliveira, Quantitative and qualitative assessment of the amorphous phase of a Class F fly ash dissolved during alkali activation reactions – Effect of mechanical activation, solution concentration and temperature, Compos. Part B Eng. 103 (2016) 1–14. https://doi.org/10.1016/j.compositesb.2016.08.001.
[122] R.L. Frost, É. Makó, J. Kristóf, E. Horváth, J.T. Kloprogge, Mechanochemical Treatment of Kaolinite, J. Colloid Interface Sci. 239 (2001) 458–466. https://doi.org/10.1006/jcis.2001.7591.
[123] Y. Guo, K. Yan, L. Cui, F. Cheng, Improved extraction of alumina from coal gangue by surface mechanically grinding modification, Powder Technol. 302 (2016) 33–41. https://doi.org/10.1016/j.powtec.2016.08.034.
[124] J. Tan, Ö. Cizer, J. De Vlieger, H. Dan, J. Li, Impacts of milling duration on construction and demolition waste (CDW) based precursor and resulting geopolymer: Reactivity, geopolymerization and sustainability, Resour. Conserv. Recycl. 184 (2022) 106433. https://doi.org/10.1016/j.resconrec.2022.106433.
[125] J.N. Yankwa Djobo, A. Elimbi, H.K. Tchakouté, S. Kumar, Mechanical activation of volcanic ash for geopolymer synthesis: effect on reaction kinetics, gel characteristics, physical and mechanical properties, RSC Adv. 6 (2016) 39106–39117. https://doi.org/10.1039/C6RA03667H.
[126] S. Rescic, P. Plescia, P. Cossari, E. Tempesta, D. Capitani, N. Proietti, F.Fratini, A.M. Mecchi, Mechano-chemical activation: an ecological safety process in the production of materials to stone conservation, 2011 Int. Conf. Green Build. Sustain. Cities 21 (2011) 1061–1071. https://doi.org/10.1016/j.proeng.2011.11.2112.
[127] Y. Luo, S. Bao, S. Liu, Y. Zhang, S. Li, Y. Ping, Enhancing reactivity of granite waste powder toward geopolymer preparation by mechanical activation, Constr. Build. Mater. 414 (2024) 134981. https://doi.org/10.1016/j.conbuildmat.2024.134981.
[128] Y. Zhao, J. Qiu, Z. Ma, X. Sun, Eco-friendly treatment of coal gangue for its utilization as supplementary cementitious materials, J. Clean. Prod. 285 (2021) 124834. https://doi.org/10.1016/j.jclepro.2020.124834.
[129] B. Jabłońska, A.V. Kityk, M. Busch, P. Huber, The structural and surface properties of natural and modified coal gangue, J. Environ. Manage. 190 (2017) 80–90. https://doi.org/10.1016/j.jenvman.2016.12.055.

[130] Standard Specification for Coal Fly Ash and Raw or Calcined Natural Pozzolan for Use in Concrete, (n.d.). https://store.astm.org/c0618-22.html
[131] E.I. Diaz, E.N. Allouche, S. Eklund, Factors affecting the suitability of fly ash as source material for geopolymers, Fuel 89 (2010) 992–996. https://doi.org/10.1016/j.fuel.2009.09.012.
[132] B. Csőke, Á. Rácz, G. Mucsi, Determination of the Bond work index of binary mixtures by different methods, Int. J. Miner. Process. 123 (2013) 78–86. https://doi.org/10.1016/j.minpro.2013.05.004.
[133] C. Burmeister, L. Titscher, S. Breitung-Faes, A. Kwade, Dry grinding in planetary ball mills: Evaluation of a stressing model, Adv. Powder Technol. 29 (2018) 191–201. https://doi.org/10.1016/j.apt.2017.11.001.
[134] ISO 13320:2020, ISO (n.d.). https://www.iso.org/standard/69111.html
[135] C191 Standard Test Methods for Time of Setting of Hydraulic Cement by Vicat Needle, (n.d.). https://store.astm.org/c0191-21.html (accessed August 9, 2025).
[136] N. Vdović, I. Jurina, S.D. Škapin, I. Sondi, The surface properties of clay minerals modified by intensive dry milling — revisited, Appl. Clay Sci. 48 (2010) 575–580. https://doi.org/10.1016/j.clay.2010.03.006.
[137] S.L. James, T. Friščić, Mechanochemistry, Chem. Soc. Rev. 42 (2013) 7494–7496.
[138] A. Zoltán Juhász, Aspects of mechanochemical activation in terms of comminution theory, Colloids Surf. Physicochem. Eng. Asp. 141 (1998) 449–462. https://doi.org/10.1016/S0927-7757(98)00245-3.
[139] Undesired Agglomeration:Methods of Avoiding or Lessening its Effect, in: Agglom. Set, John Wiley & Sons, Ltd, 2004: pp. 23–36. https://doi.org/10.1002/9783527619788.ch4a.
[140] P.L. Guzzo, F.B. Marinho de Barros, B.R. Soares, J.B. Santos, Evaluation of particle size reduction and agglomeration in dry grinding of natural quartz in a planetary ball mill, Powder Technol. 368 (2020) 149–159. https://doi.org/10.1016/j.powtec.2020.04.052.
[141] Comparative study of microstructural characteristics and stored energy of mechanically activated hematite in different grinding environments, Int. J. Miner. Process. 79 (2006) 120–139. https://doi.org/10.1016/j.minpro.2006.01.010.
[142] Two dimensions comminution of kaolinite clay particles, Powder Technol. 105 (1999) 125–134. https://doi.org/10.1016/S0032-5910(99)00127-8.
[143] F. Mádai, F. Kristály, G. Mucsi, MICROSTRUCTURE, MINERALOGY AND PHYSICAL PROPERTIES OF GROUND FLY ASH BASED GEOPOLYMERS, (2015).
[144] F. Cherblanc, J. Berthonneau, P. Bromblet, V. Huon, Influence of Water Content on the Mechanical Behaviour of Limestone: Role of the Clay Minerals Content, Rock Mech. Rock Eng. 49 (2016) 2033–2042. https://doi.org/10.1007/s00603-015-0911-y.
[145] E. Petrakis, V. Karmali, G. Bartzas, K. Komnitsas, Grinding Kinetics of Slag and Effect of Final Particle Size on the Compressive Strength of Alkali Activated Materials, Minerals 9 (2019) 714. https://doi.org/10.3390/min9110714.
[146] K.J. Pascoe, Inorganic Non-metallic Materials, in: Introd. Prop. Eng. Mater., Springer Netherlands, Dordrecht, 1978: pp. 343–364. https://doi.org/10.1007/978-94-011-7068-0_20.
[147] X. Yang, Y. Zhang, C. Lin, Microstructure Analysis and Effects of Single and Mixed Activators on Setting Time and Strength of Coal Gangue-Based Geopolymers, Gels 8 (2022) 195. https://doi.org/10.3390/gels8030195.
[148] G. Mucsi, N. Halyag Papné, C. Ulsen, P.O. Figueiredo, F. Kristály, Mechanical Activation of Construction and Demolition Waste in Order to Improve Its Pozzolanic

Reactivity, ACS Sustain. Chem. Eng. 9 (2021) 3416–3427. https://doi.org/10.1021/acssuschemeng.0c05838.
[149] B.J. Saikia, Spectroscopic estimation of geometrical structure elucidation in natural SiO2 crystal, J Mater Phys Chem 2 (2014) 28–33.
[150] F. Delogu, Mechanochemical Behavior of Surface Radicals in Ground Quartz, J. Phys. Chem. C 115 (2011) 21230–21235. https://doi.org/10.1021/jp206354p.
[151] H.P. Klug, L.E. Alexander, X-ray diffraction procedures: for polycrystalline and amorphous materials, 1974.
[152] R. Mejdoub, H. Hammi, M. Khitouni, J.J. Suñol, A. M'nif, The effect of prolonged mechanical activation duration on the reactivity of Portland cement: Effect of particle size and crystallinity changes, Constr. Build. Mater. 152 (2017) 1041–1050. https://doi.org/10.1016/j.conbuildmat.2017.07.008.
[153] Improving reactivity of fly ash and properties of ensuing geopolymers through mechanical activation, Constr. Build. Mater. 57 (2014) 151–162. https://doi.org/10.1016/j.conbuildmat.2014.01.095.
[154] S. Beinert, G. Fragnière, C. Schilde, A. Kwade, Analysis and modelling of bead contacts in wet-operating stirred media and planetary ball mills with CFD–DEM simulations, Chem. Eng. Sci. 134 (2015) 648–662. https://doi.org/10.1016/j.ces.2015.05.063.
[155] P.J. Heaney, Chapter 1. STRUCTURE AND CHEMISTRY OF THE LOW-PRESSURE SILICA POLYMORPHS, in: Silica, De Gruyter, 2018: pp. 1–40. https://www.degruyterbrill.com/document/doi/10.1515/9781501509698-006/pdf?licenseType=restricted (accessed April 29, 2025).
[156] R. Hamzaoui, F. Muslim, S. Guessasma, A. Bennabi, J. Guillin, Structural and thermal behavior of proclay kaolinite using high energy ball milling process, Powder Technol. 271 (2015) 228–237. https://doi.org/10.1016/j.powtec.2014.11.018.
[157] Mechanisms of carbonation hydration hardening in Portland cements, Cem. Concr. Res. 152 (2022) 106687. https://doi.org/10.1016/j.cemconres.2021.106687.
[158] M.S. Tuğluca, E. Teksin, K. Taj, O. Şahin, H. İlcan, E. Gülcan, M. Şahmaran, Mechanochemical transformation of waste bricks: A study on grinding optimization and pozzolanic activity, Powder Technol. 460 (2025) 121030. https://doi.org/10.1016/j.powtec.2025.121030.
[159] M. Tahmasebi Yamchelou, D. Law, R. Brkljača, C. Gunasekara, J. Li, I. Patnaikuni, Geopolymer synthesis using low-grade clays, Constr. Build. Mater. 268 (2021) 121066. https://doi.org/10.1016/j.conbuildmat.2020.121066.
[160] Y.-M. Liew, C.-Y. Heah, A.B. Mohd Mustafa, H. Kamarudin, Structure and properties of clay-based geopolymer cements: A review, Prog. Mater. Sci. 83 (2016) 595–629. https://doi.org/10.1016/j.pmatsci.2016.08.002.
[161] F. Pacheco-Torgal, J. Castro-Gomes, S. Jalali, Alkali-activated binders: A review. Part 2. About materials and binders manufacture, Constr. Build. Mater. 22 (2008) 1315–1322. https://doi.org/10.1016/j.conbuildmat.2007.03.019.
[162] M.S. Morsy, S.H. Alsayed, Y. Al-Salloum, T. Almusallam, Effect of Sodium Silicate to Sodium Hydroxide Ratios on Strength and Microstructure of Fly Ash Geopolymer Binder, Arab. J. Sci. Eng. 39 (2014) 4333–4339. https://doi.org/10.1007/s13369-014-1093-8.
[163] J. Davidovits, Geopolymer Chemistry and Applications, Geopolymer Institute, 2008. https://books.google.hu/books?id=dliw_KTYq4oC.
[164] Effect of curing temperature on the development of hard structure of metakaolin-based geopolymer, Constr. Build. Mater. 24 (2010) 1176–1183. https://doi.org/10.1016/j.conbuildmat.2009.12.023.

[165] N. Marjanović, M. Komljenović, Z. Baščarević, V. Nikolić, Improving reactivity of fly ash and properties of ensuing geopolymers through mechanical activation, Constr. Build. Mater. 57 (2014) 151–162. https://doi.org/10.1016/j.conbuildmat.2014.01.095.
[166] J.G.S. van Jaarsveld, J.S.J. van Deventer, Effect of the Alkali Metal Activator on the Properties of Fly Ash-Based Geopolymers, Ind. Eng. Chem. Res. 38 (1999) 3932–3941. https://doi.org/10.1021/ie980804b.
[167] U. Rattanasak, P. Chindaprasirt, Influence of NaOH solution on the synthesis of fly ash geopolymer, Miner. Eng. 22 (2009) 1073–1078. https://doi.org/10.1016/j.mineng.2009.03.022.
[168] J. Zeng, K. Zhang, W. Sun, Y. Zeng, Z. Zou, Mechanics and microstructure analysis of geopolymer utilizing ilmenite tailing and metakaolin powder as alkali-activated materials, Case Stud. Constr. Mater. 21 (2024) e03567. https://doi.org/10.1016/j.cscm.2024.e03567.
[169] P. Duxson, J.L. Provis, Designing Precursors for Geopolymer Cements, J. Am. Ceram. Soc. 91 (2008) 3864–3869. https://doi.org/10.1111/j.1551-2916.2008.02787.x.
[170] P.D. Silva, K. Sagoe-Crenstil, V. Sirivivatnanon, Kinetics of geopolymerization: Role of Al2O3 and SiO2, Cem. Concr. Res. 37 (2007) 512–518. https://doi.org/10.1016/j.cemconres.2007.01.003.
[171] F. Kristály, B. Török, The role of SiO_2 and silica-rich amorphous materials in understanding the origin of uncommon archeological finds, Mater. Manuf. Process. 35 (2020) 1410–1419. https://doi.org/10.1080/10426914.2020.1762210.
[172] G. Mucsi, Mechanical activation of power station fl y ash by grinding – A review, Epitoanyag - J. Silic. Based Compos. Mater. 68 (2016) 56–61. https://doi.org/10.14382/epitoanyag-jsbcm.2016.10.
[173] S. Kumar, G. Mucsi, F. Kristály, P. Pekker, Mechanical activation of fly ash and its influence on micro and nano-structural behaviour of resulting geopolymers, Adv. Powder Technol. 28 (2017) 805–813. https://doi.org/10.1016/j.apt.2016.11.027.
[174] R. Szabó, F. Dolgos, Á. Debreczeni, G. Mucsi, Characterization of mechanically activated fly ash-based lightweight geopolymer composite prepared with ultrahigh expanded perlite content, Ceram. Int. (2021). https://doi.org/10.1016/j.ceramint.2021.10.218.
[175] K. Debnath, D. Das, P. Kumar Rout, Effect of mechanical milling of fly ash powder on compressive strength of geopolymer, Mater. Today Proc. 68 (2022) 242–249. https://doi.org/10.1016/j.matpr.2022.08.321.
[176] E. Prud'homme, P. Michaud, E. Joussein, A. Smith, C. Peyratout, I. Sobrados, J. Sanz, S. Rossignol, Geomaterial foams: role assignment of raw materials in the network formation, J. Sol-Gel Sci. Technol. 61 (2012) 436–448. https://doi.org/10.1007/s10971-011-2644-z.
[177] X. Wang, F. Liu, Z. Pan, W. Chen, F. Muhammad, B. Zhang, L. Li, Geopolymerization of Coal Gangue via Alkali-Activation: Dependence of Mechanical Properties on Alkali Activators, Buildings 14 (2024) 787. https://doi.org/10.3390/buildings14030787.
[178] I. Ozer, S. Soyer-Uzun, Relations between the structural characteristics and compressive strength in metakaolin based geopolymers with different molar Si/Al ratios, Ceram. Int. 41 (2015) 10192–10198. https://doi.org/10.1016/j.ceramint.2015.04.125.
[179] A. Nana, E. Kamseu, A.-T. Akono, J. Ngouné, J.N. Yankwa Djobo, H.K. Tchakouté, M.C. Bignozzi, C. Leonelli, Particles size and distribution on the improvement of the mechanical performance of high strength solid solution based inorganic polymer composites: A microstructural approach, Mater. Chem. Phys. 267 (2021) 124602. https://doi.org/10.1016/j.matchemphys.2021.124602.
[180] Zoltán J., Mechano-chemical activation of kaolin minerals, Acta Mineral.-Petrogr. 24 (1980) 121–145.

[181] D. Wasan, A. Nikolov, B. Moudgil, Colloidal dispersions: Structure, stability and geometric confinement, Powder Technol. 153 (2005) 135–141. https://doi.org/10.1016/j.powtec.2004.12.005.
[182] F. Stenger, S. Mende, J. Schwedes, W. Peukert, Nanomilling in Stirred Media Mills, Chem. Eng. Sci. 60 (2005) 4557–4565. https://doi.org/10.1016/j.ces.2005.02.057.
[183] A.Z. Juhász, Z. Juhász, L. Opoczky, Mechanical Activation of Minerals by Grinding: Pulverizing and Morphology of Particles, Ellis Horwood, 1990. https://books.google.hu/books?id=HsJaAAAAYAAJ.
[184] L. Opoczky, Fine grinding and agglomeration of silicates, Powder Technol. 17 (1977) 1–7. https://doi.org/10.1016/0032-5910(77)85037-7.
[185] I. Tole, F. Delogu, E. Qoku, K. Habermehl-Cwirzen, A. Cwirzen, Enhancement of the pozzolanic activity of natural clays by mechanochemical activation, Constr. Build. Mater. 352 (2022) 128739. https://doi.org/10.1016/j.conbuildmat.2022.128739.
[186] The impact of mechanochemical activation on the physicochemical properties and pozzolanic reactivity of kaolinite, muscovite and montmorillonite, Cem. Concr. Res. 162 (2022) 106962. https://doi.org/10.1016/j.cemconres.2022.106962.
[187] M. Baláž, M. Birinci, K. Şentürk, M. Achimovičová, P. Baláž, I.O. Tampubolon, T. Stolar, R. Bienert, F. Emmerling, S. Erdemoğlu, H. Sis, M. Erdemoğlu, Utilizing Taguchi method and in situ X-ray powder diffraction monitoring to determine the influence of mechanical activation conditions on the physico-chemical properties and Al leachability of K-feldspar, J. Mater. Res. Technol. 32 (2024) 3886–3895. https://doi.org/10.1016/j.jmrt.2024.08.156.
[188] N. Vdović, I. Jurina, S.D. Škapin, I. Sondi, The surface properties of clay minerals modified by intensive dry milling — revisited, Appl. Clay Sci. 48 (2010) 575–580. https://doi.org/10.1016/j.clay.2010.03.006.
[189] V.V. Boldyrev, S.V. Pavlov, E.L. Goldberg, Interrelation between fine grinding and mechanical activation, Int. J. Miner. Process. 44–45 (1996) 181–185. https://doi.org/10.1016/0301-7516(95)00028-3.
[190] Structural collapse in phlogopite mica-rich mine tailings induced by mechanochemical treatment and implications to alkali activation potential, Miner. Eng. 151 (2020) 106331. https://doi.org/10.1016/j.mineng.2020.106331.
[191] W. Steele, G. Zgrablich, W. Rudzinski, Equilibria and dynamics of gas adsorption on heterogeneous solid surfaces, Elsevier, 1996.
[192] M. Thommes, K. Kaneko, A.V. Neimark, J.P. Olivier, F. Rodriguez-Reinoso, J. Rouquerol, K.S.W. Sing, Physisorption of gases, with special reference to the evaluation of surface area and pore size distribution (IUPAC Technical Report), 87 (2015) 1051–1069. https://doi.org/10.1515/pac-2014-1117.
[193] R. Arbain, M. Othman, S. Palaniandy, Preparation of iron oxide nanoparticles by mechanical milling, Miner. Eng. 24 (2011) 1–9. https://doi.org/10.1016/j.mineng.2010.08.025.
[194] P. Pourghahramani, E. Forssberg, Microstructure characterization of mechanically activated hematite using XRD line broadening, Int. J. Miner. Process. 79 (2006) 106–119. https://doi.org/10.1016/j.minpro.2006.02.001.
[195] L.G. Austin, P. Bagga, An analysis of fine dry grinding in ball mills, Powder Technol. 28 (1981) 83–90. https://doi.org/10.1016/0032-5910(81)87014-3.
[196] A. Kwade, J. Schwedes, Breaking characteristics of different materials and their effect on stress intensity and stress number in stirred media mills, Powder Technol. 122 (2002) 109–121. https://doi.org/10.1016/S0032-5910(01)00406-5.

[197] O. Altun, P. Prziwara, S. Breitung-Faes, A. Kwade, Impacts of process and design conditions of dry stirred milling on the shape of product size distribution, Miner. Eng. 163 (2021) 106806. https://doi.org/10.1016/j.mineng.2021.106806.
[198] S. Kaufhold, M. Hein, R. Dohrmann, K. Ufer, Quantification of the mineralogical composition of clays using FTIR spectroscopy, Vib. Spectrosc. 59 (2012) 29–39. https://doi.org/10.1016/j.vibspec.2011.12.012.
[199] A. Povarennykh, The use of infrared spectra for the determination of minerals, Am. Mineral. 63 (1978) 956–959.
[200] S. Chida, B. Uchino, M. Senna, A topochemical study on the microplastic deformation and preferred dissolution of pure silicon single crystal, Solid State Ion. 39 (1990) 263–272. https://doi.org/10.1016/0167-2738(90)90405-G.
[201] R.K. Mishra, M. Weibel, T. Müller, H. Heinz, R.J. Flatt, Energy-effective Grinding of Inorganic Solids Using Organic Additives, CHIMIA 71 (2017) 451–451. https://doi.org/10.2533/chimia.2017.451.
[202] N.V. Chukanov, A.D. Chervonnyi, Infrared spectroscopy of minerals and related compounds, Springer, 2016.
[203] M. Kumar, L. Goswami, A.K. Singh, M. Sikandar, Valorization of coal fired-fly ash for potential heavy metal removal from the single and multi-contaminated system, Heliyon 5 (2019). https://doi.org/10.1016/j.heliyon.2019.e02562.
[204] Y. Liu, B. Sun, L. Tajcmanova, C. Liu, J. Wu, Effect of carbon residues structures on burnout characteristic by FTIR and Raman spectroscopy, Spectrochim. Acta. A. Mol. Biomol. Spectrosc. 272 (2022) 120947. https://doi.org/10.1016/j.saa.2022.120947.
[205] X. Liu, D. Song, X. He, B. Nie, L. Wang, Insight into the macromolecular structural differences between hard coal and deformed soft coal, Fuel 245 (2019) 188–197. https://doi.org/10.1016/j.fuel.2019.02.070.
[206] L. Zhu, C. Liu, G. Duan, Z. Liu, L. Jin, Y. Zhou, K. Fang, Research on the Mechanical Activation Mechanism of Coal Gangue and Its CO2 Mineralization Effect, Sustainability 17 (2025) 2364. https://doi.org/10.3390/su17062364.
[207] JoséV. Ibarra, E. Muñoz, R. Moliner, FTIR study of the evolution of coal structure during the coalification process, Org. Geochem. 24 (1996) 725–735. https://doi.org/10.1016/0146-6380(96)00063-0.
[208] E.C. Leonel, E.J. Nassar, K.J. Ciuffi, M.J. dos Reis, P.S. Calefi, Effect of high-energy ball milling in the structural and textural properties of kaolinite, Cerâmica 60 (2014) 267–272. https://doi.org/10.1590/S0366-69132014000200016.
[209] Y. Taha, M. Benzaazoua, R. Hakkou, M. Mansori, Coal mine wastes recycling for coal recovery and eco-friendly bricks production, Miner. Eng. 107 (2017) 123–138. https://doi.org/10.1016/j.mineng.2016.09.001.
[210] S. Gao, L. Guo, Application of Coal Gangue as a Coarse Aggregate in Green Concrete Production: A Review, Materials 12 (2021). https://doi.org/10.3390/ma14226803.
[211] A. Mitrović, M. Zdujić, Mechanochemical treatment of Serbian kaolin clay to obtain high reactive pozzolana, J. Serbian Chem. Soc. 78 (2013) 579–590. https://doi.org/10.2298/JSC120829107M.
[212] I. Tole, K. Habermehl-Cwirzen, A. Cwirzen, Mechanochemical activation of natural clay minerals: an alternative to produce sustainable cementitious binders – review, Mineral. Petrol. 113 (2019) 449–462. https://doi.org/10.1007/s00710-019-00666-y.
[213] V.A. Baki, X. Ke, A. Heath, J. Calabria-Holley, C. Terzi, M. Sirin, The impact of mechanochemical activation on the physicochemical properties and pozzolanic reactivity of kaolinite, muscovite and montmorillonite, Cem. Concr. Res. 162 (2022) 106962. https://doi.org/10.1016/j.cemconres.2022.106962.

[214] J. Mañosa, A. Alvarez-Coscojuela, J. Marco-Gibert, A. Maldonado-Alameda, J.M. Chimenos, Enhancing reactivity in muscovitic clays: Mechanical activation as a sustainable alternative to thermal activation for cement production, Appl. Clay Sci. 250 (2024) 107266. https://doi.org/10.1016/j.clay.2024.107266.
[215] Effects of mechanical grinding on pozzolanic activity and hydration properties of quartz, Adv. Powder Technol. 31 (2020) 4500–4509. https://doi.org/10.1016/j.apt.2020.09.028.
[216] R. Delhez, T.H. De Keijser, J.I. Langford, D. Louer, E.J. Mittemeijer, E.J. Sonneveld, Crystal imperfection broadening and peak shape in the Rietveld method, Rietveld Method 5 (1993) 132–166.
[217] G. Yao, Z. Wang, J. Yao, X. Cong, C. Anning, X. Lyu, Pozzolanic activity and hydration properties of feldspar after mechanical activation, Powder Technol. 383 (2021) 167–174. https://doi.org/10.1016/j.powtec.2021.01.042.
[218] B. Wei, Y. Zhang, S. Bao, Preparation of geopolymers from vanadium tailings by mechanical activation, Constr. Build. Mater. 145 (2017) 236–242. https://doi.org/10.1016/j.conbuildmat.2017.03.234.
[219] É. Makó, R.L. Frost, J. Kristóf, E. Horváth, The Effect of Quartz Content on the Mechanochemical Activation of Kaolinite, J. Colloid Interface Sci. 244 (2001) 359–364. https://doi.org/10.1006/jcis.2001.7953.
[220] J. Chen, X. Guan, M. Zhu, J. Gao, Mechanism on Activation of Coal Gangue Admixture, Adv. Civ. Eng. 2021 (2021) 5436482. https://doi.org/10.1155/2021/5436482.
[221] S.P.K. Kohobhange, C.H. Manoratne, H.M.T.G.A. Pitawala, R.M.G. Rajapakse, The effect of prolonged milling time on comminution of quartz, Powder Technol. 330 (2018) 266–274. https://doi.org/10.1016/j.powtec.2018.02.033.
[222] I. Tole, K. Habermehl-Cwirzen, M. Rajczakowska, A. Cwirzen, Activation of a Raw Clay by Mechanochemical Process—Effects of Various Parameters on the Process Efficiency and Cementitious Properties, Materials 11 (2018) 1860. https://doi.org/10.3390/ma11101860.
[223] É. Makó, R.L. Frost, J. Kristóf, E. Horváth, The Effect of Quartz Content on the Mechanochemical Activation of Kaolinite, J. Colloid Interface Sci. 244 (2001) 359–364. https://doi.org/10.1006/jcis.2001.7953.
[224] C. Zhao, Z. Li, S. Peng, J. Liu, Q. Wu, X. Xu, State-of-the-art review of geopolymer concrete carbonation: From impact analysis to model establishment, Case Stud. Constr. Mater. 20 (2024) e03124. https://doi.org/10.1016/j.cscm.2024.e03124.
[225] A. Alujas, R. Fernández, R. Quintana, K.L. Scrivener, F. Martirena, Pozzolanic reactivity of low grade kaolinitic clays: Influence of calcination temperature and impact of calcination products on OPC hydration, Appl. Clay Sci. 108 (2015) 94–101. https://doi.org/10.1016/j.clay.2015.01.028.
[226] P.S.L. Souza, D.C.C. Dal Molin, Viability of using calcined clays, from industrial by-products, as pozzolans of high reactivity, Cem. Concr. Res. 35 (2005) 1993–1998. https://doi.org/10.1016/j.cemconres.2005.04.012.
[227] N. Essaidi, B. Samet, S. Baklouti, S. Rossignol, Feasibility of producing geopolymers from two different Tunisian clays before and after calcination at various temperatures, Appl. Clay Sci. 88–89 (2014) 221–227. https://doi.org/10.1016/j.clay.2013.12.006.
[228] M. Frías, M.I. Sanchez de Rojas, R. García, A. Juan Valdés, C. Medina, Effect of activated coal mining wastes on the properties of blended cement, Cem. Concr. Compos. 34 (2012) 678–683. https://doi.org/10.1016/j.cemconcomp.2012.02.006.
[229] H.Y. Zhang, G.H. Qiu, V. Kodur, Z.S. Yuan, Spalling behavior of metakaolin-fly ash based geopolymer concrete under elevated temperature exposure, Cem. Concr. Compos. 106 (2020) 103483. https://doi.org/10.1016/j.cemconcomp.2019.103483.

[230] Unraveling the characteristics of geopolymer mortars: A deep dive into the impact of marble powder as fine aggregate and varied activators, Constr. Build. Mater. 422 (2024) 135767. https://doi.org/10.1016/j.conbuildmat.2024.135767.
[231] H. Xu, J.S.J. Van Deventer, The geopolymerisation of alumino-silicate minerals, Int. J. Miner. Process. 59 (2000) 247–266. https://doi.org/10.1016/S0301-7516(99)00074-5.
[232] L.N. Tchadjie, S.O. Ekolu, Enhancing the reactivity of aluminosilicate materials toward geopolymer synthesis, J. Mater. Sci. 53 (2018) 4709–4733. https://doi.org/10.1007/s10853-017-1907-7.
[233] M. Zhang, M. He, J. Zhang, Mitigation of efflorescence for multi-componential geopolymer: Influence of steel slag, flue gas desulfurization gypsum and pre-curing periods, J. Clean. Prod. 403 (2023) 136835. https://doi.org/10.1016/j.jclepro.2023.136835.
[234] Z. Zhang, J.L. Provis, X. Ma, A. Reid, H. Wang, Efflorescence and subflorescence induced microstructural and mechanical evolution in fly ash-based geopolymers, Cem. Concr. Compos. 92 (2018) 165–177. https://doi.org/10.1016/j.cemconcomp.2018.06.010.
[235] Z. Zhang, J.L. Provis, X. Ma, A. Reid, H. Wang, Efflorescence and subflorescence induced microstructural and mechanical evolution in fly ash-based geopolymers, Cem. Concr. Compos. 92 (2018) 165–177. https://doi.org/10.1016/j.cemconcomp.2018.06.010.
[236] W. Zhang, L. Lang, C.-X. Dong, Z. Qi, Z.-R. Zhang, J.-S. Li, Comprehensive study on coal gangue-based geopolymer activated by phosphoric acid: From macroscale properties to molecular simulation, Constr. Build. Mater. 438 (2024) 137271. https://doi.org/10.1016/j.conbuildmat.2024.137271.
[237] M.S. Elfwal, N.H. El-Ashkar, N.M. Nagy, A.H. Shalan, Utilization of electric arc furnace slag and metakaolin as precursors in alkali-activated paste: microstructure and mechanical properties, Innov. Infrastruct. Solut. 9 (2024) 343. https://doi.org/10.1007/s41062-024-01657-5.
[238] I.S. Abbas, M.H. Abed, H. Canakci, Development and characterization of eco- and user-friendly grout production via mechanochemical activation of slag/rice husk ash geopolymer, J. Build. Eng. 63 (2023) 105336. https://doi.org/10.1016/j.jobe.2022.105336.
[239] B. Luzu, M. Duc, A. Djerbi, L. Gautron, High performance illitic clay-based geopolymer: Influence of thermal/mechanical activation on strength development, Appl. Clay Sci. 258 (2024) 107445. https://doi.org/10.1016/j.clay.2024.107445.
[240] Y. Luo, Z. Jiang, D. Wang, Y. Lv, C. Gao, G. Xue, Effects of alkaline activators on pore structure and mechanical properties of ultrafine metakaolin geopolymers cured at room temperature, Constr. Build. Mater. 361 (2022) 129678. https://doi.org/10.1016/j.conbuildmat.2022.129678.
[241] P. Duxson, A. Fernández-Jiménez, J.L. Provis, G.C. Lukey, A. Palomo, J.S.J. van Deventer, Geopolymer technology: the current state of the art, J. Mater. Sci. 42 (2007) 2917–2933. https://doi.org/10.1007/s10853-006-0637-z.
[242] A.D. Hounsi, G.L. Lecomte-Nana, G. Djétéli, P. Blanchart, Kaolin-based geopolymers: Effect of mechanical activation and curing process, Constr. Build. Mater. 42 (2013) 105–113. https://doi.org/10.1016/j.conbuildmat.2012.12.069.
[243] M.B. Ogundiran, S. Kumar, Synthesis and characterisation of geopolymer from Nigerian Clay, Appl. Clay Sci. 108 (2015) 173–181. https://doi.org/10.1016/j.clay.2015.02.022.
[244] A. Fernández-Jiménez, A. Palomo, Mid-infrared spectroscopic studies of alkali-activated fly ash structure, Microporous Mesoporous Mater. 86 (2005) 207–214. https://doi.org/10.1016/j.micromeso.2005.05.057.

[245] K. Komnitsas, D. Zaharaki, V. Perdikatsis, Geopolymerisation of low calcium ferronickel slags, J. Mater. Sci. 42 (2007) 3073–3082. https://doi.org/10.1007/s10853-006-0529-2.
[246] K. Chen, W.-T. Lin, W. Liu, Effect of NaOH concentration on properties and microstructure of a novel reactive ultra-fine fly ash geopolymer, Adv. Powder Technol. 32 (2021) 2929–2939. https://doi.org/10.1016/j.apt.2021.06.008.
[247] A. Bach Delpeuch, F. Maillard, M. Chatenet, P. Soudant, C. Cremers, Ethanol oxidation reaction (EOR) investigation on Pt/C, Rh/C, and Pt-based bi- and tri-metallic electrocatalysts: A DEMS and in situ FTIR study, Appl. Catal. B Environ. 181 (2016) 672–680. https://doi.org/10.1016/j.apcatb.2015.08.041.
[248] Understanding the gel compatibility and thermal behavior of alkali activated Class F fly ash/ladle slag: The underlying role of Ca availability, Cem. Concr. Res. 170 (2023) 107198. https://doi.org/10.1016/j.cemconres.2023.107198.
[249] Y.-S. Wang, Y. Alrefaei, J.-G. Dai, Silico-Aluminophosphate and Alkali-Aluminosilicate Geopolymers: A Comparative Review, Front. Mater. 6 (2019). https://www.frontiersin.org/articles/10.3389/fmats.2019.00106 (accessed January 2, 2023).
[250] H.E. Elyamany, A.E.M. Abd Elmoaty, A.M. Elshaboury, Setting time and 7-day strength of geopolymer mortar with various binders, Constr. Build. Mater. 187 (2018) 974–983. https://doi.org/10.1016/j.conbuildmat.2018.08.025.
[251] A.J. Kinloch, Mechanisms of adhesion, in: A.J. Kinloch (Ed.), Adhes. Adhes. Sci. Technol., Springer Netherlands, Dordrecht, 1987: pp. 56–100. https://doi.org/10.1007/978-94-015-7764-9_3.
[252] B.O. Bateup, Surface chemistry and adhesion, Int. J. Adhes. Adhes. 1 (1981) 233–239. https://doi.org/10.1016/0143-7496(81)90071-3.
[253] G. Mucsi, A review on mechanical activation and mechanical alloying in stirred media mill, Chem. Eng. Res. Des. 148 (2019) 460–474. https://doi.org/10.1016/j.cherd.2019.06.029.
[254] Zheng Yi Fu, Shi Liu Wei, Mechanochemical activation of calcium oxide powder, Powder Technol. 87 (1996) 249–254. https://doi.org/10.1016/0032-5910(96)03094-X.
[255] P.J. Sánchez-Soto, M. del Carmen Jiménez de Haro, L.A. Pérez-Maqueda, I. Varona, J.L. Pérez-Rodríguez, Effects of Dry Grinding on the Structural Changes of Kaolinite Powders, J. Am. Ceram. Soc. 83 (2000) 1649–1657. https://doi.org/10.1111/j.1151-2916.2000.tb01444.x.
[256] Z.A. Juhász, Colloid-chemical aspects of mechanical activation, Part. Sci. Technol. 16 (1998) 145–161. https://doi.org/10.1080/02726359808906792.
[257] A. Bouaziz, R. Hamzaoui, S. Guessasma, R. Lakhal, D. Achoura, N. Leklou, Efficiency of high energy over conventional milling of granulated blast furnace slag powder to improve mechanical performance of slag cement paste, Powder Technol. 308 (2017) 37–46. https://doi.org/10.1016/j.powtec.2016.12.014.
[258] P.N. Kuznetsov, L.I. Kuznetsova, A.M. Zhyzhaev, V.I. Kovalchuk, A.L. Sannikov, V.V. Boldyrev, Investigation of mechanically stimulated solid phase polymorphic transition of zirconia, Appl. Catal. Gen. 298 (2006) 254–260. https://doi.org/10.1016/j.apcata.2005.10.002.
[259] L. Petra, P. Billik, Z. Melichová, P. Komadel, Mechanochemically activated saponite as materials for Cu2 + and Ni2 + removal from aqueous solutions, Appl. Clay Sci. 143 (2017) 22–28. https://doi.org/10.1016/j.clay.2017.03.012.
[260] D. Myers, Surfaces, interfaces, and colloids, Wiley New York, 1999.